Laser controlled cycloaddition and reversion of crossdimers

Dissertation

zur Erlangung des Doktorgrades der Naturwissenschaften (Dr. rer. nat.)

dem Fachbereich Chemie

der Philipps-Universität Marburg

vorgelegt von

Dipl. Chem. Philipp Johannes Behrendt

aus München

Marburg/Lahn 2013

Erstgutachter: - Prof. Dr. Norbert Hampp

Zweitgutachter: - Prof. Dr. Gerhard Hilt

Prüfungstermin: 18.07.2013

Hochschulkennziffer: 1180

„Thunder is good, thunder is impressive;

but it is lightning that does the work”

Mark Twain

Publications

Paper:

- "Two-photon absorption triggered drug delivery from a polymer for intraocular lenses in presence of an UV-absorber"

D. Kehrloesser, P. J. Behrendt, N. Hampp, *Journal of Photochemistry and Photobiology A: Chemistry* **2012**, *248,* 8-14.

- "Laser-based Depletion Zone Photoreaction: Selective Synthesis of [2+2]-Crossdimers of coumarin and 5-Fluorouracil"

P. J. Behrendt, H.-C. Kim, N. Hampp, *Journal of Photochemistry and Photobiology A: Chemistry* **2013**, *264*, 67-72.

- "Photochemical cleavage of the stereoisomers of coumarin with 5-fluorouracil via single- and two-photon excitation"

P. J. Behrendt, H.-C. Kim, N. Hampp; in preparation

Presentations:

- CAS NIMTF Sino German Symposium; March 2011, Ningbo, China
- XXX EL.B.A. Nanoforum; April 2012, Genova, Italy

Posters:

- 502. WE-Heraeus Seminar; April 2012, Bad Honnef, Germany
- XXIV IUPAC Symposium on Photochemistry; July 2012, Coimbra, Portugal

Table of contents

Publications 3

Abstract 6

Zusammenfassung 7

List of abbreviations 8

1. Introduction 10

1.1. Cataract treatment / ACTIOL 10

1.2. Advantages of photoreactions 11

1.3. Photo-physics 12

1.4. Sensitizer 15

1.5. [2+2]-cycloadditions 17

1.6. Photochemistry of coumarin 19

1.7. Cyclobutane structures in nature and for synthesis 22

1.8. Advantage of crossdimerization / motivation 22

2. Results and discussion 24

2.1. Composition 26

2.1.1. Different assemblies 26

2.1.2. Different concentrations 27

2.1.3. Diffusion 30

2.1.4. Triplet promoter / additives 32

2.1.5. Different crossdimers 33

2.2. Activation/excitation 37

2.2.1. Light source 37

a) Additional wavelength 40

2.2.2. Photon distribution 43

2.2.3. Intrinsic values 45

2.2.4. Set ups 47

2.2.5. Activation/depletion zone/suppression 49

2.3. Reaction 56
2.3.1. Side reactions 57
2.3.2. Dispersion of energy 59
a) Heat 59
b) Fluorescence; *Stern-Volmer* plot 61
c) Phosphorescence 64
2.3.3. Singlet or Triplet reaction 65
2.3.4. Kinetics 66
a) Constant concentration 71
b) Constant absorption (OD) 74
c) Reaction rates 79
d) Quantum yield 81

2.4. Reversibility 82
2.4.1. Single photon absorption (SPA) 82
2.4.2. Two photon absorption (TPA) 86
2.4.3. Films 92
2.4.4. After-treatment 94
2.4.5. Combining laser and thermal recycling 95

2.5. Derived reactions 98
2.5.1. [4+2]-heterocycloaddition 98
2.5.2. Photoremovable protective group 101

2.6. Summary and outlook 105

3. Materials and methods 107
3.1. Synthesis 109

References 123
Supplements 128
Acknowledgment 129
Curriculum vitae 130
Erklärung 131

Abstract

To treat cataract, the major cause for blindness, the original eye lenses are removed and artificial lenses are implanted. With this procedure, the side effect of secondary cataract has become of interest to research. The treatment thereof calls for the development of a molecular integrated and covalently bound photolinker system for the controlled release of cytostatica. To load the polymeric intraocular lens, crossdimers of the photolinker coumarin together with the antimetabolite 5-fluorouracil are synthesized. After incorporation in the lens, the specific release via cycloreversion then is best realized with a two photon process which offers high spatial resolution, and which uses visual light to pass the cornea.

The backbone of this work is the light driven, intermolecular and coumarin based crossdimerization and its reversion. To achieve this goal, the options given for photoreactions, like set up, substrates, and excitation are considered and their variables are evaluated. The choice of photolinker is narrowed down and a comparison between these absorbing substrates provided by kinetic measurements. A list of possible molecule types of the non-absorbing reaction partner for the crossdimerization is given, by which a huge variety of crossdimers can be build up. The commonly used lamp based light sources such as a *Rayonet* reactor are compared to the novel favored laser system. The sun is also utilized to project a large scale, energetically economic process. The laser, as a new tool for molecule synthesis, exhibits improvements to cycloaddition reactions in a number of experiments. Additives like sensitizers and triplet promoters are shown to be unnecessary with this high energy illumination. The laser fueled set up is analyzed and the photon distribution, together with the photon flux, is determined to be crucial. With parameters attuned to the lifetime of the excited state, the diffusion controlled dimerization reaction can be controlled and steered towards the principal generation of crossdimer.

The reversibility of the dimerization reaction caused both by heat and light is demonstrated. Thermal cleavage is used in addition to laser synthesis in the specialization towards exclusive crossdimer synthesis. Light is primarily used in the customary laser based two photon absorption for specific single and two bond cleavage. Hereby the ever more popular two photon cycloreversion is measured of individual stereoisomers.

All methods, developed for the dimer generation, belong to the general concept for the extended application of photoreaction in synthesis. Additional examples in form of a sequential photoreaction and photoremovable protective groups are presented accordingly.

Zusammenfassung

Um Katarakt, was die häufigste Ursache für Blindheit darstellt, zu behandeln werden die ursprünglichen Augenlinsen entfernt und durch künstliche ersetzt. Wegen dieser Behandlung wurde der Nebeneffekte des sekundären Katarakts von Interesse für die Forschung. Die diesbezügliche Behandlung benötigt die Entwicklung eines kovalent gebundenen, auf molekularer Ebene integrierten und licht-gesteuerten Freisetzungssystems für Zytostatika. Für die Beladung der polymeren, interokularen Linsen werden dazu Kreuzdimere des fotoaktiven Kumarins mit dem Antimetaboliten 5-Fluoruracil synthetisiert. Nach dem Einbringen in die Linse, wird die dosierbare Freisetzung mittels Zykloreversion am besten gesteuert durch einen örtlich hochaufgelösten Zweiphotonenprozess, welcher sichtbares Licht verwendet um die Kornea zu passieren.

Rückgrat dieser Dissertation ist die lichtgetriebene, intermolekulare, auf Kumarin basierende Kreuzdimerisierung und dessen Reversion. Um dieses Ziel zu erlangen wurden die Möglichkeiten an Aufbauten, Substraten und Anregungen verglichen und deren Variablen evaluiert. Die Auswahl an absorbierenden Linkern wird eingeengt und eine Vergleichbarkeit über kinetische Messungen gegeben. Eine Liste an möglichen Molekültypen, so wie der nicht absorbierenden Reaktionspartner, für die Kreuzdimerisierung wird angeführt, mit derer sich eine große Menge möglicher Kreuzdimere herstellen lässt. Die herkömmlichen lampenbasierenden Lichtquellen, wie der Rondellreaktor, werden mit dem neuen Lasersystem verglichen. Sonnenlicht wird außerdem verwendet um einen energieökonomischen Großmaßstabsansatz zu veranschaulichen. Der Laser, als ein neues Instrument für die Molekülsynthese, zeigt in einer Reihe an Experimenten Verbesserungen. Zusätze, wie Sensibilisatoren und Triplettpromotoren, zeigen sich als unnötig für solch eine hochenergetische Bestrahlung. Der lasergetriebene Aufbau wird untersucht wobei sich der Photonenfluss und Photonenverteilung als Kernpunkte heraus stellen. Mit den richtigen Parametern kann diese diffusionsabhängige Reaktion, welche zusätzlich abhängig von der Lebensdauer des angeregten Zustandes ist, kontrolliert und gesteuert werden, um vornehmlich Kreuzdimer zu produzieren.

Die Umkehrbarkeit dieser Dimerisierungsreaktion wird sowohl mit Licht als auch mit Hitze demonstriert. Thermische Zersetzung wird dabei, zusätzlich zur Lasersynthese, für die Spezialisierung hingehend zur ausschließlichen Kreuzdimerisierung verwendet. Licht hingegen wird hauptsächlich in der bekannten Zweiphotonenabsorption für den selektive ein- und zweifach Bindungsbruch eingesetzt. Dabei wird die, immer beliebtere, Zweiphotonen-zykloreversion für individuelle Stereoisomere gemessen.

Alle Methoden, welche für die Dimererzeugung entwickelt wurden, gehören zu dem übergeordneten Konzept zur erweiterten Anwendung lichtgetriebener Reaktionen in der Synthese. Zusätzliche

Beispiele in der Form von aneinandergereihten Lichtreaktionen und lichtentfernbaren Schutzgruppen sind diesbezüglich angeführt.

List of abbreviations

Because of a limited number of letters in the alphabet sometimes a symbol has different meanings (indicated by //). However each symbol is assigned in the text accordingly and no two meaning are used within one section.

5FU	5-fluorouracil
A	acceptor // excitable substrate // area
abs	absorption
ACN	acetonitrile
ACTIOL	active intraocular lens
AIBN	azoisobutylnitrile
a.u.	arbitrary units
B	ground state, reaction partner/ quencher
c	concentration // captiv/capto
cal	calorie
CD	crossdimer
d	dativ
D	donor
DCM	dichloromethane
DSC	differential scanning calorimetry
DNB	dinitrobenzyl
DOE	diffractive optical element
E	energy
E_A	activation energy
EDG	electron donating group
em	emission
EWG	electron withdrawing group
FWHM	full width at half maximum
FRET	*Förster* resonance energy transfer
GM	*Göppert Meyer* (GM = 10^{-50} cm·s·photons^{-1})

H5 / H5FU	1-heptanoly-5-fluorouracil
HD	homodimer
hh	head to head
HOMO	highest occupied molecular orbital
HPLC	high pressure liquid chromatography
ht	head to tail
I	intensity // intermediate
IC	internal conversion
ISC	inter system crossing
IUPAC	International union of pure and applied chemistry
k	constant
L	linker
LA	Lewis acid
LIPS	laser induced plasma spectroscopy
LUMO	lowest unoccupied molecular orbital
MMA	methylmetacrylate
NMR	nuclear magnetic resonance
OD	optical density
P	product
PMMA	poly-methacrylic acid
ppg	photoremovable protective group
R	rest (chemical group) // reaction rate
Re	reactant
RT	room temperature
S	singlet // substrate
SPA	single photon absorption
SOMO	single occupied molecular orbital
T	triplet
TC / TBSCum	7-*tert.*butyldimethylsilyloxycoumarin
TEMPO	tetramethylpiperidinoxyl
THF	tetrahydrofuran
TPA	two photon absorption
TTET	triplet-triplet energy transfer
wt	weight
X	any variety of substrates B

1. Introduction

1.1. Cataract treatment / ACTIOL

In our ever more aging society and in developing countries, cataract is a growing problem. Caused by maladies and mal nourishment or generated by medication, this opacification of the eye lens is one of the most abundant diseases.[1,2] Often beginning at the age of 65, the clouding of the lens evokes deteriorating sight, increased sensibility to brightness and eventually blindness.[3] The treatment is to surgically replace the natural lens with an artificial intraocular lens (IOL). In Germany around 600,000 of these operations are made every year. Unfortunately, in about 50 % of all cases epithelial cell migrate onto the anterior and posterior sides of the new lens and form the so called secondary cataract.[4,5] The common procedure is then to destroy these cells by laser irradiation. But often times the high intensities thereby damage the lens or the retina.[6] The solution hence is to inhibit the growth of cells on the IOL. To do so, approaches tired to change the surface geometry and wetability.[7-10] An elegant way is the internal medication via a drug loaded active intraocular lens (ACTIOL). Therefore the photolinker coumarin is used to reversibly bind the antimetabolite 5-fluorouracil within the polymer matrix of the artificial lens (Figure 1). This drug has already been clinically studied and proved to be effective.[11-13] To release the drug in a single photon absorption process (SPA) light of wavelengths below 300 nm is required. Because the cornea transmits only visible light, a two photon absorption process (TPA) with a laser determined wavelength of 532 nm is used (Figure 2). This TPA allows a dose specific and high spatially resolved drug release, only within the vocal volume of the focused laser beam (Figure 3). Therewith, multiple and locally concentrated treatments are possible.

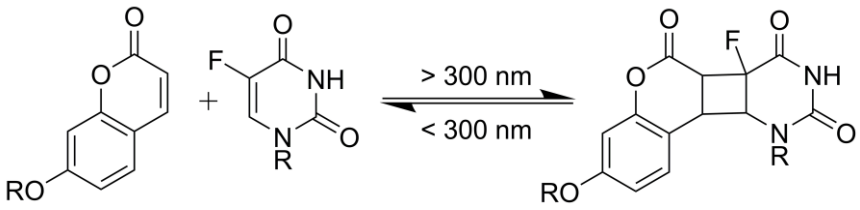

Figure 1: Reversible crossdimer TC-H5FU formation.

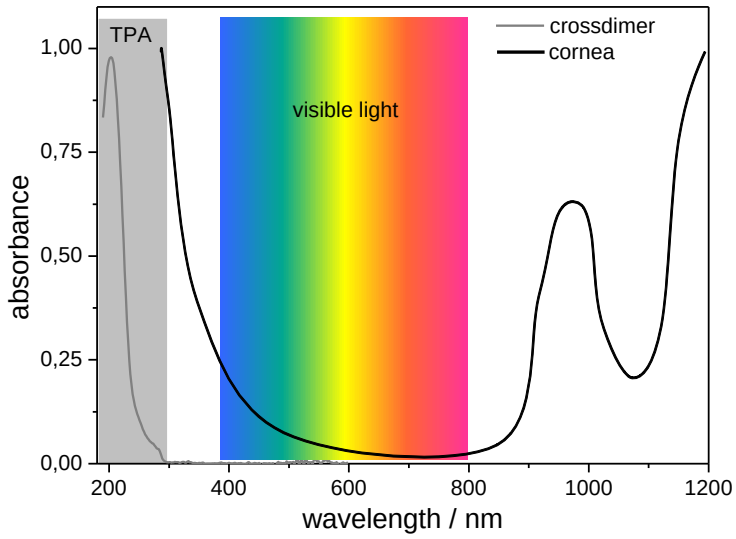

Figure 2: Absorption of crossdimer and absorption of human cornea.[14]

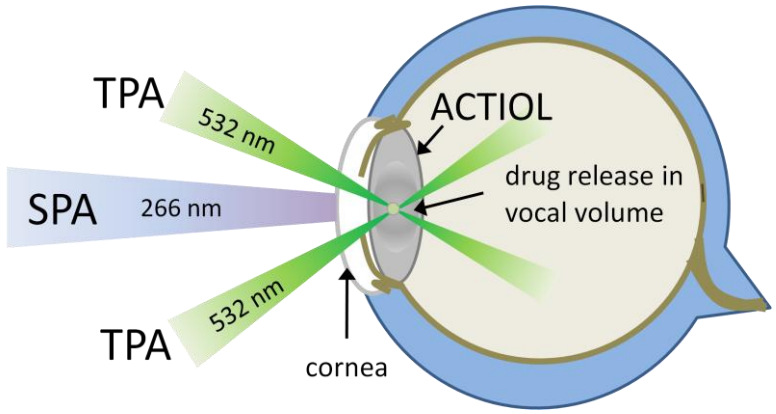

Figure 3: TPA process in ACTIOL.

1.2. Advantages of photoreactions

Reactions driven by light belong to the oldest reactions on earth, even though specific scientific use only exists for around 200 years.[15-17] Still, today thermal and electrochemical processes are favored by the industry. The irony is that light is the only free energy source, whereas heat and electricity need to be generated.

When all three are compared, the thermal energy is the easiest to insert in the reaction system, but offers the least amount of control. The electric energy has varying currents and a direction of force field as features, but cannot locally activate specific molecules. Light on the other hand incorporates a number of influential reaction parameters. Its direction of force field can be used in laser induced

plasma spectroscopy (LIPS) or optical tweezers. The coherence of photons is used for coherent control and the two photo absorption reactions discussed later on. Concomitantly, the energy or wavelength can be accurately tuned and the intensity can be altered instantly. Furthermore, photo-reactions are fast, because they can take place within the excited molecule itself. Then again, it is possible to use the specific activation of a chromophor in the molecule and to directly address a particular transition energy gap. Reactions induced by light are clean, too. Only the absorbing species of molecules is activated and just the energy needed is locally induced, which offers a high spatial resolution, especially in TPA processes. Often time, photo-reactions are reversible as well, making them interesting for advanced applications such as drug release, refractive index shift, polymer healing, and many more. Light can also be measured fast and accurately.

1.3. Photo-physics

The *Stark-Einstein* law states, that every absorbed photon will cause a chemical or physical reaction. Once a chromophor absorbs a photon (or light energy) the energy is dispersed over the molecule and a variety of energy outlets are used to dispose of this extra energy. Depending upon the stiffness, the number, and place of functional groups, the presence of heavy atoms, and the condition of its surrounding, a number of different transitions can take place. Either radiation less decay or radiant fluorescence or phosphorescence, with previous inter system crossing, are possible. Each of these passage ways requires different time spans. A general overview of these intervals is presented in Figure 4. Organic photoreactions essentially use the energy out of the S_1 and T_1 state to generate products.

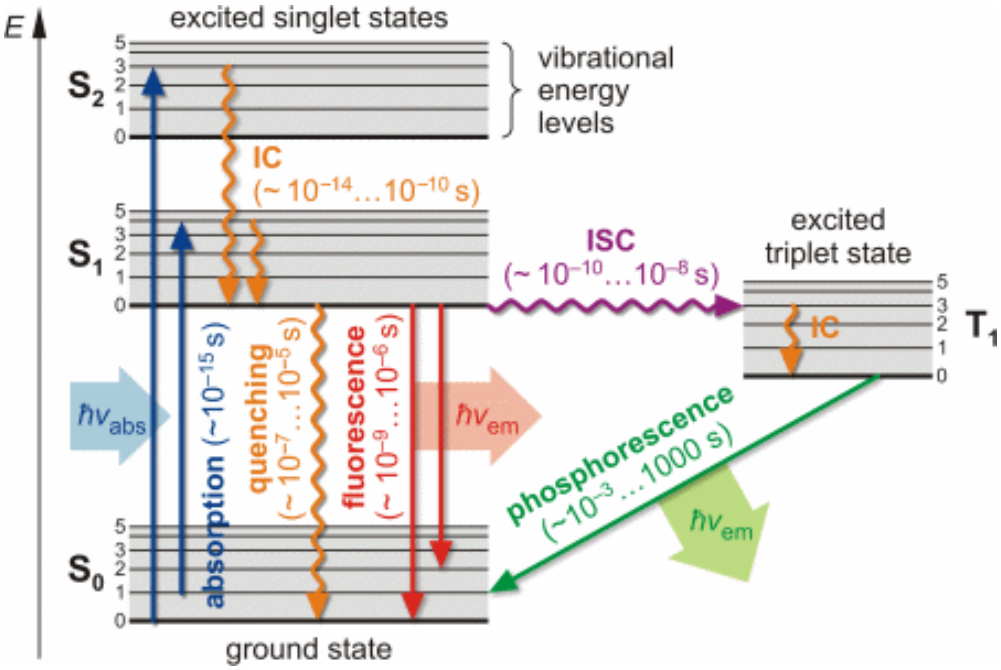

Figure 4: *Jablonski* diagram.[18]

In more detail the absorbed energy is used to excite the reactant (Re) into an activated state from which it can form a product. It therefore needs to reach lower lying troughs in the potential energy surface. In case the entire reaction takes place on a single potential energy surface of one excited state and the excess energy is released through radiation, then this reaction is called adiabatic. If several potential energy surfaces are involved, then it is a diabatic reaction (Figure 5).

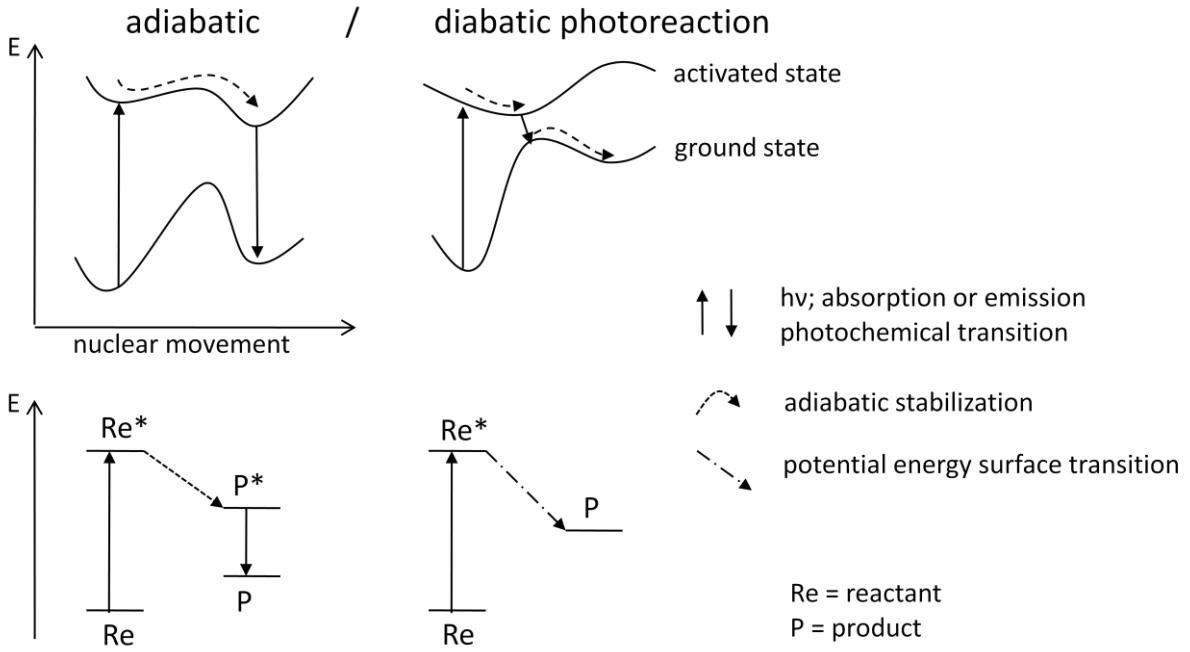

Figure 5: Adiabatic and diabatic photo-reaction.

In essence, every total photo-reaction is a diabatic reaction. Adiabatic reactions only occur involving small structural changes and minor alterations in covalent bonding (e.g. proton transfer and complex formation). This mechanism is responsible for most chemiluminescent processes. Diabatic reactions on the other hand need spontaneous transitions to lower energy surfaces, which require small inter-surface energy gaps and efficient spin-orbit coupling (as devised in the *Marcus* theory.[19]). These mechanism regulated transitions happen voluntarily, but due to coincidental de-excitation into the initial ground state, the quantum efficiencies are rather low.

Simultaneously to a single photon absorption (SPA) process, any absorption can be achieved with two coherent photons (TPA) with twice the wavelength. This concept, which has been created by Mrs. *Goeppert-Mayer* in 1931, stands in contradiction to the *Stark-Einstein* law, but could be proven experimentally in 1961 with the development of high intensity pulsed lasers.[20,21] A very high photon density is needed in order to populate virtual levels, with life times of 10^{-17} up to 10^{-15} s. The second absorption has to take place during this short amount of time before relaxation to the ground state occurs. Generally, a monochromatic light source is used, but so called non-degenerate TPAs with two different wavelengths are also possible. With the coumarin dimer and its absorption below 300 nm a high intensity, green 532 nm laser is suited for TPA dimer cleavage. This visible radiation thus can pass through the cornea, allowing the application of coumarin in lenses (s. Fig. 3).
There are different selection rules for SPA and TPA, because of angular momentum preservation; therefore the excited states are not identical. TPA for example just allows transitions with an even parity. This is used in two-photon-spectroscopy to populate electronic states which are difficult to access via SPA. Additionally, the TPA, in contrast to SPA, displays a non-linear dependence between absorption rate and light intensity. The following formula 1 depicts the quadratic relation of the intensity I of a monochromatic radiation with the absorbed energy per time:

$$\frac{dW}{dt} = \frac{8\pi^2\omega}{n^2c^2} \cdot I^2 \cdot Im(\chi^{(3)}) \qquad (1)$$

W: absorbed energy, n: refractive index, ω: frequency of irradiation, I: Intensity,
Im($\chi^{(3)}$): imaginary part of susceptibility tensor of 3. degree

Only with the employment of high intensities will a TPA process exhibit a measurable reaction rate, which permits high spatial resolution within the focus of the laser beam, avoiding any kind of reactions outside of the focus. Regular, low intensity day light is unable to evoke any reaction.
To quantify the process, the two-photon absorption cross-section σ of the molecule at a specific wavelength is denominated. Comparable to a rate constant it can be calculated by insertion in $\frac{dW}{dt} = \frac{dN_P}{dt} \cdot h\upsilon$ in the above formula:

$$\frac{dN_P}{dt} = \delta \cdot N \cdot F^2 \quad (2)$$

N_p: absorbed photons, N: absorbing molecules per volume, F: photon flux,

δ: two-photon cross-section ($\delta = 8\pi^2 h\nu^2 n^{-2} c^{-2} N \cdot \mathrm{Im}(\chi^{(3)})$), h: Planck constant

The two-photon absorption cross-section is stated in the unit of *Goeppert-Mayer* (1 GM = 10^{-50} $cm^4 \cdot s$), which compared to a single photon absorption cross-section is approximately 30 magnitudes smaller. To verify the quadratic dependence of a TPA process, its velocity time rule has to be calculated and logarithmized.

$$\frac{dc}{dt} = \delta \cdot c_0 \cdot \Phi_{TPA} \cdot I^2 = k \cdot I^2 = v_0 \quad (3)$$

$$\rightarrow \ln v_0 = \ln k + 2ln\, I \quad (4)$$

When plotted as a double logarithmic graph of the initial reaction velocity against the intensity, given by the pulse intensity, the slope will be around 2.

Photoactive materials have always been of high interest, especially the ones working with TPA processes. To get a high two-photon absorption cross-section is crucial and can be achieved with the addition of acceptor- and donor substituents to the conjugated part of the chromophor.[22] Besides this chemical improvement, it is an important part of this thesis to find out whether different stereoisomers of the same molecule have varying cross-sections, which could be used to decrease the radiation time, or total amount of energy induced into the material.

1.4. Sensitizer

The majority of intermolecular photo-addition-reactions occur out of a long existing triplet state, which is more stable than a fast depleting singlet state. It is therefore crucial to have as many molecules as possible within this triplet state. Organic molecules in general can reach this state with inter system crossing by themselves, but the quantum yields for this process are usually rather low and only about a few per cent. To boost the number of triplet molecules, sensitizers are added to the reaction mixture. These molecules are normally rather stiff, composed of annulated rings and include hetero-atoms. As sensitizers they should have a high absorption cross-section and a high inter system crossing probability. Generally, all organic molecules can be sensitizers, but a couple of prominent and efficient are listed in Figure 6.

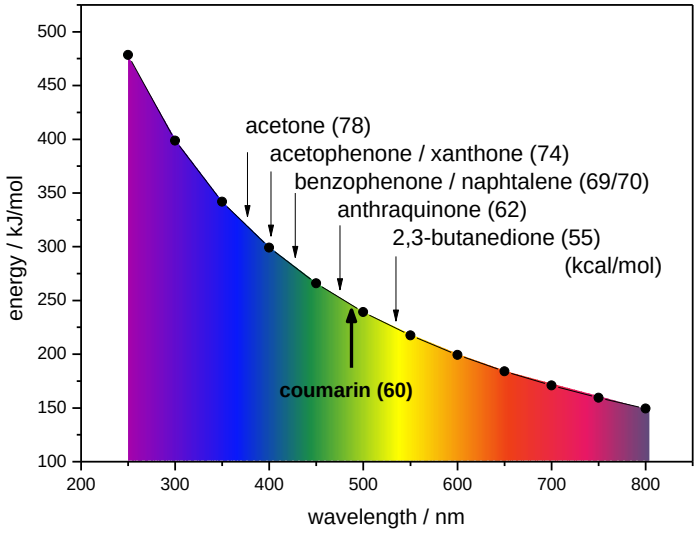

Figure 6: Triplet energies of organic sensitizers.

Sensitizers are available over a wide wavelength range. In order to choose the right one for a particular reaction, it is important to notice that the energies of the triplet states of the sensitizers and of the targeted molecules cannot be too far apart. The energy transfer from the sensitizer to the acceptor molecule is a two-electron process during a collision between them. In contrast to the long range *Förster* energy transfer (FRET), the molecules in the triplet-triplet energy transfer (TTET) have to come as close as the *van-der Waals* contact radius which is around 10 Å. During their brief contact the molecules exchange their electronic configuration via the *Dexter* mechanism. This mechanism works for singlet, as well as for triplet excited states, but only the triplet transfer is of importance here (Figure 7).

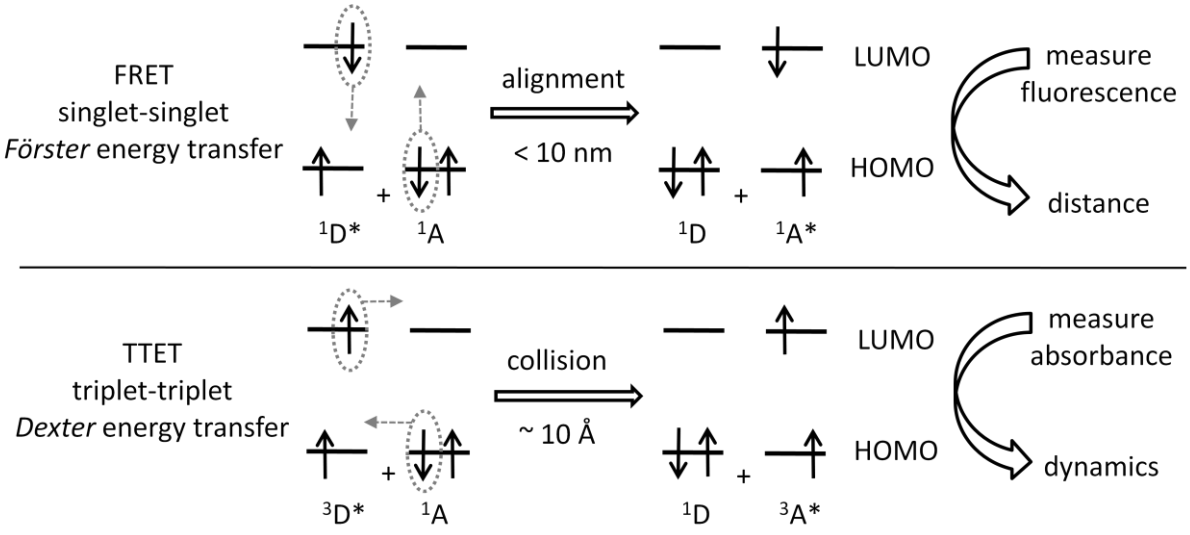

Figure 7: FRET and TTET between donor D and acceptor A.

In case there is singlet transfer, the fluorescence intensity of the acceptor correlates to the distance of the donor. If triplet energy transfer is occurring, the absorbance of the acceptor will decrease as its triplet state becomes populated. Another possibility for observing the initial state of the acceptor is also to monitor the fluorescence. This intensity will drop when sensitization occurs. Measurements like this are used later in the *Stern-Volmer* experiments (s. 2.3.2. b)).

1.5. [2+2]-cycloadditions

In order to form a cyclobutane ring via a [2+2]-cycloaddition, two double bonds are sacrificed to generate two energetically more stable single bonds. On the down side, the novel four-membered ring does not allow the carbon atoms at each corner to adapt to their preferred sp^3-configuration with interbond-angles of 109.5°, which causes this reaction to be endothermic. The substituents therefore have strong electronic and steric influences on this strained ring and create a stereochemic oriented, regioselective product distribution. Generally, the reaction mechanism is regarded to be pericyclic and concerted, which includes the scission and creation of chemical bonds within one step. The formation of side products is avoided, as is generally the case for cycloaddition reactions. The theory for these reactions, whether it be [4+2] (so called *Diels-Alder* reactions) or [2+2] electron reactions, was installed by *Woodward, Hoffmann* and *Fukui*.[23] The energy and orientation of the frontier orbitals are most important for the consideration whether such an addition will happen. In each case the highest occupied molecular orbital (HOMO) of one substrate reacts with the lowest unoccupied molecular orbital (LUMO) of the second one. To gain binding interactions, the orbital lobes of the frontier orbitals have to have matching polarities and should have a comparable size or amount of energy. When the polarity of the orbital lobes within the transition state is in phase, it is a suprafacial alignment and if the polarity is asymmetric, it is an antarafacial arrangement. With a thermal induced [2+2]-cycloaddition-reaction a suprafacial orientation of the molecules is forbidden and an antarafacial orientation is allowed, but very improbable due to steric hindrance of the substituents in the orthogonal configuration (Figure 8). Only through high temperature reactions or within confinements are products formed this way.[24-26]

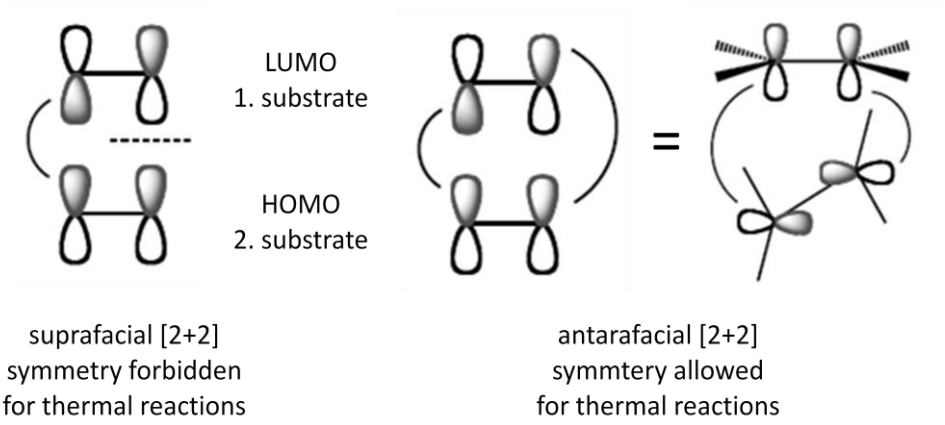

Figure 8: Thermal [2+2]-cycloaddition only allowed with antarafacial geometry.

On the other hand, the suprafacial [2+2]-reaction can be conducted with light. One substrate is photo-chemically excited by promoting one electron of the HOMO into the LUMO, creating two single occupied molecular orbitals (SOMO). This activated molecule then can react with a ground state molecule in its reach (Figure 9).

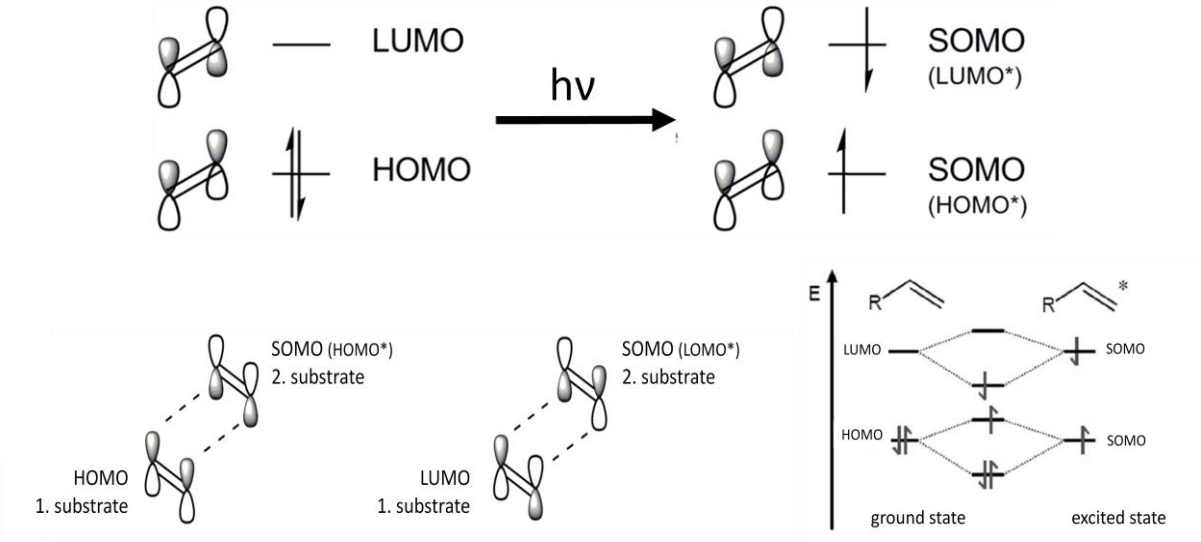

Figure 9: Photo-excitation and interaction between double bonds.

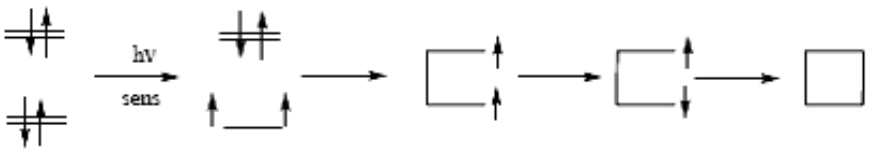

Figure 10: Biradical mechanism.

In reality though, this reaction might not be concerted or overly stereoselective, but can proceed via the formation of a 1,4-biradical intermediate (Figure 10). This concept was first introduced in 1970 by *Bauslaugh* and exhibits a triplet state, of which its stabilization and life time are of utmost

importance.[27,28] The more stable these radicals are, the more thermodynamically favored are the products. After a concept of *Viehe* a radical can be stabilized by adjacent electron-donating (d = dativ) and electron-accepting (c = captiv) groups. This combined capto-dativ effect of both groups can lower the energy of the radical by up to 25 kJ/mol and can thus have an impact on the speed of the reaction, as well as the isomer formation (Figure11).[29,30]

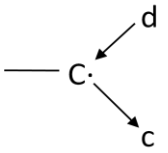

d = EDG: -NH_2,-NR_2, -OH, -OR, -R
c = EWG: -NO_2, -COOH, -COR

Figure 11: Capt-dative effect for radical stabilization.

When coumarin, as an aromatic or conjugated enone is excited and it is quenched with an olefin, a cyclobutane ring is formed. Guidelines for these addition-reactions have been set up by *Turro*:[31]

1. The enone will react out of a T^3-state, which can have n,π^*- or π,π^*-configuration.
2. Electron deficient olefins react slower than electron rich ones.
3. The addition of electron rich olefins is regioselective.
4. The reaction causes the loss of the configuration of the olefin.

1.6. Photochemistry of coumarin

Coumarin is a fragrant substance found in many plants. It has been used for photochemical reactions for over 200 years, by simply exposing solutions of it to sun light for extended periods of time.[32] Depending upon the loci and the electronic nature of its substitutions, the wavelength needed to dimerize coumarin via a [2+2]-cycloaddition can vary from around 300 up to 350 nm.[33-36] The reversible cycloreversion reaction regenerates the coumarin. The reversibility requires shorter wavelengths below 300 nm of about 250 nm, because the conjugated system is discontinued. Varying the radiation wavelength can therefore be used to make or break bonds and switch between monomer and dimer (Figure 12).

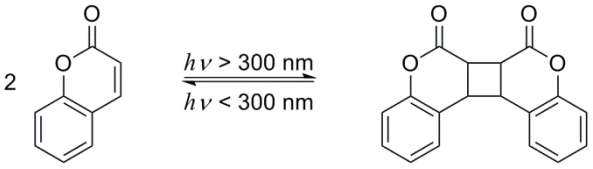

Figure 12: Photochemical dimerization or cycloreversion of coumarin.

The dimer molecules can have four stereo-isomeric forms (Figure 13).[37,38] The selective formation of any one of these four possible stereoisomers can depend upon the polarity of the solvent, the addition of sensitizers, and steric preference.[39,40] In nonpolar solvents the excited singlet state is insufficiently stabilized, resulting in low yields. Through inter system crossing or with the addition of a sensitizer, coumarin is promoted into a triplet state, which reacts to a 1,4-biradical. The stabilization of this biradical then predominantly determines the formation of either the syn- or the anti-hh dimer. In polar solvents the excited state prefers the assembly of syn-hh dimers. Through the addition of Lewis acids, such as borontrifluoride, the anti-hh form can again be favored.[41] The distribution of the isomers, of which three out of four are generally formed, can be distinguished with NMR-spectroscopy.[37]

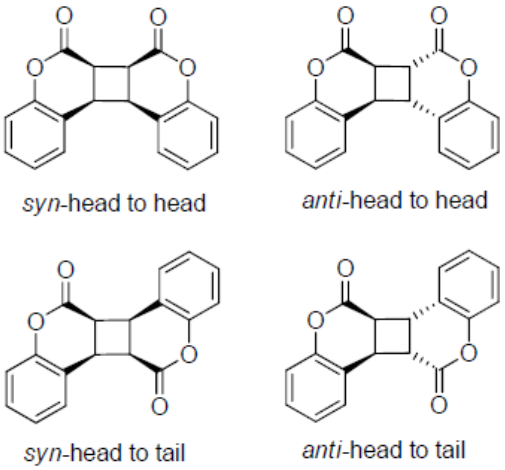

Figure 13: Stereoisomers of coumarin homodimer.

The common synthetic approach to form cyclobutane derivates is via photochemical [2+2]-cycloadditions. The earliest reports of [2+2]-photocycloadditions for the synthesis of coumarin homodimers even date back before *Woodward and Hoffmann's* pioneering work[42,43; 37] in which they introduced a general concept of the mechanism in 1969. Since then, the synthetic applications have increased and studies on mechanistic,[27] stereoselective,[44,45] regioselective,[46-48] and enantiomeric[49,50] aspects were done. Coumarin is one of the prime molecules for photo-cycloadditions. The homodimerization reactions of coumarins have been thoroughly examined with respect to solvent dependency and stereoselectivity.[51-55] Furthermore, the reversibility of this reaction has been investigated, resulting in practical applications for photoactive materials.[56-59] Recent approaches attempt to locally change the refractive index[60] or the fluorescence.[61,62] Improvements have been reported by forcing the reactions into a confined space, adding a Lewis acid, or applying an individual and specialized catalyst.[63-66] One newer development is the employment of coumarins as functional building blocks in light-triggered drug delivery devices.[67,68] Whereas the above mentioned examples study homodimers (HD) of two identical molecules, so

called crossdimers (CD) or heterodimers with two diverse components have been studied comparatively seldom.[69-74] Versatile applications make crossdimers very appealing,[75] but in general the yields of the crossdimerization reactions are low, because the homodimerization is mechanistically favored.[76] Coumarin crossdimerizations need lengthy reaction times and the crossdimer yield is a challenge. Only with a sensitizer like benzophenone, or the availability of a directing coordination site does the yield rise.[77-80] The problem with intermolecular crossdimerization reaction in solution is that the homodimerization of the activated species is often the dominant reaction. It is therefore important to find ways to generate crossdimers quickly and efficiently.

With the addition of 1-heptanoly-5-fluorouracil (H5FU) to 7-*tert.*butyldimethylsilyloxycoumarin (TC), crossdimers of the two components can be formed in four stereoisomeric forms (Figure 14). Generally, only two or three stereoisomers are formed, depending on the velocity of the reaction and the influence of additives.

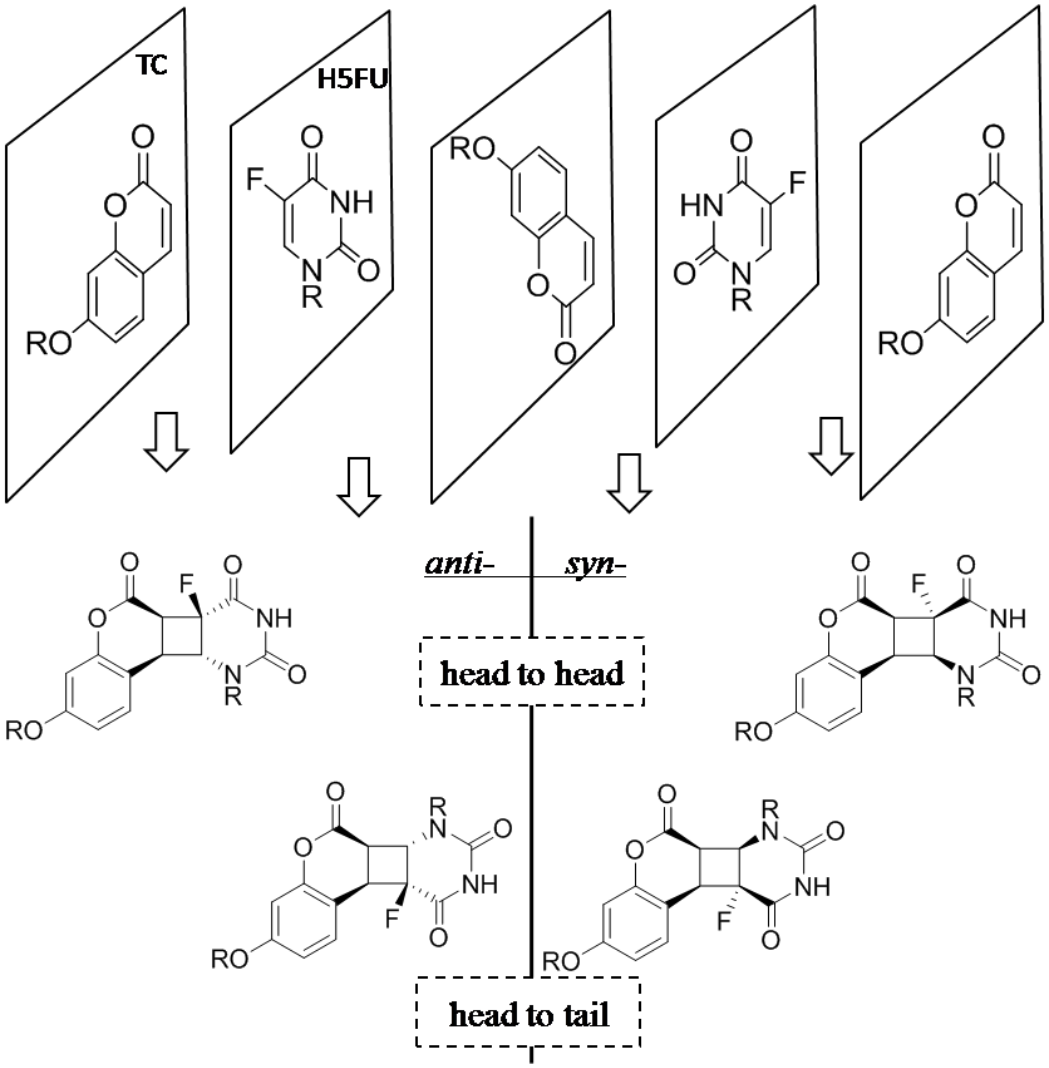

Figure 14: Stereoisomers of crossdimers TC-H5FU and formation from substrates.

The dimerization reaction is completely reversible, as long as the lactone ring of the coumarin has not opened. The ring strain of the cyclobutane ring facilitates the opening of the lactone ring by nucleophiles, like hydroxide ions, amines, or primary alcohols. This concludes the possibility of an unsymmetrical photo cleavage and loss of reversibility.[81-84]

1.7. Cyclobutane structures in nature and for synthesis

The cyclobutane motive appears in a variety of bioactive natural products, such as caryophyllene, grandisol, lineatin, and others.[85;75] They are secondary natural products and are less abundant than naturally occurring cyclopropanes. In general, they belong to the family of terpenes. The TC-H5FU crossdimer focused on in this work can be called a cyclobutane containing alkaloide. Nature uses enzymes, photoisomerations, and oxidative ring closure reactions to build up these four-membered rings.[86] However, a big part of the existing cyclobutane molecules has been created artificially. Nowadays, they are intermediates on the synthetic routes to more complex molecules. With ring opening or ring enlargement reactions a variety of sequential molecules can be created and cyclobutane molecules can be used to produce amino acids, peptides, and nucleosides.[87] What makes the cyclobutane so special, is the fact that it consists of a pair of the few chemical bonds that can be specifically and selectively formed or cleaved with light or heat. Both methods will be depicted in this thesis.

1.8. Advantage of crossdimerization / motivation

The cornerstone of this work is the drug release out of intraocular lenses with laser irradiation to cure secondary cataract. The key ingredient in this photoactive material is the photoactive crossdimer. Especially the build up of these dimers is difficult. Loading the linker functionalized polymer with the drug molecule proofed to be impractical, because of cross linking within backbone. The best and most direct method is to generate the crossdimers and to covalently bind them to the material. My overall goal therefore is to efficiently produce dimers with two different parent molecules. In the literature, only a few examples exist of the formation of crossdimers in solution. Generally, the homodimer formation is the predominant response for intermolecular reactions. In case two distinguishable chemicals in solution are used, the homodimerization is inevitable occurring

besides the requested crossdimerization. In principle, the homodimerization is the preferred reaction, because of equal orbital size/energy and geometry and π-stacking of benzene rings and other aromatics. To favor the crossdimerization, most often the photo-inactive component is already used as the solvent. This substrate thus has to be cheap or available in a great amount, while the work up becomes difficult.

To employ the facile homodimerization to generate photoactive materials has been seized in a vast number of publications with different applications (s. 1.6). So why would crossdimerization be desirable, when it seems more cumbersome? The answer is simple, because like the depiction of the word crossdimer, the final dimer will to some extent have a crossing/combination of the properties of the parent molecules. It will have a different polarity, which is important for its solubility. Crossdimers will also have a much greater variation in size. This presents itself in steric hindrance, different diffusion constants, and molar volumes (interconnected to the refractive index). Moreover, the dipole moment of the final dimer molecule can be influenced better to vary its absorption wavelength and to produce a faster reaction and good quantum yield. This is relevant for the two photon cleavage reaction of the drug release and because of the fact that there are only a small number of available laser wavelengths.

In essence, the direct approach to combine molecules, rather than to modify the photoactive linker molecule, requires less synthetic steps, encountering fewer problems. That way, an ordinary photolinker can be used and only the reaction parameters need to be adjusted to manufacture crossdimers with desired characteristics. This concept is feasible for a wide quantity of crossdimers, which are clearly more diverse than the number of available linker homodimers. With regards to the coumarin based photoreactions, on which my work is based, a number of physical and chemical properties can be induced in order to deduce reaction dependent information and to obtain specific products.

The goal is to find the best set up for a photo-reaction, to conduct it, to steer it, and ultimately to use photochemistry as commonly as familiar organic routines.

2. Results and discussion

The main body of this work features photo-reactions with a predominant synthetic objective. Even more specific, photocycloadditions or photocycloreversions are the most frequently mentioned reactions. My chief goal is the intermolecular crossdimerization in solution. This synthesis is a complex reaction which has a simple mechanism and still is difficult to put into numbers. How fast, how much, or how frequently is many times not answered in publications, a simple yield must unfortunately oftentimes do. The question therefore needs to be answered why this reaction is so complicated.

First and foremost, the 3-dimensional activation of molecules is something thermal reactions do not claim, as long as the heater is on and the stirring is vigorous, activation is of no particular importance. In contrast, the number of photons and their spatial distribution is crucial to photoreactions. Constantly varying concentrations also influence thermal reactions but make studying photoreactions immensely difficult. The trouble of several different time regimes for the excitation, diffusion, and collision process of the molecule to form a product, maybe via a biradical intermediate, is challenging to say the least. These intermediates and transition states want to be stabilized, so an energy quenching solvent is more harmful than with a purely heat driven reaction. Together, everything accumulates in a temporary balance between physics and chemistry. The following Figure 15 a) gives an overview of parameters that can be varied and that can be read out during, or after the reaction.

All reactions conducted in solution follow a standardized synthesis pattern, which is given in section 3. Every method explored in the next chapters uses this pattern if not stated otherwise. Specifics for the reaction are given in their respective paragraphs. An overview of the matrix of variables that have been examined is shown in Figure 15 b), with the most important variables in green highlights.

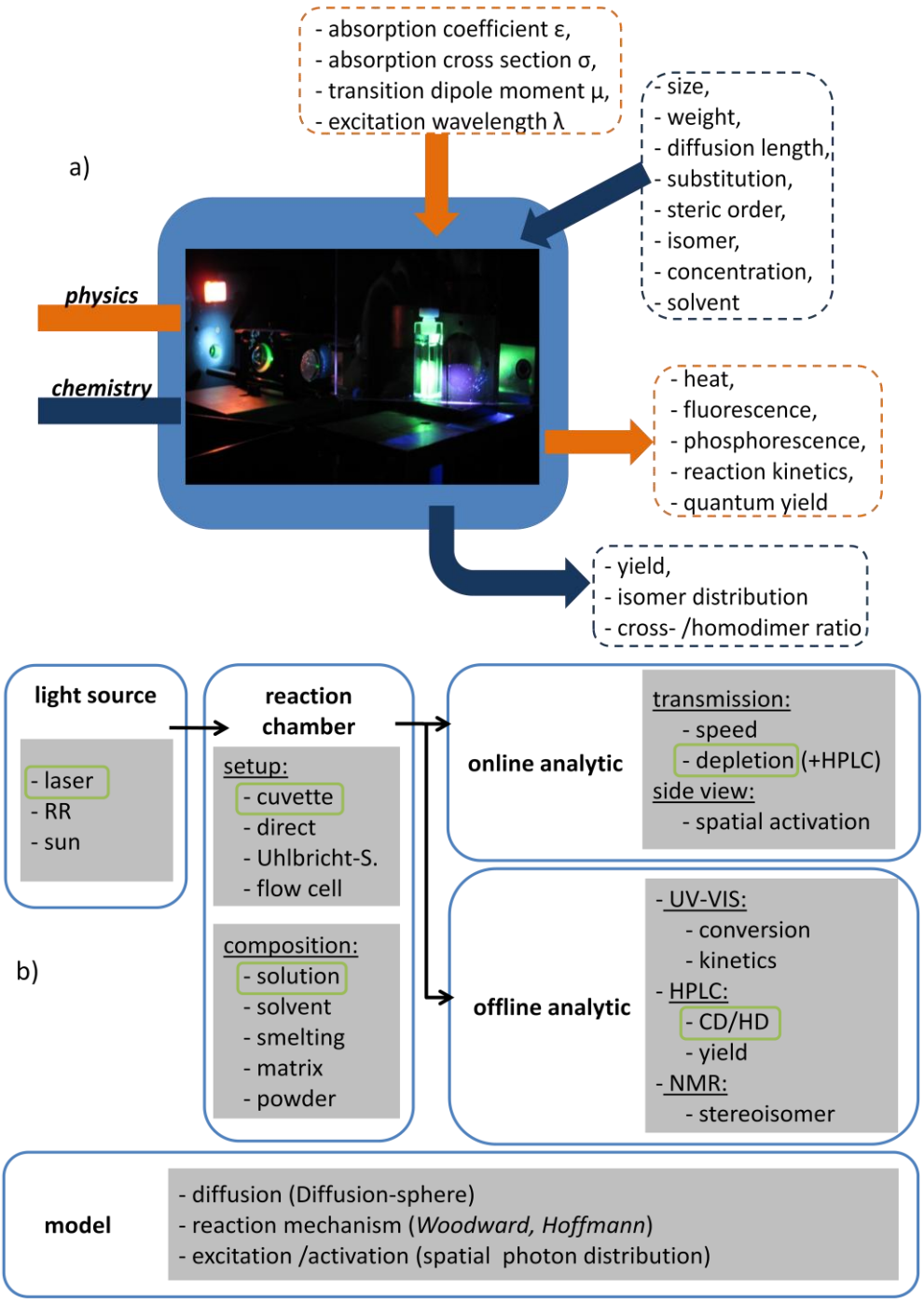

Figure 15: a) Theoretical interaction of physics/physical chemistry and chemistry in photochemistry; b) Matrix of experiments, analytics, and models - green highlights the standard method.

The main part of this thesis is divided into five parts. First is the **composition** of the material that is going to be irradiated. Than the **excitation** of the photoactive substance is studied, before the investigation of the **reaction** itself and of how the energy is used. The **reversibility** of some reactions is important and practical, whereas **derived reactions** demonstrate versatility.

2.1. Composition

2.1.1. Different assemblies

#	Composition	Comment	Picture	A / TBS-Cum B / monomer solvent
I	A in solvent B	• B needs to be a liquid or liquefiable (less variety); • A has to be soluble in B (varying diffusion distances); + high concentration of A (good chance of exclusive crossdimer formation)	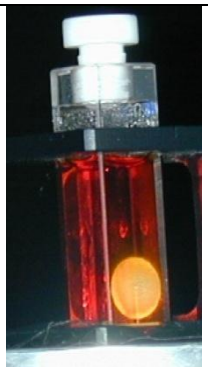	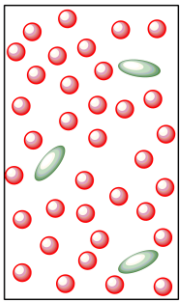 A dissolved in B
II	A and B in solution	• A and B have to be soluble in solvent in high concentrations + common synthetic approach; easy to work with; lots of combinations		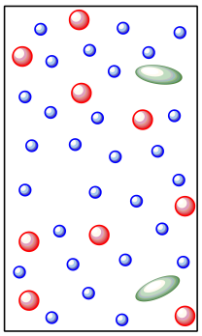 solution
III	A, B in matrix (polymer/film)	• deficient yield because of geometrical strains; low CD/HD ratio + quick reaction in both ways; predetermined allocation	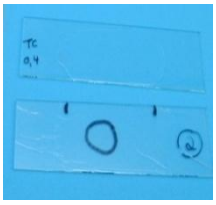	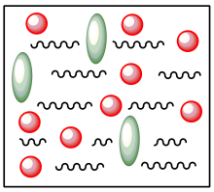 film
IV	smelting of A,B	• one of the substances has to be meltable; (preferably eutectic) + laser can also deliver heat		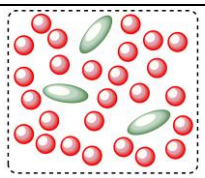 smelting
V	powder mixture of A, B	• inhomogeneous blend; bad heat distribution + quick and easy		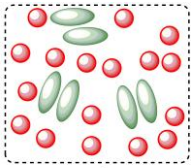 powder

Table 1: Different assemblies of substrates with varying states.

The intermolecular formation of crossdimers constitutes the core of this research. In an abstract sort of way, it will be helpful to define an excitable linker as simply A. This entity will absorb the light and undergo a photo-reaction, making it the premium ingredient in the reaction mixture. The ground state (non-laser absorbing) reaction partner or quencher will be nominated as B. Therefore, if A and B are present, the strict photoaddition-reaction could yield AA homodimers and AB crossdimers in all kind of isomeric forms. Even though A is most often represented by coumarin, or some kind of its variations, the methods demonstrated further down apply to any kind of species A. The same holds true for the manner of the reaction, which is a photoaddition and prevalently a [2+2]-cycloaddition, which can be transferred to all sorts of photoreactions. There are several ways to assembly a photoreaction for the synthesis of crossdimers. Table 1 presents an overview.

It is a question of reason whether one uses a solvent as in case No. II or prefers to omit it. The reality is that the majority of chemical reaction is still made in solution and the kinetics, as well as the heat distribution are much better understood. The entire reaction is easier to handle and most analytical practices, like HPLC and NMR, also require solutions. These methods work and I have used them all, but No. II excels. Assemblies No. III-V are better for changing material properties than drug release, whereas No. I shows the highest yield, but can only be used for a small number of combinations.

2.1.2. Different concentrations

To favor the crossdimerization, an excess of the non-activated reaction partner is obviously helpful. Therefore, concentration assays of 20 mM TC and a varying H5FU multiple of 1 up to 10 dissolved in acetonitrile were made. Therewith, the chance of an activated coumarin molecule to react with H5FU rather than with another coumarin increases, because of shorter required diffusion distances. The following graph shows a row of 10 experiments analyzed by HPLC. Only above a 3.3 time surplus does the dimer ratio favor the crossdimer (Figure 16). This indicates coumarins strong desire to form homodimers, which might be the result of π-stacking and its valence orbital size and density. In general, the yields of the crossdimerization reactions in solutions are low. Improvements require special additives and confinements (s. 1.6).

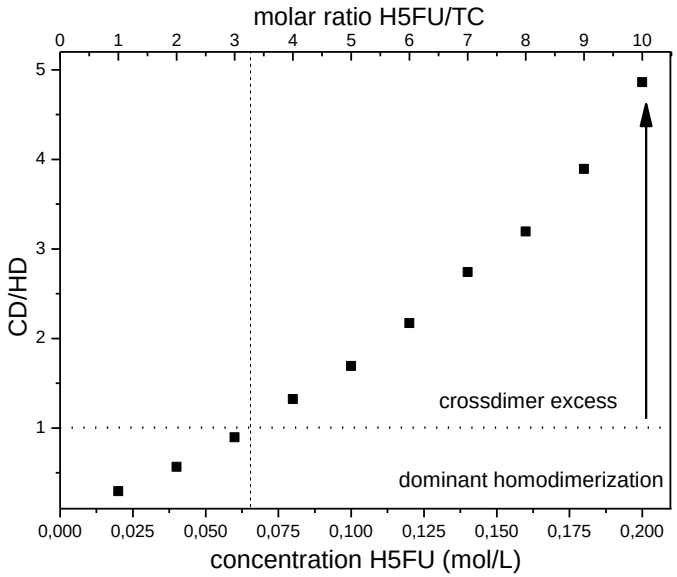

Figure 16: Crossdimer (TC-H5FU) to homodimer (TC-TC) ratio after 20 min irradiation at 0.7 W, with a varying molar ratio of H5FU to TC. A crossdimer excess is observed only above a 3.3:1 ratio of H5FU over TC.

In addition to a crossdimer preference, the excess H5FU increases the velocity of the reaction and shortens the reaction time needed for a complete turnover of TC into dimers.

The next graph represents a transmission measurement behind the irradiated cuvette. The more TC is worked off, the more light will pass through the cell. This measurement thus poses an online concentration monitoring like in a UV-VIS measurement and allows for the determination of a completed reaction (Figure 17). If the conversion percentage values at a fixed time (420 s) are plotted against their respective concentration, it is clear to see, that an almost linear dependence exists (Figure 18). This is not too obvious considering that the concentration differences work in three dimensions of the reaction volume and any kind of collision with a molecule can cause quenching. The graph indicates a weak interaction of the ground state molecule H5FU with the activated TC*. A ten fold excess only increases the reaction to three times the speed, and in order to double the reaction speed roughly five times more partner substance B has to be added. An effective set up that will produce a fast reaction hence is relevant.

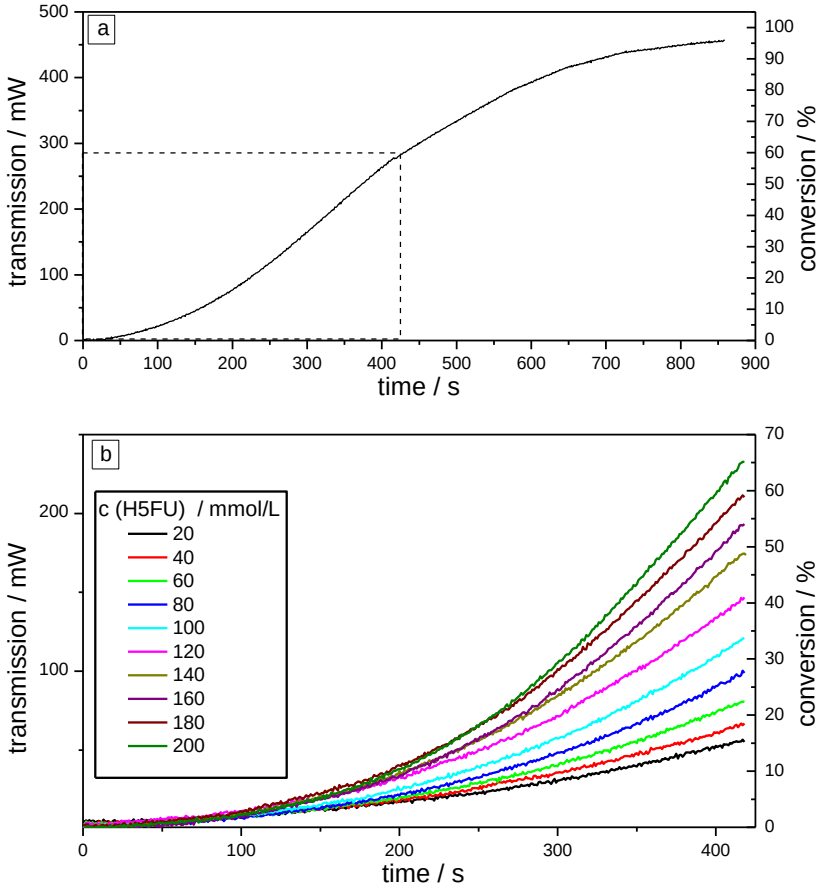

Figure 17: Laser transmission depending on reaction time. a) Indirectly linked to the concentration of TC, the transmission reflects the TC conversion. b) Enlargement of dotted rectangle from above. Increasing H5FU concentration results in improved reaction rates and in more transmission.

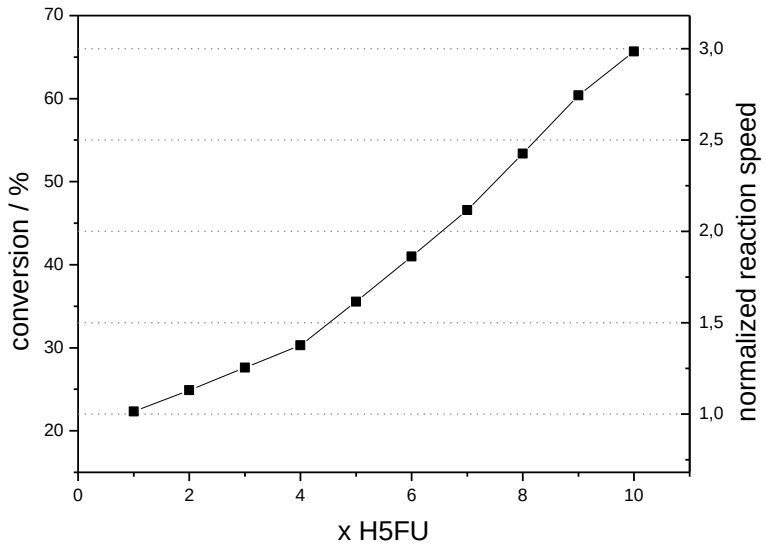

Figure 18: Conversion % at 420 s of reaction, indicating the TC turnover ~ reaction speed.

2.1.3. Diffusion

An interesting aspect, which I like to consult in my line of reasoning, is the diffusion of substances within another component or solvent, called heterodiffusion. The heterodiffusion coefficient D can be calculated with the following empiric formula, introduced by *Wilke* and *Chang*:[88]

$$D = 7.4 \cdot 10^{-8} \cdot \frac{T \cdot \sqrt{C \cdot M_2}}{\eta \cdot V_1^{0.6}} \tag{5}$$

In this formula the T is temperature (300 K), C the association factor (ACN: 1.2; DCM: 1.2), M_2 the molecular weight of the solvent (ACN: 41 g/mol; DCM: 84 g/mol), η the dynamic viscosity (ACN 0.35 mPa·s; DCM: 0.43 mPa·s at 22 °C), and V_1 the molar volume of the diffusing molecule (TC: 800 cm³/mol). With this diffusion coefficient and the lifetime τ of the excited molecule, the average 3-dimensional diffusion length Δx, can be calculated:

$$\Delta x = \sqrt{6D\tau} \tag{6}$$

Therewith, it is possible to determine the diffusion volume V in form of a sphere:

$$V = \frac{4}{3}\pi \cdot \Delta x^3 \tag{7}$$

Within this diffusion sphere the excited molecule can then find N reaction partners with:

$$N = c \cdot V \cdot N_A \tag{8}$$

Table 2 lists all values for both primarily used solvents and an excited lifetime for TC of 1 µs.

solvent	D / m²/s	Δx / m	V / m³	N(TC)	N(H5FU)
ACN	$8.06 \cdot 10^{-10}$	$6.95 \cdot 10^{-8}$	$1.41 \cdot 10^{-21}$	17000	170000
DCM	$9.39 \cdot 10^{-10}$	$7.51 \cdot 10^{-8}$	$1.77 \cdot 10^{-21}$	21000	210000

Table 2: Heterodiffusion values.

There are more reaction partners in a diffusion sphere with DCM than with ACN, which should result in a faster reaction. The transmission intensity behind the cuvette can be regarded as indication for the turnover, because of the decreasing TC during the dimerization reaction. In Figure 19 can be seen how the reaction in ACN somehow starts faster, before the DCM reaction catches up and ends up being the faster one. Apparently, the irradiated volume in the ACN takes longer to be refilled with ground state molecules from the surrounding reservoir. (More on the depletion of the irradiated volume in chapter 2.2.5) The DCM reaction is faster but produces less crossdimer (Table 3).

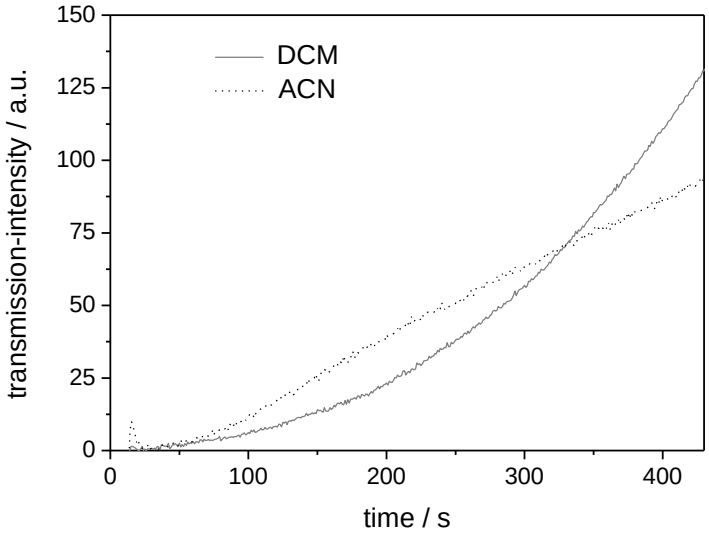

Figure 19: Transmission of reactions in different solvents.

solvent	TC/H5FU /mM	time / min	yield / %	CD/HD
ACN	20/200	10	95	3.0
ACN	20/200	20	100	4.0
ACN	10/100	10	88	2.5
DCM	20/200	10	100	2.6
DCM	10/100	10	100	2.0

Table 3: Different reaction times in different solvents.

The isomer distribution varies as well, because of the varying electronic stabilizing effects of the solvents for different intermediate states (Table 4).

solvent	syn ht	syn hh	anti ht
ACN	4.2	3.2	1
DCM	3	1.4	1

Table 4: Stereoisomer distribution of reactions in ACN and DCM.

The solvent thus is a key component of the mixture and can change the speed and outcome of the photoreaction.

2.1.4. Triplet promoter / additives

The term triplet promoter is not a standard term. I use it to refer to any substance which, added to the reaction mixture, will promote molecules into their triplet state. These molecules are any kind of organic sensitizer or molecules utilizing the heavy atom effect.[89-91] The heavy atom effect has been most prominently measured with iodine, bromine and a number of brominated chemicals. Defined by IUPAC it is: „The enhancement of the rate of a spin-forbidden process by the presence of an atom of high atomic number, which is either part of, or external to, the excited molecular entity. Mechanistically, it responds to a spin-orbit coupling enhancement produced by a heavy atom."[92] Within my diploma thesis I could already show that the addition of organic sensitizers or inorganic additives does not necessarily improve the number of triplet molecules. The organic sensitizers have big absorption cross-sections and get destroyed by the intense laser, generating unwanted debris. The inorganic metal salts probably do not evoke a strong heavy atom effect, but can use coumarin and H5FU as ligands and play more of a coordinating role. This leads to different isomer mixtures but does not affect the coumarin triplet state.

heavy atom substance	radiation time / min	yield / %	cross-/homodimer
-	10	95	2.9
dibromoethane	10	95	3.2
bromanisole	10	94	3.3
bromoehtylbenzene	10	97	3.1

Table 5: Laser reaction in ACN inside 2mm cuvette with 0.01 mol/L bromo-substance.

The heavy atom effect itself was tested by adding bromide-containing substances to the reaction mixture. Table 5 summarizes the outcome. No significant improvement of the triplet state population and the therefrom produced crossdimers can be detected, which would vindicate the addition of a heavy atom substance. In order for these substances to work, they have to be in close proximity of the coumarin, or have to form a complex therewith. In solution, without confinement, the contact time between these two molecules seems to be too short-lived.

Another complementary find is the addition of *Lewis* acids to the reaction mixture. Already proven to support coumarin dimerizations, three acids were tested.[41,54]

***Lewis* acid**	**homodimer / remaining TC**	**crossdimer / homodimer**
-	1.0	2.8
$SnCl_4$	0.68	3.6
$ALCl_3$	0.42	3.2
$BF_3 \cdot OEt_2$	0.78	3.6

Table 6: Addition of *Lewis* Acids.

Again, the strong laser also obliterated any additional effect the *Lewis* acids could have (Table 6). The dimer ratio did improve, but the TC turnover stagnated and a number of unidentifiable side products were generated.

In summary, no additive seems to improve a high intensity laser reaction, which is convenient and economical, maintaining a simple reaction mechanism, which causes less side products.

2.1.5. Different crossdimers

It is important to notice the versatility of the synthetic practice which is presented throughout this thesis. With just a single linker molecule, like the protected hydroxycoumarin species (TC), a wide variety of crossdimer molecules can be fabricated. These molecules can be different in size, polarity, and shape or reaction efficiency. The choice is only limited by their absorption, solubility, and concurrent side reaction with biradicals. The issue of absorption will be discussed in a later chapter (s. 2.2.1), whereas the other two are apparent. The following Table 7 gives several examples of molecules that form crossdimers with TC.

A number of factors determine the outcome of a dimerization reaction, so there is no clear cut answer to which substrate will work. In the table below is a variety of big monomers, closed rings, open chains, mono-/di-and tri-substituted double bonds, and different functional groups. In comparison, small molecules and rings work better than open chains (M11, 12), sterically hindered molecules are less reactive (M16, 17), and alcohols barely work (M5, 14). The quinones (M1, 2) work well because of their radical catching ability. Other quinones were also tested but it was not clear whether a cyclobutane or single bond conjugate was formed. Altogether there is an endless number of crossdimers with unique characteristics.

monomer (M #)		chemical structure	$M_{monomer}$ $M_{crossdimer}$ / g·mol^{-1}	mass by LCMS	CD/HD	yield CD / %
1	2,6-dimethyl-*para*-benzochinone	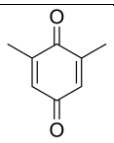	136; 412	413 (M^+ + H) 475 (M^+ + K + Na + H)	1.0	10
2	2,6-dimethoxy-*para*-benzochinone	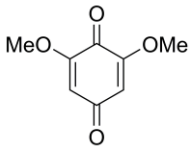	168; 444	445 (M^+ +H) 507 (M^+ + Na + K + H)	7.7	5.7
3	*(E)*-stilbene	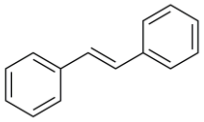	180; 456	525 (M^+ + 3Na) 553 (M^+ + 2K)	10.7	21.3
4	4-hydroxy-stilbene	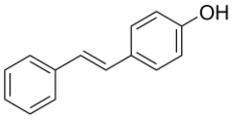	196; 472	496 (M^+ + Na + H) 513 (M^+ + Na + NH_4) 525 (M^+ + $3NH_4$ – H)	4.9	3.4
5	3-phenyl-2-propen-1-ol	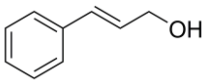	134; 410	583 (M^+ + $M_{Monomer}$ + K) 327 (monomerether + $3NH_4$ + Na)	-	-
6	3-phenyl-2-propenal	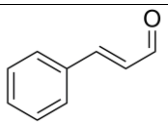	232; 408	507 (M^+ + 4Na + H) 544 (M^+ + 3K + NH_4 + H)	2.1	5.9
7	3-phenyl-2-propenoic acid	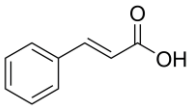	148; 424	469 (M^+ + 2Na – H) 487 (M^+ + K + Na + H) 484 (M^+ + Na + $2NH_4$ + H)	3.7	10
8	4-vinylbenzylchloride	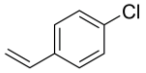	153; 429	469 (M^+ + K)	1.9	6.9
9	trimethoxychalcone	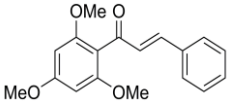	298; 574	637 (M^+ + K + Na + H)	1.1	11.2
10	2,5-furandione	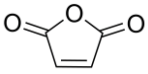	98; 374	415 (M^+ + Na + NH_4) 500 (M^+ + 2K + $2NH_4$) 477 (M^+ + 2Na + K + NH_4)	2.1	12.5
11	*cyclo*-pentenone	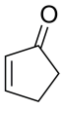	82; 358	382 (M^+ + Na + H)	18.9	13.4
12	3,4-dihydropyrane		84; 360	401 (M^+ + Na + NH_4)	15.6	11.9
13	*N*-vinyl-2-pyrrolidinone	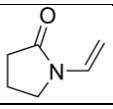	222; 387	452 (M^+ + $3NH_4$ + 2Na + H)	8.3	16.6

monomer (M #)		chemical structure	$M_{monomer}$ $M_{crossdimer}$ / $g \cdot mol^{-1}$	mass by LCMS	CD / HD	yield CD / %
14	4-penten-1-ol	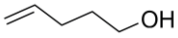	86; 362	363 (M^+ + H) 425 (M^+ + Na + K + H)	0.16	2.8
15	diethyl-*(Z)*-2-butenedioate	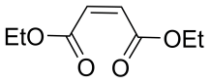	172; 448	511 (M^+ + K + Na + H)	1.04	9.8
16	3-methyl-2-butene-1-ol	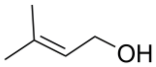	86; 362	423 (M^+ + Na + $2NH_4$ + H)	0.3	2.5
17	3-methyl-2-butenoic acid	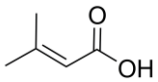	100; 376	502 (M^+ + 2Na + 2K + H) 461 (M^+ + 2Na + K)	0.4	3.8
18	2,3-dimethylbut-2-ene		84; 360	361 (M^+ + H)	7.6	8.6
19	tetrachloroethene	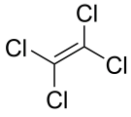	166; 442	443 (M^+ + H) 466 (M^+ + Na + H)	2.6	7.8
20	dimethylthymin	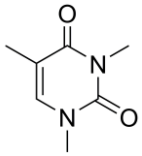	154; 430	471 (M^+ + Na + NH_4) 493 (M^+ + K + Na + H)	2.4	4.5

Table 7: Generated crossdimers.

In case the reaction partner B is a liquid itself and does not absorb 355 nm light, the crossdimerization can also be done, dissolving the TC within the B component and irradiating the mixture. With *N*-vinyl-2-pyrrolidinone and dihydropyrane this procedure is feasible. Increasing the TC concentrations over the common 20 mmol/L is no problem, also increasing the total dimer concentration after the reaction (Figures 20 and 21).

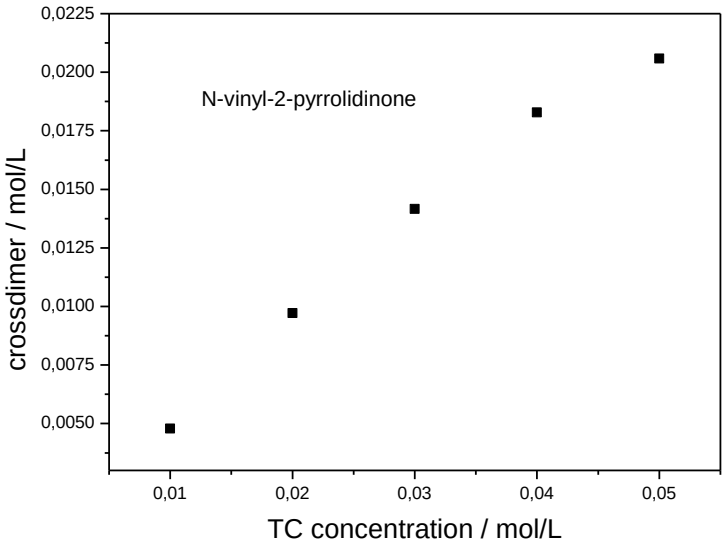

Figure 20: TC-*N*-vinyl-2-pyrrolidinone crossdimerization after 7 min irradiation.

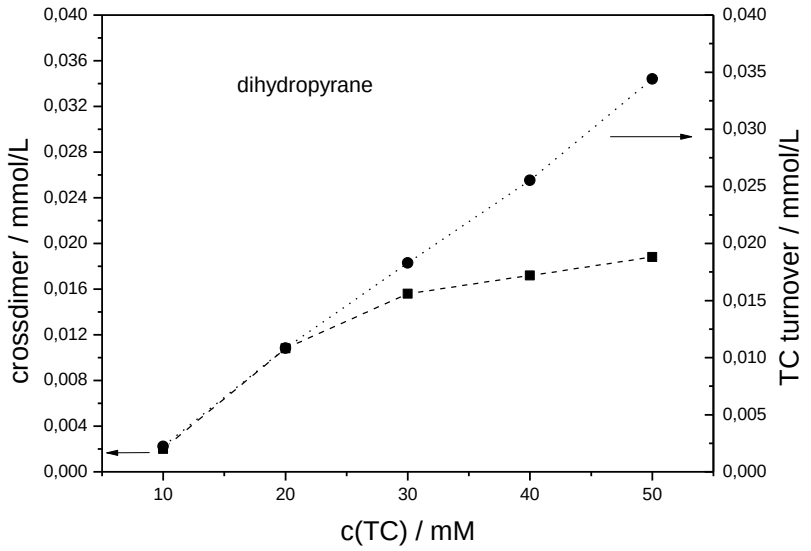

Figure 21: TC-dihydropyrane crossdimerization after 7 min irradiation.

The second crossdimerization is not linear in CD output to TC input, but the TC turnover already indicates (even without HPLC measurements shown here) the generation of homodimers above 20 mmol/L of TC. This again demonstrates the preference of TC to form homodimers even if TC is surrounded by heterodimer-forming partner molecules.

2.2. Activation/excitation

Next to what is put into the reaction vessel and what product one would like to obtain, it is very important to figure out how much and what kind of light will be needed. Light is an evermore sought-after energy source because it can very easily be controlled. Compared to heat it has a direction and electromagnetic force; it is quantized and can be aligned, tuned, modulated, and measured very well. It allows me to selectively excite molecules and to specifically activate certain photo-reactions.
In theory, a light driven reaction has a by one increased reaction order; that is to say with the addition of the photon. The number of photons and their distribution within the cuvette thus is decisive. No other variables, such as the solvent or the temperature, have as much influence on the outcome of the reaction. This section then will expose the intrinsic core values of photochemistry; how they can be measured, what can be learned, and how a photoreaction can be steered.

2.2.1. Light source

The light source is crucial for any kind of photochemical reaction. It determines how and how strong the reaction vessel will be irradiated. Every kind of light source comes with its advantages and limitations. But it is vital to utilize the unique parameters to best perform a light driven reaction. Light is very manageable, so that the ideal photoreaction selectively excites one molecule entity, transition, or photoreaction.
The three mayor light sources I have used throughout this work are: a 355 nm pulsed laser, a *Rayonet* reactor, and the natural sun light of central Germany. Each emission was measured with a sensor or fiber optic spectrometer. The laser only emits a single wavelength whereas the other two occupy a broader wavelength range. To selectively run the photoreaction it is essential to only excite the linker species. Figure 22 also displays the absorption spectra of TC, H5FU and their homo- and crossdimers. In order to make sure that no side reactions or cleavage reactions occur, only the coumarin substrate needs to be activated. Therewith, the dimer formation of the partner uracil is avoided. The laser also differs from the broad band emitter in that it has a hard excitation which specifically addresses few micro-states of the coumarin sample. The broad emitters, on the other hand, evoke a soft and broad excitation which can result in different vibration-selected reaction paths and side products.

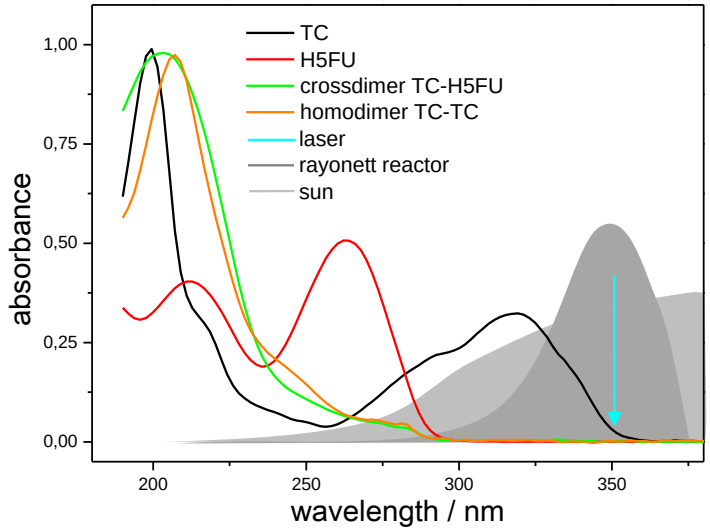

Figure 22: UV-Vis spectra of the substrates TC and H5FU, the homodimer (TC-TC) and crossdimer (TC-H5FU) products. The excitation wavelength of 355 nm is indicated by the blue arrow. Emission of the sun and the *Rayonet* reactor are given in grey. The 355 nm laser exclusively excites the TC contingent.

All three light sources can produce slightly different isomers constitutions. Figure 23 shows how the laser irradiation in DCM has one less isomer (probably the anti hh) than the other two broad band light sources. This might be a result of the faster, more kinetically driven reaction with laser light.

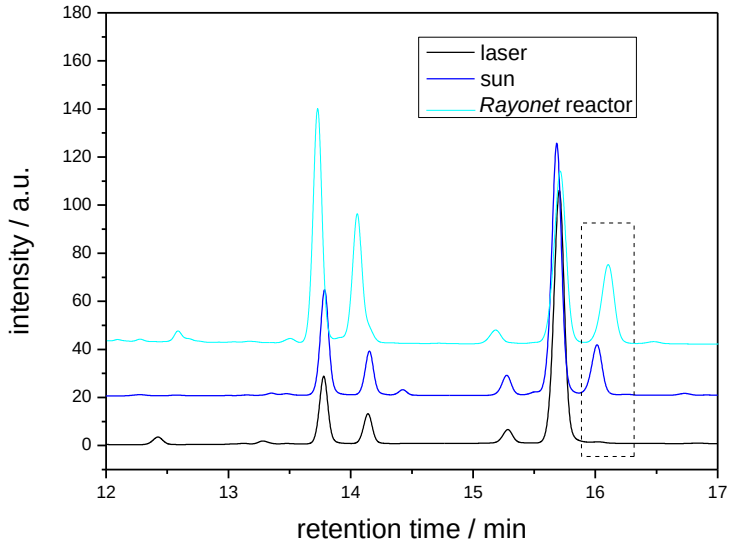

Figure 23: HPLC chromatograms of homodimer isomers from different light sources.

If the three light sources from above are compared, the laser offers by far the highest intensity per area at the required wavelength. The area that can be irradiated is the smallest with the laser, e.g. a cuvette, whereas the photo-reactor can be equipped with around a 1 L flask and the sun is for free and could potentially produce huge amounts. The laser is monochromatic and has by far the best coherence, it is also best when it comes to tunability, while the others are fairly limited in that regard. The low-to-mid intensity broad band light sources might be able to populate charge transfer or varying other excited states. Table 8 gives an overview of the specifics for each light source.

light source	**device**	**characteristics**	**advantages**
laser		- high intensity - monochromatic 355 nm - polarized light - gaussian beam profile - pulse length 20 ns	+ no side reactions + generation of heat + fast
photo-reactor / *Rayonet* reactor / marry-go-round reactor		- mid intensity - broadband (centre at 350 nm FWHM 50 nm) - working temperature 35 °C	+ high volume + parallel experiments
parabolic sun reflector (18 inch, polished aluminum)	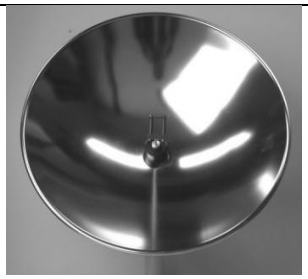	- low intensity - broadband (UV-A - NIR)	+ free energy + heat generation + up scaling

Table 8: Light sources and characteristics.

The high intensity laser can be used to alter the reaction conditions inside of the reaction vessel which will be examined later. The *Rayonet* reactor in general does not deliver a satisfying CD/HD ratio, but can be used to run different batches at the same time. The sun was used as an eco-friendly alternative with future potential and resulted in a very good CD/HD ratio of 16.

As the photon flux is important for the comparison the exact irradiation time of the laser is needed. To determine the pulse length of the laser an ultra fast photodiode was used to measure the peak shape (Figure 24).

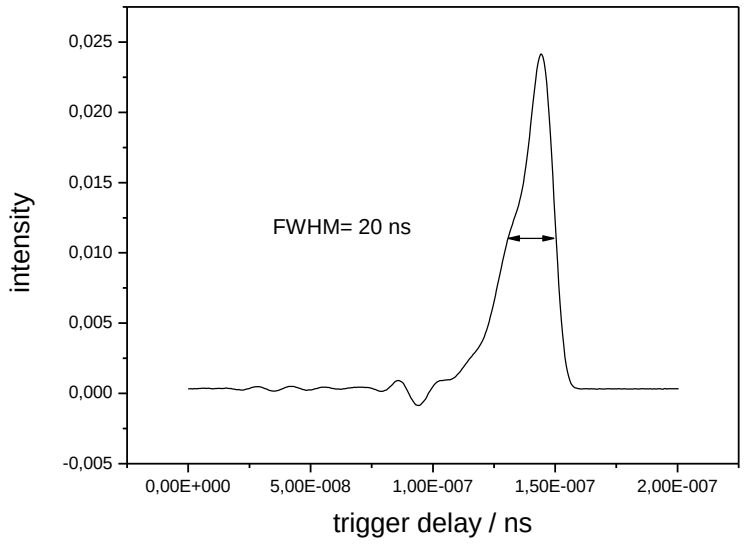

Figure 24: Pulse width determination with ultra fast diode.

To compare the light sources (laser, *Rayonet* reactor [RR] and sun) five criteria are chosen (Figure25): a) The reaction time it takes for a complete conversion. b) The photon flux influences the speed and dimer ratio. c) The volume is important with regard to scalability. d) The variables, which represent the user´s possibilities to influence the reaction. e) The dimer ratio as the general focus of this work.

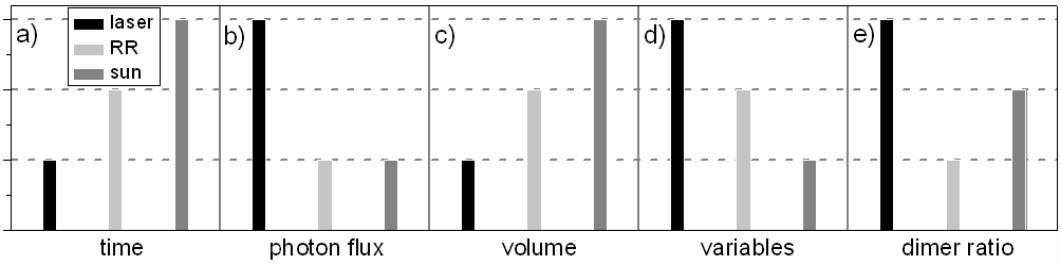

Figure 25: Light source criteria.

a) Additional wavelength

This effect is difficult to measure and enticing in its core proposition. The influence of additional wavelength irradiation during the actual laser treatment is subtle and will only partially alter the outcome of the reaction. It is supportive in order to get an idea of how and why light can be used to operate photoreactions. A schematic set up is presented in the Figure 26. The additional wavelengths are a continuous wave 633 nm HeNe Laser and a blue diode laser with a wavelength range of 380 to 400 nm. Both lasers were directed onto the laser spot of the 355 nm laser with the same polarization at small lateral angles (set up caused).

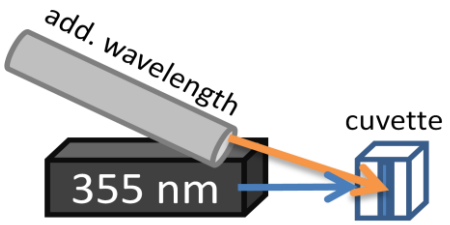

Figure 26: Set up between 355 nm laser and additional laser with equal polarization.

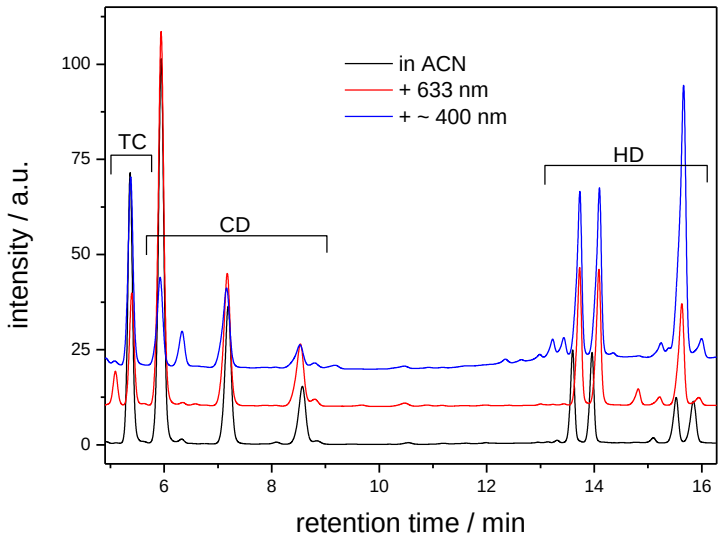

Figure 27: Additional wavelength product distribution in HPLC.

The red light causes the reaction to be more efficient, with a higher crossdimer yield and a predominant formation of the first two homodimers in the HPLC chromatogram (Figure 27). A plausible explanation for this kind of behavior is the orientation of TC molecules due to the continuous electromagnetic field of the red light. This slower frequency works well with movement speed in solution and has been shown in literature to aid preorientation before the laser pulse hits.[93] This can be regarded as an external effect. The blue light on the other hand can have intrinsic influence through charge separation. IUPAC defines charge transfer as: "A process in which, under the influence of a suitable driving force (e.g. provided by photoexcitation), electronic charge moves in a direction that increases the difference in local charges between donor and acceptor sites. Electron transfer between neutral species is one of the most important examples."[94] This intramolecular electron transfer is one of the main types of adiabatic photoreactions. The electronic structure of the ground state is altered and the dipole moment between ground and excited state change. Succeeding relaxation processes such as pyramidalization or planarization, linearization, bending, or twisting etc. cause modification in the electronic structure of the excited molecule. Figure 28 shows that in theory the absorption of a charge separated molecule is bathochromic

shifted, which corresponds to the blue diode laser. For the TC reaction a changed crossdimer isomer distribution of 3:3:1 and unfortunately less turnover can be documented. The extra light probably causes extreme intermediates which do not undergo rapid product formation. Examples can be seen in Figure 27 around the homodimers and in the extra peak at 6.3 min blue line. This shifted charge transfer caused absorption can be used, which has already been shown in experiments for the dimerization of stilbene.[95,96]

In essence light can be used to influence molecules in solution and change their excited state which can result in a change of yield and a variation of isomer distribution. None of these factors are compulsive, because photoreactions are so complex, but it is vital to determine principle tendencies of interactions.

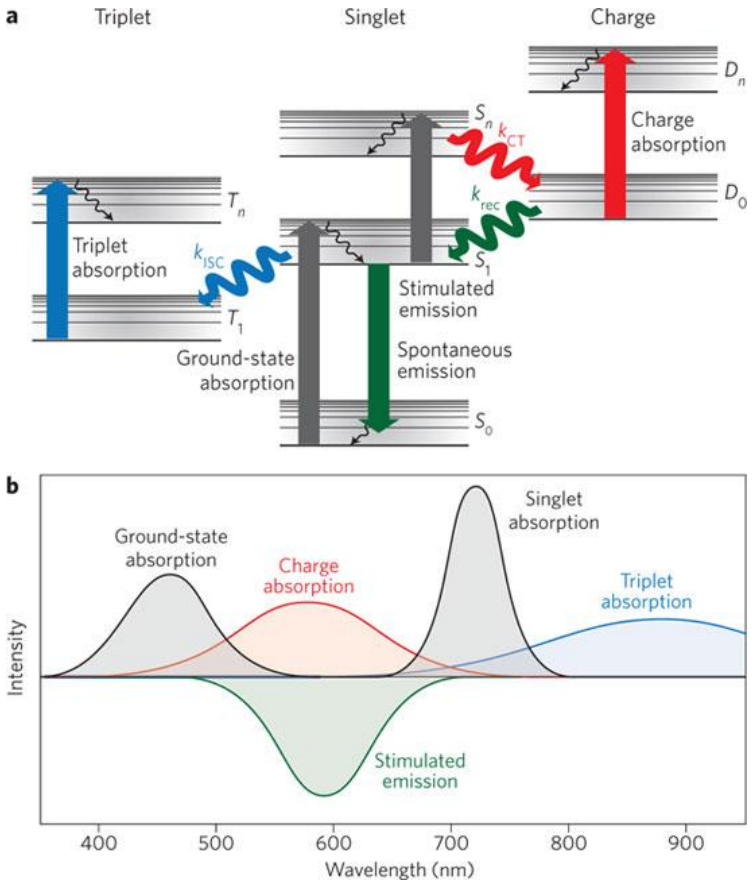

Figure 28: a) *Jablonski* diagram for charge separation; b) Absorption spectra.[97]

2.2.2. Photon distribution

This point is actually ambiguous, not straightforward, or simple. It represents why photons are used, what they feature, and how they are used. One of its key aspects has already been mentioned above in chapter 2.2.1. The specific activation (355 nm) of few sublevels or micro-states of vibration of TC molecules singles out a transition during the absorption process. The result is less side reactions in contrast to broad band irradiation experiments. No B-component dimers or charge transfer side products can be seen. As a reminder: Just the addition of ~30 nm bandwidth, like with the blue diode in the previous section, generated unwanted byproducts.

Next, with this particular wavelength only the wing of the absorption band of TC is targeted and a smaller than maximum absorption cross section is utilized. Therefore, the photons, even though there are less of them than molecules, can enter deep inside the cuvette instead of being absorbed at the laser facing front. The effective reaction volume increases and consequentially the cross-reaction with the ground state partner substrate is favored.

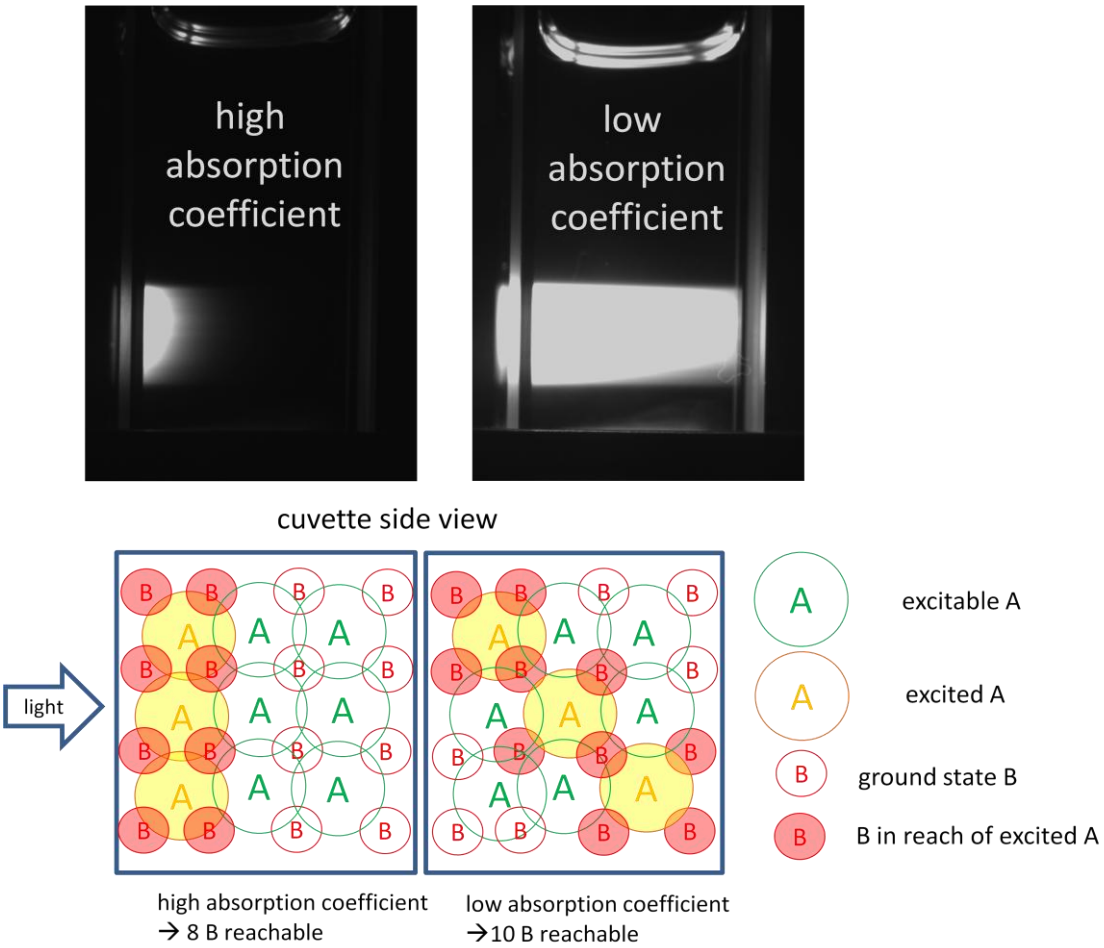

Figure 29: (top) Fluorescence of the laser penetration with high/low absorbing substrate. (bottom) 2D model for crossdimerization probability. The distribution of excited molecules inside cuvette contributes to the crossdimerization preference.

Figure 29 shows a side view of a cuvette with a 5.0 mmol/L high (benzophenone) and a low (TC) 355 nm absorbing substance. At equal laser intensities the light can penetrate the right cuvette much deeper. Below the picture, a model illustrates how a bigger illuminated volume favors the crossdimerization. In case the substrate absorbs the light well, the diffusion controlled reaction can only deliver a slight crossdimer probability. If the substrate instead is low absorbing, then the reaction volume increases and more ground state reaction partners can be reached with an equivalent amount of excited molecules. On the contrary, the dimerization reaction is not very wavelength dependent for a one photon absorption but the two photon absorption will vary with the wavelength because of the very low absorption probability.[98]

Diffusion has already been a topic of interest and continues to be one of the most influential parameters in an intermolecular reaction. For this model to apply, there has to be at least one excited TC* in each of the yellow diffusion spheres from Figure 29. Depending upon the lifetime of the TC* the pulse intensity needed for that varies. However, every intensity value of Table 9 is below the commonly used 66 µJ. Every additional photon over the pulse energy stated results in more than one TC* per diffusion sphere and consequentially in the suppression of the homodimerization reaction by that number. For medium intensities this suppression does not have influence but with high intensities or lower concentrations of TC that effect can be used.

lifetime τ /µs	**distance Δx / m**	**TC in sphere**	**pulse intensity for 1TC* per diffusion sphere / µJ**
1	$7.0 \cdot 10^{-8}$	$1.7 \cdot 10^{4}$	39.3
2	$9.8 \cdot 10^{-8}$	$4.8 \cdot 10^{4}$	13.9
5	$1.6 \cdot 10^{-7}$	$1.9 \cdot 10^{5}$	3.52
10	$2.2 \cdot 10^{-7}$	$5.4 \cdot 10^{5}$	1.24
20	$3.1 \cdot 10^{-7}$	$1.5 \cdot 10^{6}$	0.44
30	$3.8 \cdot 10^{-7}$	$2.8 \cdot 10^{6}$	0.24
50	$4.9 \cdot 10^{-7}$	$6.0 \cdot 10^{6}$	0.11
100	$7.0 \cdot 10^{-7}$	$1.7 \cdot 10^{7}$	0.04

Table 9: Required pulse intensity for adjacent occupied diffusion spheres to have one TC*.
(Calculated with *Lambert Beer law* and ε = 990 L/mol·cm)

So far, I have recorded the spatial distribution of photons within the reaction chamber. Now I want to change viewpoints and look at the photons themselves. A single photon is characterized by its direction, wavelength, and polarization. Regular non-polarized light has an even angular distribution over all electric field vector directions. Laser light however is polarized and just has one polarization. Coumarin, like any bigger, asymmetric organic molecule has a considerable dipole moment. The best light-molecule interaction exists when the dipole moment of the transition is aligned to the polarization of the light. Deviations thereof follow the distribution of the *Malus´* law. In solution the

rotational distribution of coumarin is isotropic. A non-polarized laser pulse therefore should exhibit an increased yield.

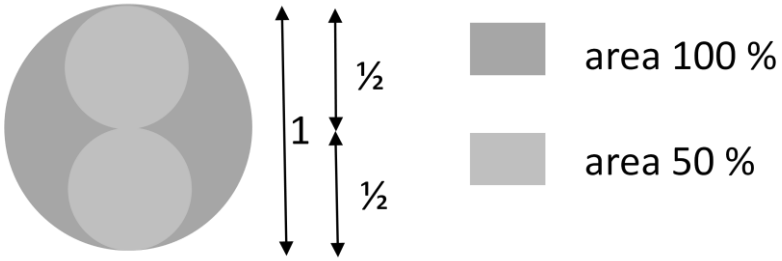

Figure 30: Rotational absorption distribution: - large dark grey circle with diameter 1 and area A. - smaller light grey circles represent model angular absorption distribution with diameter 0.5 A and 0.25 A area each.

Figure 30 illustrates a mathematical model for the absorption. If the light is non-polarized, the bigger circle represents the angular absorption distribution in solution. If the molecule is stationary, as during a laser pulse, the smaller circles can be used to represent the angular absorption.[99,100] The math indicates a 50 % improvement with non-polarized light. When a quarter wave-plate (355 nm) is used to form circular polarized light, an acceleration in TC turnover of 30 % is found. The difference can come from the fact that circular light is not equal in absorption probability to non-polarized light or because the linear polarized light could partially align the molecules and therefore elude the model. The overall result is for circular polarized light to have a higher absorbance although mostly homodimer was produced with this polarization. Once the molecules in every orientation can absorb the light the system behaves comparable to an increase of the absorption cross section. As seen above the crossdimer preference will suffer with these conditions.

2.2.3. Intrinsic values

Parts of the absorption process are the intrinsic, molecule inherent parameters. There is the absorption coefficient ε which can be measured with an UV-VIS spectrometer and expressed as the molar absorption coefficient α. This value can provide the molar absorptivity or molecular absorption cross section σ. If we integrate the absorption spectrum, we can get the integrated absorption coefficient (IAC) (Figure 31).

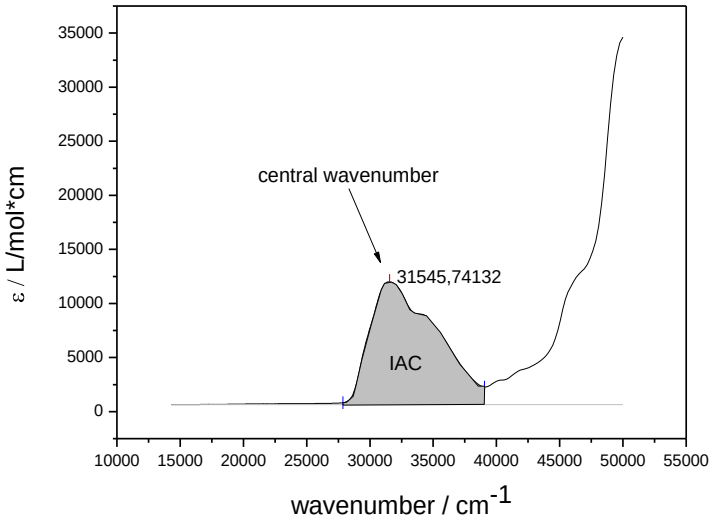

Figure 31: Integrated absorption coefficient IAC.

This IAC can be used to calculate the oscillator strength *f*, the 1. *Einstein* coefficient A, which stands for a spontaneous emission rate. The 2. *Einstein* coefficient, which includes induced emission and absorption, can be calculated, too. Moreover the transition dipole moment μ and the electric field amplitude E_{el} or Intensity I_{el}, at which the transition is saturated, can be deduced. The following Table 10 includes all these values for TC.[101,102]

parameter	formula	value (TC)
ε (355nm)	ε=A/cd	990 L/(mol·cm)
α (355 nm)	ln(10)·ε	2280 L/(mol·cm)
σ	$\sigma_{355} = \frac{ln(10) \cdot \epsilon_{355}}{10 N_A}$	$3.79 \cdot 10^{-22}$ m²
IAC	(plot in wavenumbers!)	$6{,}96 \cdot 10^{8}$ m/mol
f	$f = \frac{(4\pi\varepsilon_0) c^2 m_e \ln 10 (IAC)}{\pi q^2 N_0}$	0,301
μ	$\mu_{21}{}^2 = \frac{3hc \ln 10 (IAC)}{8\pi^3 N_A \omega}$	$5{,}33 \cdot 10^{-48}$ J/m³ = $5.93 \cdot 10^{-58}$ C²m²
A	$A_{21} = \frac{8\pi c \omega^3 \ln 10 (IAC)}{N_A}$	$2{,}89 \cdot 10^{8}$ 1/s
B	$B = \frac{\ln 10 (IAC)}{h \omega N_A}$	$3{,}35 \cdot 10^{12}$ s/kg
E_{el}	$\omega = \mu_{21} E / \hbar$	660 V/m
I_{el}	$I(\omega) = \frac{1}{2} c \varepsilon_0 E^2$	580 W/m²

Table 10: Intrinsic TC absorption values.

ε_0 = dielectric constant; q = electron charge; ω = angular frequency; m_e = electron mass; c = light speed; h = planck constant.

All the values are not particular striking themselves but it is important to grasp the fact that we can get so much information with just one measurement. Later on, I will illustrate the use of the 1. *Einstein* coefficient and the electric field intensity to obtain an otherwise difficult to get lifetime (s. 2.3.2. b)) and to discuss a non-linear absorption phenomenon.

The absorption cross-section is great to compare effectiveness in photoreactions and can furthermore be used to estimate the two-photon-absorption quality of a dimer. This value for TC is only about as large as the one of the main absorption of benzene [103] but I am only exciting within the wing of the broad absorption band of TC which is important to reach deep into the cuvette.

2.2.4. Set ups

The reaction set up has turned out to be a crucial and quickly alterable factor for the photon distribution. Most important is hereby to consider the solubility of the substrates and the intensity of the light source. On one hand, the concentration of my reaction mixture is limited with the solvent of choice. On the other hand, the laser does only provide a certain energy output. Whether the reaction time or the heat distribution is the key, there is a good set up for every preference. Table 11 shows four of my frequently used set ups. The direct irradiation is best in terms of excess heat removal and does result in a CD/HD ratio of ~ 10. The cuvette is the standard and most common vessel for photoreactions (CD/HD ≥ 10). The *Ulbricht* sphere is a special manufactured, highly reflective surrounding with the idea not to waste any kind of transmission but to disperse the light and to excite more molecules simultaneously. This sphere, for example, can shorten the reaction time for a complete turnover by 14 % and improve the CD/HD ratio by 36 % (from 5.5 to 7.5 at 66 µJ/pulse). The flow cell allows a large scale (≥ 200 mL / ≥ 1 g) batch to be run.

set ups	picture / scheme	advantage
direct irradiation	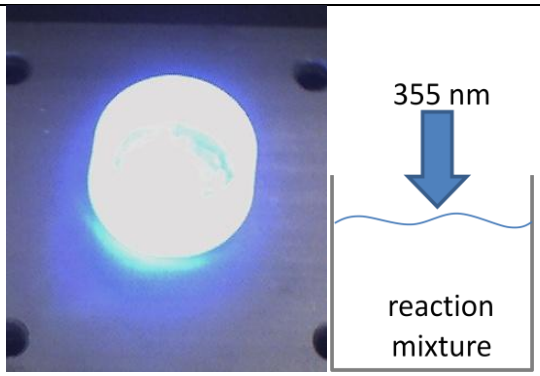	+ simple + scalable
in cuvette	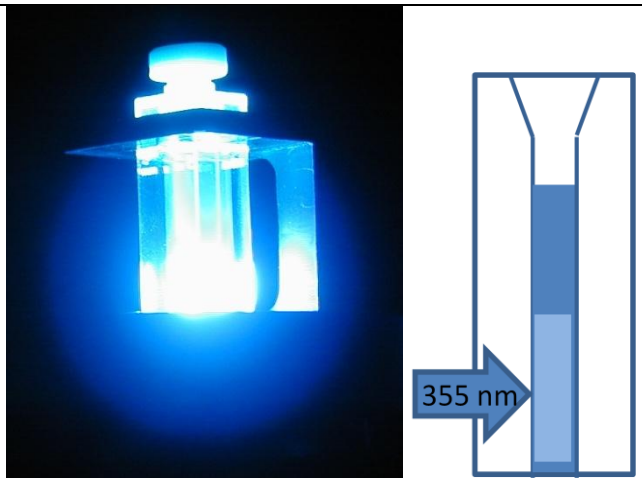	+ parallel kinetic measurement (UVVIS) + parallel turn over determination (transmission) + different thicknesses
Uhlbricht sphere (high reflective, optic PTFE)	 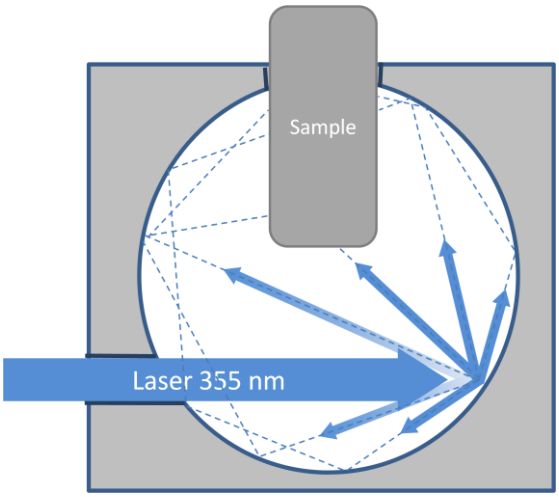	+ 98% reflective for 355 nm = no photons wasted

set ups	picture / scheme	advantage
flow cell	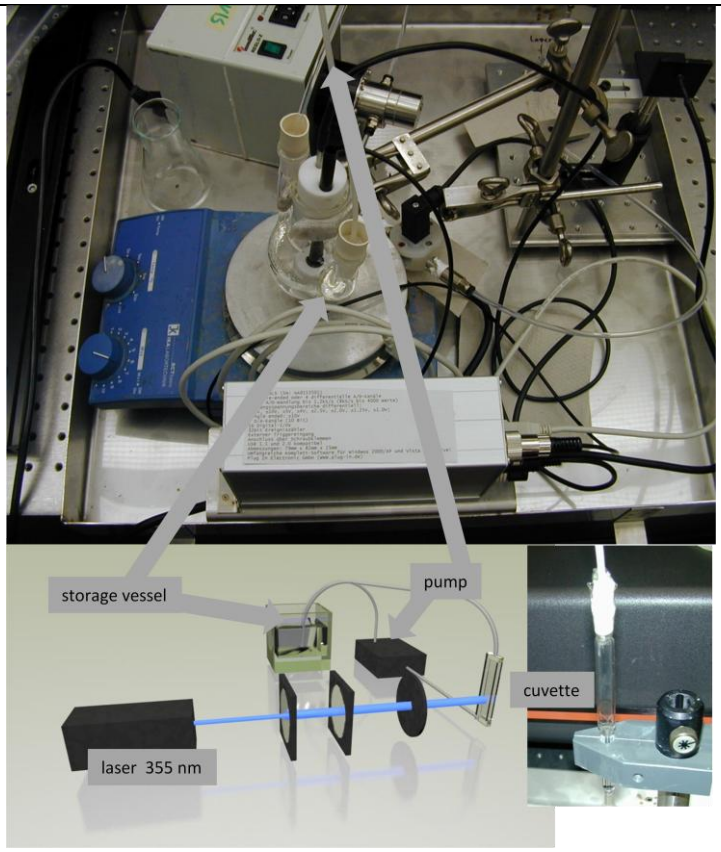	+ larger volume + parallel analysis (HPLC)

Table 11: Set ups for laser dimerization.

2.2.5. Activation/depletion zone/suppression

By far the highest significance belongs to the degree of activation, which indicates the number of photons per molecule at a certain depth in the cuvette or the irradiated volume. Depending upon the reaction vessel and concentration, together with the absorption cross-section of the substance, the photons can only penetrate a certain depth before they are absorbed. To follow the model of chapter 2.1.3: If there are adjacent diffusion spheres, which have at least one excited TC* molecule in them, the thickness d of this activated layer correlates with the concentration. (I want to mention that because of *Lambert Beer* law an increase in pulse intensity would not enlarge the thickness of the layer [at a fixed concentration] but increase the number of excited TC* per diffusion sphere because the percentage of absorbed light is constant) Table 12 lists the layer thicknesses for different concentrations.

concentration / mmol/L	OD	TC* at 66 µJ	d activated / mm
0.02 (100 %)	$7.92 \cdot 10^{-5}$	$2.15 \cdot 10^{10}$	0.22
0.015 (75 %)	$5.94 \cdot 10^{-5}$	$1.61 \cdot 10^{10}$	0.29
0.01 (50 %)	$3.96 \cdot 10^{-5}$	$1.08E \cdot 10^{10}$	0.44
0.005 (25 %)	$1.98 \cdot 10^{-5}$	$5.37 \cdot 10^{9}$	0.88
0.002 (10%)	$0.08 \cdot 10^{-5}$	$2.15 \cdot 10^{9}$	2.19
0.0002 (1 %)	$0.008 \cdot 10^{-5}$	$2.15 \cdot 10^{9}$	21.93

Table 12: Activated layer thickness in dependence of concentration.

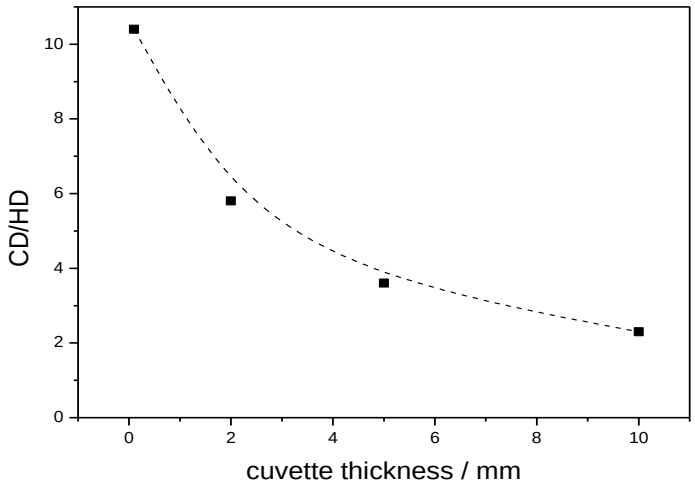

Figure 32. CD/HD-ratio depending on the cuvette thickness. The samples were irradiated with 66 µJ/pulses at 10 kHz. The exposure time was adapted to the volume to have an equal amount of photons per molecules applied in each sample (e.g. 30 min for 0.5 mL).

Figure 32 illustrates the thickness relationship. The laser pulse intensity is kept constant and the cuvette thickness is reduced to a completely activated initial volume which in the end produces a CD/HD ratio over 10. The smaller reaction volume thus equals more photons per molecules overall which results in a better CD/HD-ratio.

Of course the concentration can be diluted but then the photoreaction is not efficient. Longer diffusion distances are required, the reaction will take longer, and the quantum yield will decline. Therefore, the reaction parameters have to be measured and need to be coordinated and matched to assist each other. As already explained above, the photoreaction can only occur if an excited molecule collides with a ground state one. In case two activated molecules strike each other, no dimerization reaction takes place. With this information it is possible to design a photoreaction for every need. Using the mechanism, two strategies can be explored. One is to influence the dimer ratio by varying the irradiated volume to boundary area. Within the irradiated volume the crossdimerization should be favored and at the boundary to the non-irradiated part, the

homodimerization should take place. The second one is to vary the photo flux in order to populate the excited TC* state and to locally accelerate the reaction.

I have tried to investigate the irradiated area to volume relationship in solution but without any conclusive results, though it was possible to measure off the 2D phenomenon inside the cuvette. The dark-light interface, at which the homodimerization should be favored, was still too short compared to the illuminated volume. Figure 33 shows how a spatial laser resolution was generated through a black aluminum grid. A *Normarski* prism was also used but resulted in fringed edges whereas the grid attenuated the laser intensity. A possible solution for a high area to irradiated volume set-up could be a two dimension interference grid, a multilens plate, or a diffractive optical element (DOE) with a higher spatial resolution.

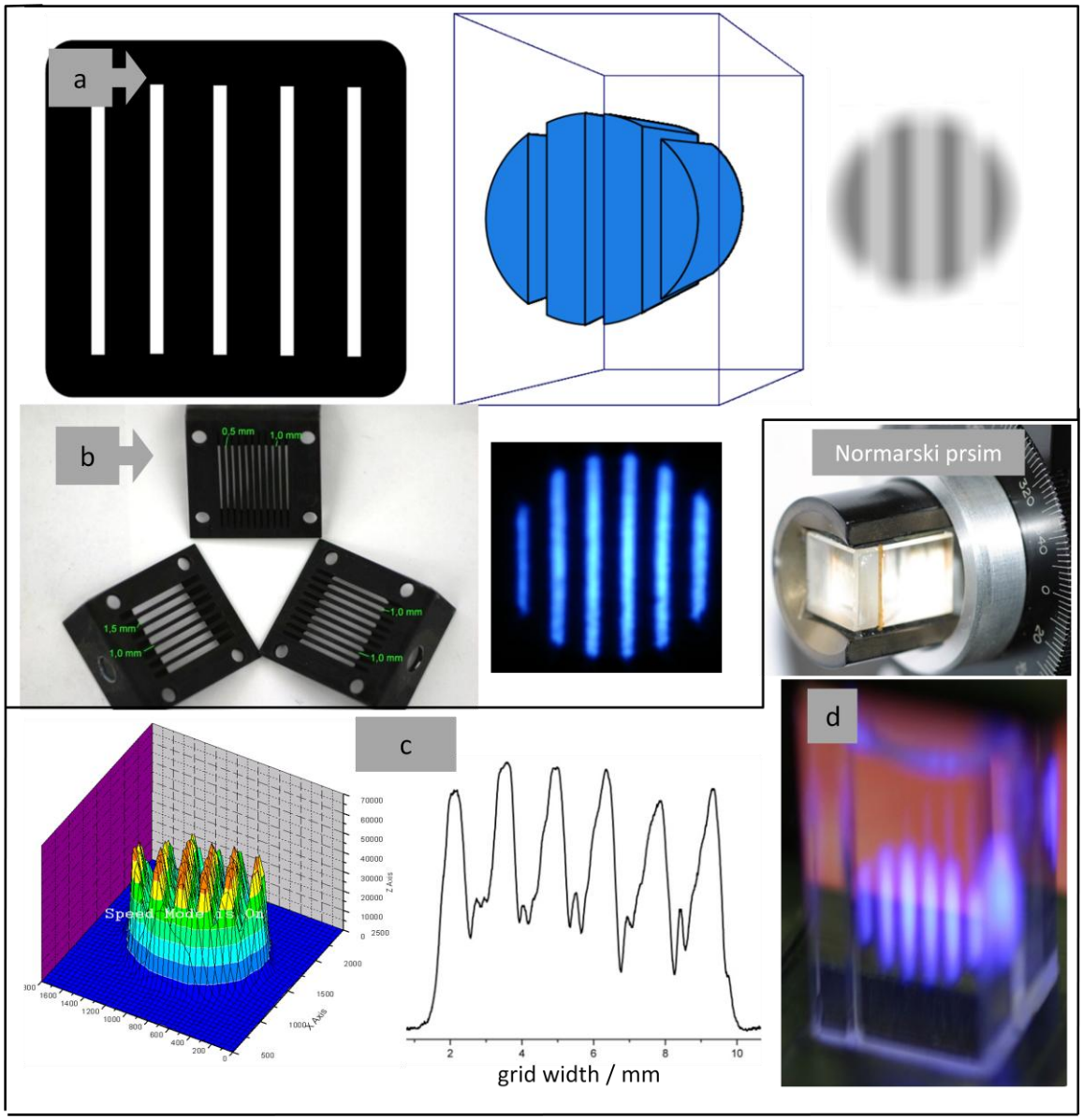

Figure 33: a) Scheme of grid generated laser parts and transmission shape; b) Photo of grids - photo of transmission; c) 3D profile and cross-section of *Normarski* prism transmission; d) Fluorescing volumes inside cuvette.

grid (slit width)	boundary / cm^2	illuminated volume / mm^3	homodimer/TC
-	0.5	100	1.0
1.5 mm	1.0	61	0.97
1.0 mm	1.3	49	0.95
0.5 mm	1.5	33	0.97

Table 13: Irradiation of 400 µL; 20mM TC at 0.27 W for 10 min.

Table 13 presents the parameters and shows that the boundary to volume ratio change is only 9. A far higher ratio is needed to show this effect.

The illuminated area is too difficult to control, but the sheer number of photons can be controlled comparatively easy. At first, I want to concentrate on the mechanism and how excitation can help me to have influence on the reaction instead of merely accelerating it.

Dimer formation of coumarin-type molecules occurs through collision quenching of an excited substrate with another ground state molecule. The higher the photon density is, the more TC molecules are excited. At very high intensities the homodimerization can be suppressed to some extent, enforcing the crossdimerization, because two excited TC molecules TC* cannot form a dimer together. Starting with a 10:1 mixture of H5FU and TC the initial statistical probability for an excited TC* to form a crossdimer, as compared to its probability to form a homodimer is about 10:1, disregarding the factual preference for homodimerization. As more and more TC is converted, the remaining TC has an ever increasing probability P to form crossdimer. In fact, when 10 % TC remains the mathematical chance is 91:1 towards crossdimerization. It therefore makes sense to execute this reaction until a high or complete conversion is achieved, as the last molecules have the best chance to form crossdimer. The following Figure 34 depicts the statistical probability for the remaining % of TC to form crossdimer.

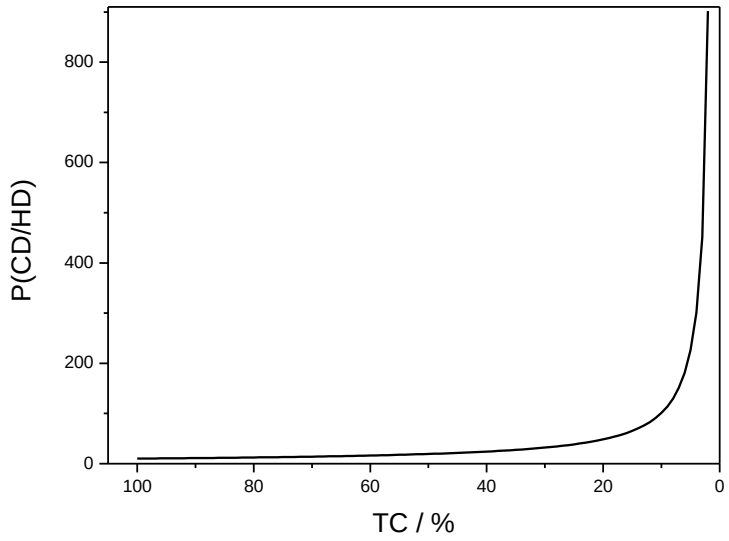

Figure 34: Crossdimer formation probability P.

But this intramolecular dimerization is diffusion controlled, so the last few percent of turnover will take considerably longer than the first few. The decreasing concentration will result in less activated TC* to find reaction partners during their lifetime. The laser with its high photon flux excites more molecules and is faster than lamp based reactors which allows for a quick and complete conversion. For the generally used 66 µJ laser pulses with 20 ns pulse width, the expanded beam has a photon flux of $F = 9.3 \cdot 10^{21}$ photons$\cdot s^{-1} \cdot cm^{-2}$. This value is roughly 100,000-times higher than common high pressure mercury lamps achieve and about 500,000-times of that the *Rayonet* reactor is able to provide. The reaction rate R for laser-supported dimer synthesis (66 µJ$\cdot$pulse^{-1}) is $R = 3.0 \cdot 10^{-3}$ mol$\cdot L^{-1} \cdot min^{-1}$ measured in TC degradation. The *Rayonet* reactor, with its much larger volume, still is slower with. $R = 1.3 \cdot 10^{-5}$ mol$\cdot L^{-1} \cdot min^{-1}$. Interestingly, the reaction rate of the laser is so high that the irradiated volume within the cuvette gets depleted of the absorbing TC in contrast to the rest of the solution. Diffusion, *Brownian* motion, and the stronger heat convection together can not negate this effect, thus the transmission behind the cuvette is higher than HPLC measurements of the equalized solution would exhibit. The laser consequently creates an artificial high conversion scenario favoring crossdimerization (Figure 35). The concentration difference of the illuminated volume and its surrounding will expand over the time of the reaction and later on diminish as the total concentration declines. The center of the irradiated volume thereby is depleted first and exposes the highest transmission. From the inside out, the *Gaussian* beam will gradually allow more and more absorbing TC molecules to be present. The smaller the number of TC molecules, the better the dimer ratio will be.

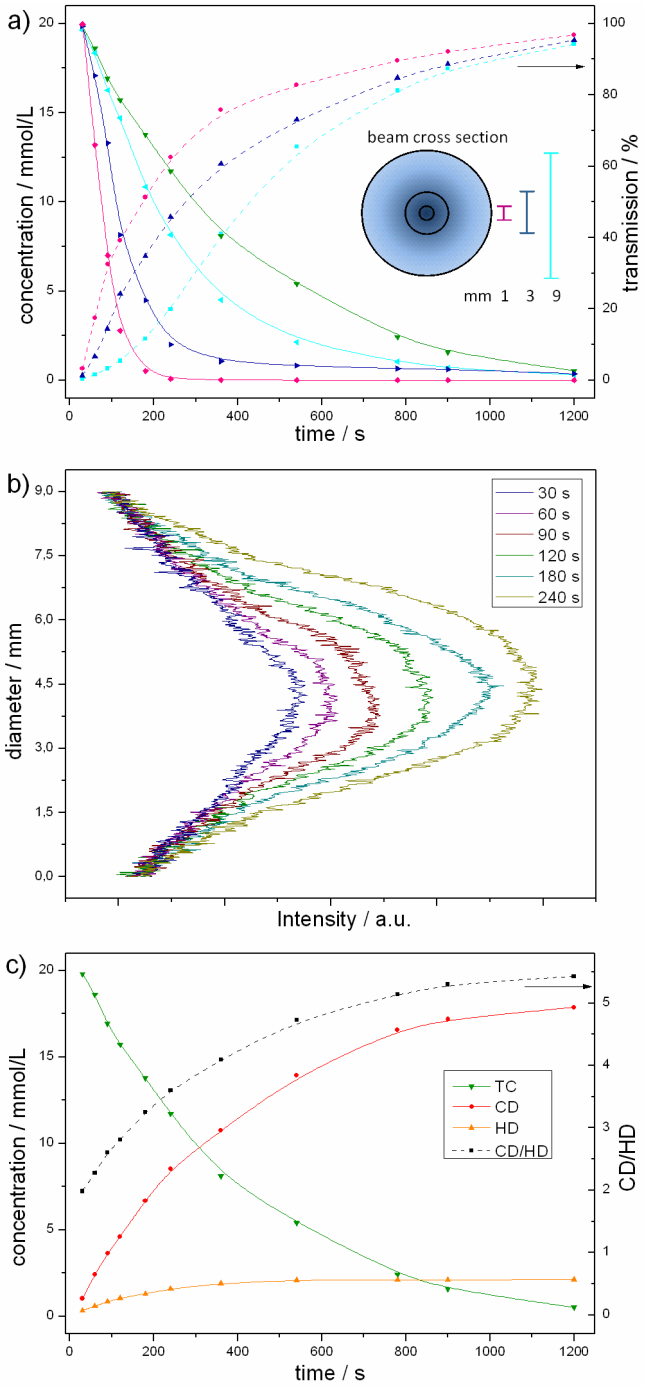

Figure 35: Establishing and maintaining the TC depletion zone and overall kinetics. a) The green solid line represents the TC concentration of the mixed solution measured by HPLC. The cyan, blue, and purple dashed lines show the transmission of 355 nm light on the right axis in dependence on the diameter of the cross-section of the *Gaussian* beam profile measured, i.e. 9 mm (cyan), 3 mm (blue), 1 mm (purple). The solid curves of same color show the derived concentrations. The depletion zone is established within the first 200 s of the reaction and is preserved until all the TC substrate has been used up completely. b) Intensity profile behind the cuvette at the beginning of the reaction. c) HPLC measurements during the reaction with 66 µJ/pulse energy. The solid lines represent the time

dependence of the concentrations of the TC substrate and the dimers. 100% concentration = 20 mmol/L TC. The dashed line shows the resulting CD/HD-ratio on the right axis.

This intensity dependent benefit can be seen in the CD/HD ratio and it is extended when the intensity is increased. That high photon flux crossdimer ratio gain will stagnate with the growing unused transmission until at very high intensities suppression of the homodimerization sets in. Mechanistically, two excited molecules can not form a dimer together. So, as a lot of TC is excited simultaneously, the homodimerization probability is diminished by that proportion. In Figure 36 the dependence of the CD/HD-ratio on the laser pulse energy at a constant applied total energy is shown. Each cuvette has been exposed to a total energy of 800 J converting 100% of TC to dimers. With low intensity pulses a meager CD/HD-ratio below 2 is obtained which increases to about 12 at pulse energies of about 9000 µJ. In the lower right corner of Figure 36 the percentage of excited TC-molecules is shown.

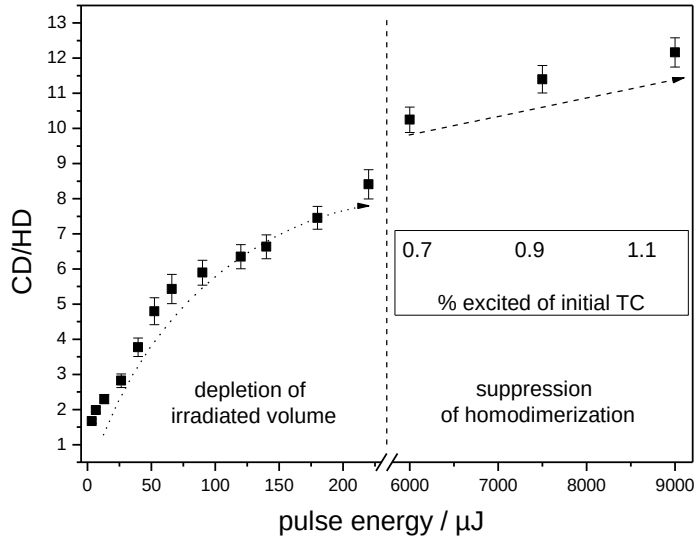

Figure 36. CD/HD-ratio in dependence of pulse energy. Each sample was exposed to the same total energy of 800 J. The CD/HD-ratio increases with increasing pulse energy.

The graph indicates a direct but non-linear relation between pulse intensity and dimer ratio. Due to the *Gaussian* laser beam profile, the 3-dimensional cuvette penetration thereof causes some non-linear correlation at low to medium intensities (≤ 100µJ).

The laser consequently is important for the crossdimerization reaction, because the high photon flux can cause a difference between the irradiated volume and its surrounding. The advantages manifest themselves in the CD/HD ratio and the conversion. In general, I can say that the more photons per

molecules there are the better the dimer ratio will turn out to be. In every slice of the cuvette from the foremost part, where the laser initially hits, to the last layer there is a drop in photon density. The more highly illuminated, or the fewer badly photon loaded layers there are, the more homodimerization is suppressed and concomitantly crossdimerization enforced. In essence, the reaction can be steered by the pulse intensity to produce either more homo- or crossdimers.

A precise theory with an exact prediction of the dimer ratio is difficult to deduce. There is the three-dimensional *Gaussian* beam profile, the constantly changing concentrations, with diffusion, and excitation in completely different time regimes. Then there are what I like to call the intrinsic values like absorbance probability, inter system crossing probability, and the lifetime. The empiric result however is concise and predicts more crossdimer with high photon flux. The depletion zone hence combines three features. It uses the laser intensity to artificially produce a low concentration zone in which every molecule will be excited and the entire volume is activated. The TC*/TC ratio is good, and the reaction is as fast as the diffusion allows it to be. Therewith, the homodimerization dominance can be eliminated and high crossdimer yields can be produced.

2.3. Reaction

Now that the energy is installed in the absorbing molecule, several opportunities exist to disperse it. The molecule can emit the energy or convert it into heat. Also, the higher electronic state can wander the path of a chemical reaction. These main reactions coexist with side reactions. All form different products with variable speeds and the probability and efficiency for each reaction channel deviate.

2.3.1. Side reactions

There is a range of possible side reactions depicted in Figure 37, all of which lead to different products. I listed eight different, theoretically possible starting steps for the TC molecule when irradiated.

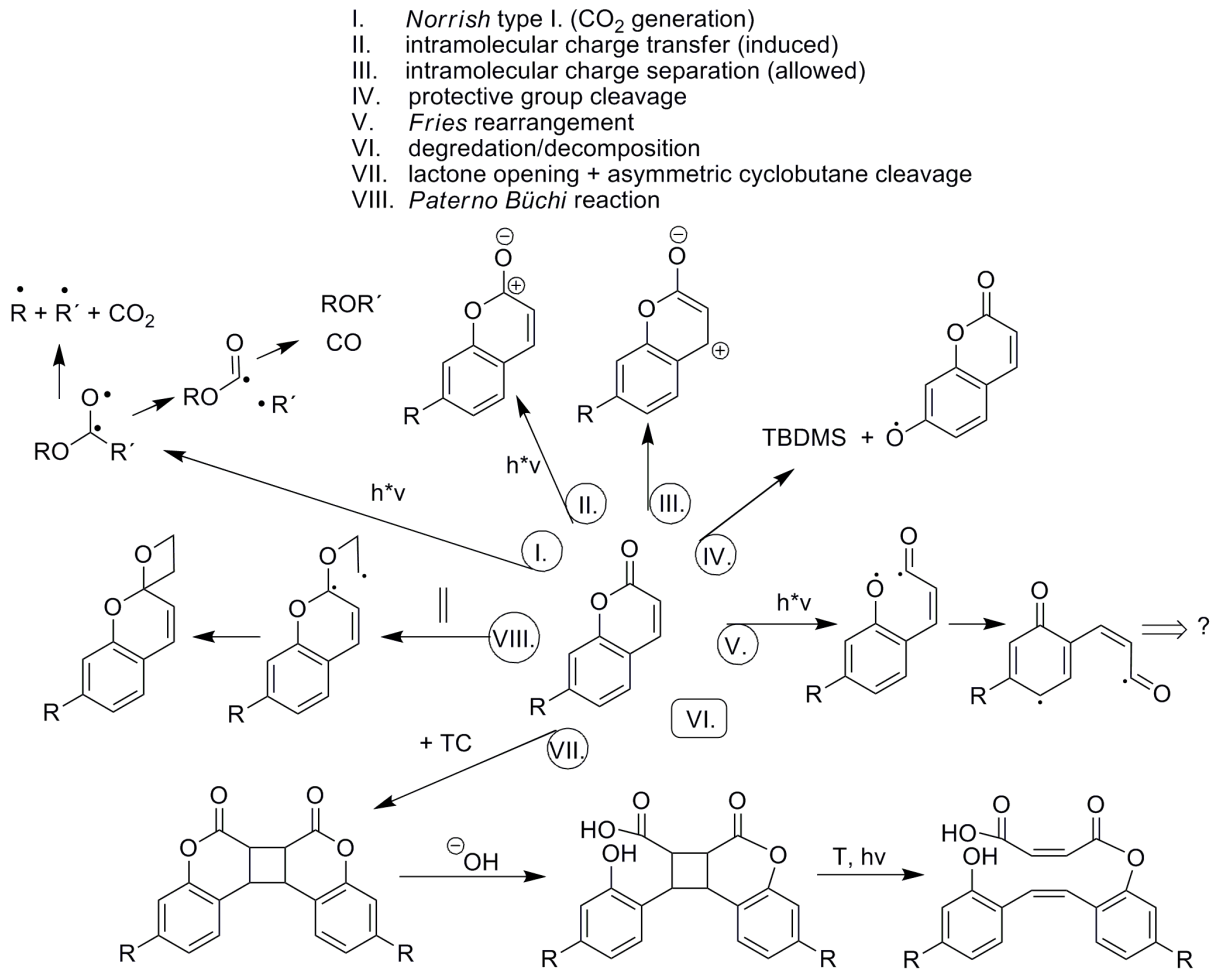

Figure 37: Possible TC side reactions after photo-excitation.

The π* excited states of carbonyl compounds display a rich chemistry. The CO-group behaves like an alkoxy radical, since the oxygen has an unpaired electron. The first side reaction is the *Norrish* type I reaction, which results in some kind of bond cleavage next to the CO group. Type II reactions would include a hydrogen atom abstraction of another molecule, making the prediction of products very difficult. Instead, type I reactions with coumarin can end up in the release of CO_2 or CO. Investigating the release of these gases proved to be insuperable because of the very small quantities that are released. NMR-studies indicate some kind of ring breaking that is not the simple lactone-ring opening in the aromatic region (Figure 38). The *Fries* rearrangement (number V.) is theoretically possible, too.

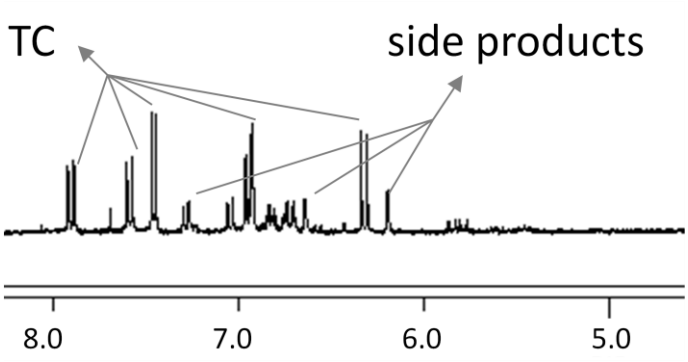

Figure 38: NMR clipping from broken lactone-ring .

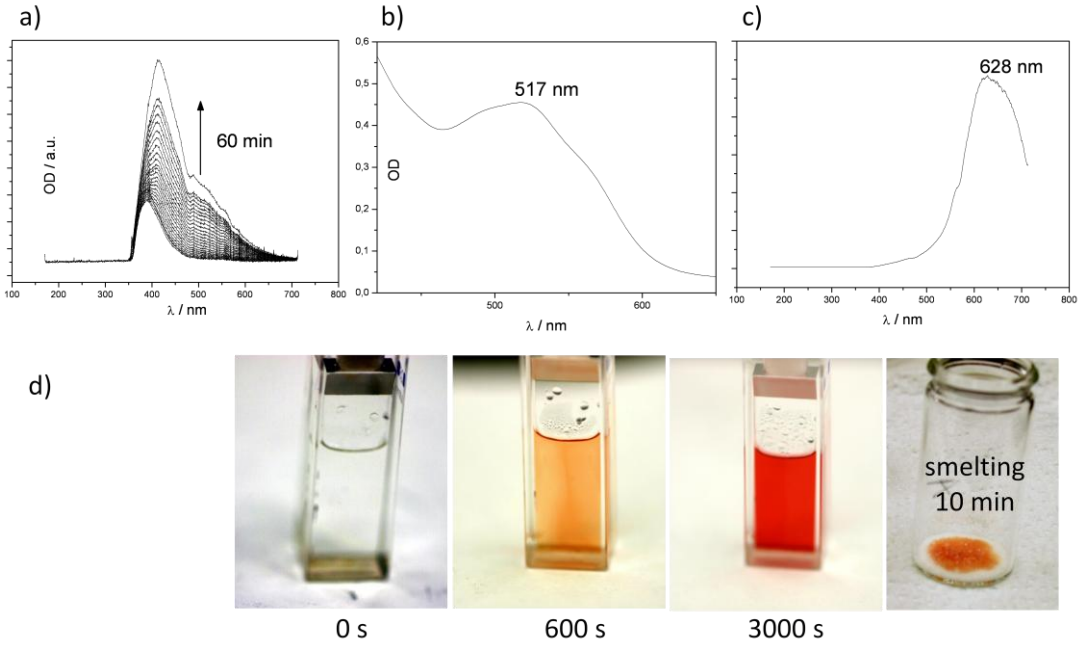

Figure 39: Reddening of (200 mmol/L H5FU + 20 mmol/L TC solution in 2 mm cuvette; 50 kHz @ 90 µJ) reaction mixture; a) Fluorescence measurements after multiple irradiations; b) UV-VIS measurement after 10 min; c) White light transmission; d) Photos of solution and smelting.

Side reaction number II. and III. are interesting because in both cases charges are generated which increase the transition dipole moment. This includes a simultaneous bathochromic shift. In a previous section (2.2.1. a)) I have shown how this broader low energy transition might be applied to use different reaction channels. Under harsh conditions and high intensities (> 30 kHz and W > 5 W) the TC substrate forms a red intermediate which is quite stable in solution and in powder form but vanishes over the time of days. Literature indicates a charge separation reaction for this coloring.[104] The amazingly strong red color, which forms during irradiation, supports this assumption (Figure 39). The protective group cleavage can be found in the LC-MS after longer light reactions (M^+= 160 g/mol) contrary to numerous unidentifiable decomposition parts form random degradation. The lactone-ring opening is only a problem under basic conditions and is a lot less common in crossdimers. The

possible asymmetric cyclobutane ring cleavage demands this side reaction to be avoided. The last, listed, and unwanted reaction is the famous *Paterno-Büchi* reaction which pleasantly does not work very well with enone structures but can occur with isolated carbonyl groups. At last, I would like to mention that there is a small possibility for higher order excitation during irradiation because of the long ns laser pulses and the long lived T-state of coumarin. However, the products should be comparable.

2.3.2. Dispersion of energy

As soon as the light energy has been absorbed by the molecule, the system tries to dispose of it. As seen in the *Jablonski* diagram (s. 1.3), there can be radiative decay with fluorescence and phosphorescence, non-radiative decay in the form of heat, or the dispatch while collision quenching which can also form a photo-product, like a dimer.

a) Heat

Heat is the most likely form of the energy release. As soon as a substance absorbs light, internal conversion will stimulate motion in form of vibration which can be transferred to the environment. Light induced, thermal energy causes density fluctuations inside the reaction mixture, as well as the creation of small eddies. Figure 40 shows how the thermal updraft from the laser at the beam facing front causes a TC ground state accumulation at the lower end (Fig. 40 c). The rise of heated low density fluid can be visualized in the absorption e), or interferogram d). The irradiated solution practically stirs itself and does not need a stirrer. Minutes long measurements with and without stirring bar deliver the same results.

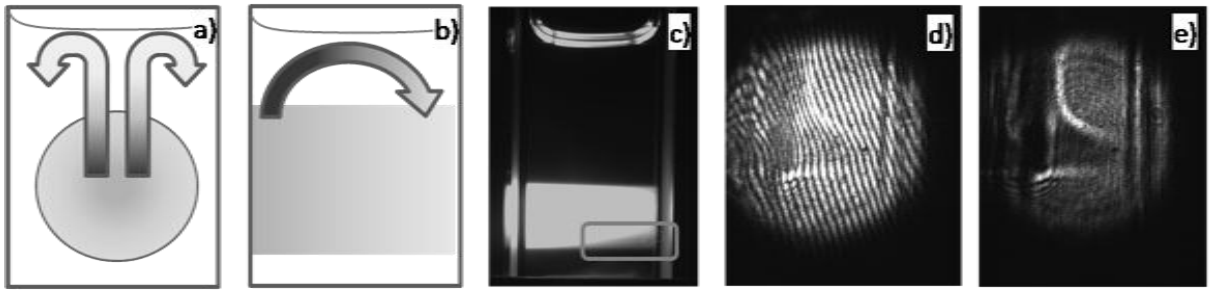

Figure 40: a) Frontal view of cuvette during irradiation, laser causes updraft; b) Side view, eddies are created; c) Side view photo of fluorescence, ground state TC accumulation in lower right corner; d) Interferogram; e) Transmission of 633 nm secondary wavelength, different densities cause varying transmission.

To measure how much hotter than the rest of solution the beam indent is thermal images are taken. Under direct laser irradiation the solution heats up. The difference of the incident laser pickup point and the surrounding solution is only 10 °C (Figure 41).

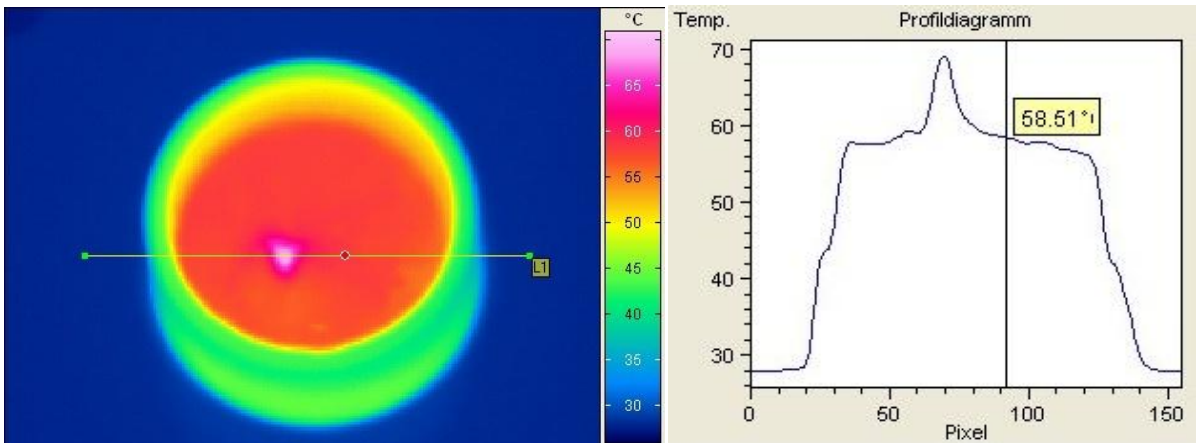

Figure 41: Thermal image of direct on top irradiation. Laser spot pickup point is 10 °C hotter then surrounding solution.

In solution the created heat can be dissipated within the cuvette volume and the temperature can not reach above the boiling point of the solvent. In solid powder form heat is not that easily spread. The amount of heat generated in the powder can be steered with the laser power. The heat is trapped as soon as it is generated, therefore a linear dependence exists (Figure 42).

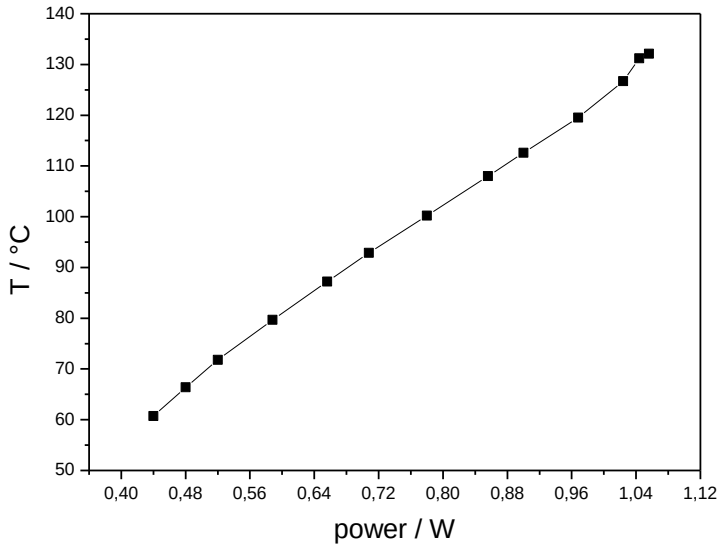

Figure 42: Laser power dependent temperature induction into TC powder/smelting.

Thermal images of irradiated TC powder show a quick temperature rise and uniform TC melting over ~ 85 °C (Figure 43).

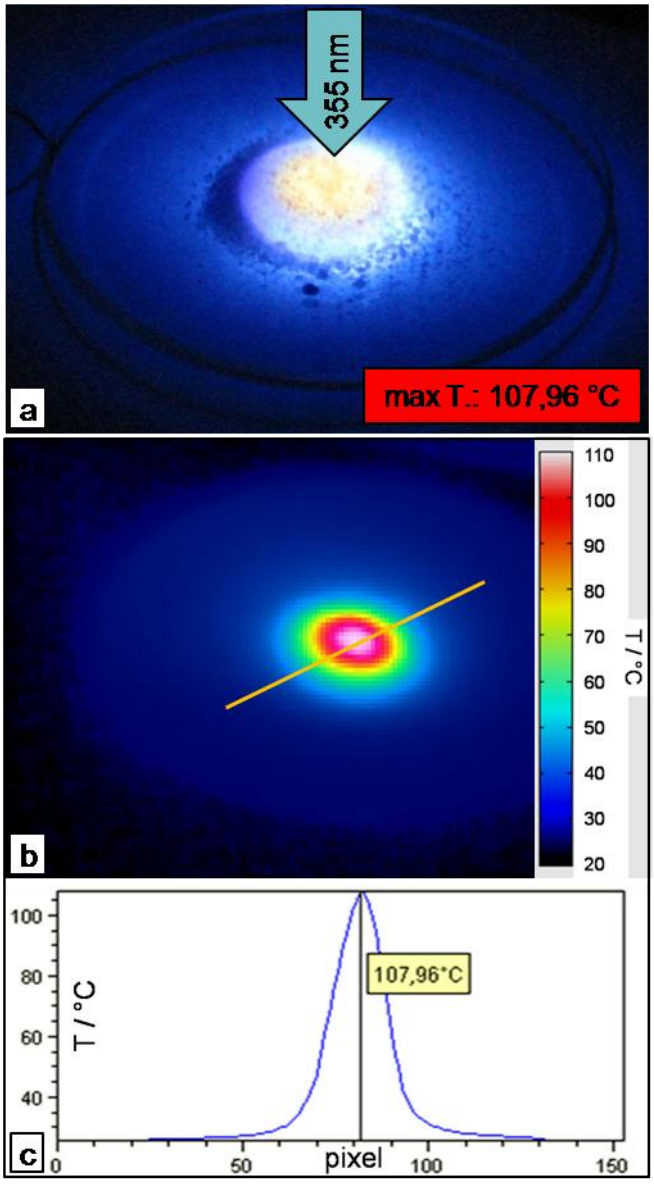

Figure 43: a) Photo of laser irradiated blend of TC and H5FU powder; b) Thermographic IR-image of the irradiation with temperature indication; c) Temperature profile along yellow line, resembling the *Gaussian* intensity distribution of the laser beam.

b) Fluorescence; *Stern-Volmer* plot

The dimerization reaction proceeds via collision quenching of the excited molecule with the ground state reaction partner. In general, most of the dimer will result out of a triplet state. To get there the excited singlet state has to undergo inter system crossing. To find out more about the singlet state reactivity fluorescence quenching experiments are done.

As soon as the molecule is photoexcited into the ^{1}S-state, any kind of non-radiative energy transfer, like a photoreaction, competes with the fluorescence of the molecule. Adding a fluorescence quencher can provide information about the interaction between these molecules. Two theoretical forms of quenching exist. In dynamic quenching both molecules experience only weak through space

coupling interactions and the energy is transferred without irradiation with either a FRET or *Dexter* mechanism. When the concentration of the quencher is raised, the probability for a collision increases which causes the lifetime of the excited species and its fluorescence intensity to drop. The relationship of quencher concentration and singlet lifetime or fluorescence is represented in the *Stern-Volmer* equation:

$$\frac{Q_f^0}{Q_f} = \frac{I_f^0}{I_f} = \frac{\tau_0}{\tau} = 1 + k_q \tau_0 \; Q \tag{9}$$

Q_f = fluorescence quantum yield, I_f = fluorescence intensity, τ = excited state life time, k_q = rate constant of quenching in $M^{-1} \cdot s^{-1}$, [Q] = concentration of the quencher;

The other possible process is static quenching, in which there is a strong coupling between the two partners. This association results in a ground state complex. Adding quencher this time increases the probability of association which decreases the fluorescence intensity but has no effect on the lifetime. In this instance the *Perrin* model of quenching can be used to determine the radius of a sphere-of-action in which the coupling reaction occurs as soon as the reaction partner enters into this active sphere.[105]

$$\ln \frac{I_f^0}{I_f} = \frac{4}{3} \pi r^3 \; Q \tag{10}$$

r = radius of the reaction sphere;

If both forms, the dynamic and the static, simultaneously occur, then the non-linear *Stern-Volmer* relation can be consulted:

$$\begin{aligned} &\frac{I_f^0}{I_f} = k_q \cdot \tau_0 \cdot k_{Eq} \cdot \; Q \;^2 + \; k_q \cdot \tau_0 + k_{Eq} \; \cdot \; Q \; + 1 \\ &\sim y = ax^2 + bx + 1; \\ &a = k_q \cdot \tau_0 \cdot k_{Eq} \\ &b = k_q \cdot \tau_0 + k_{Eq} \end{aligned} \tag{11}$$

k_{Eq} = equilibrium constant for complex formation;

Increasing the quencher concentration in this case causes the lifetime to decrease gradually and the fluorescence intensity to fall rapidly.

To find out how efficient TC can be quenched, fluorescence measurements with three substances are made. For example, Figure 44 shows how increasing *cyclo*-pentenone concentration causes the fluorescence intensity to decreases. *Stern-Volmer* plots for all measurements are shown in Figure 45 and the results are summarized in Table 14.

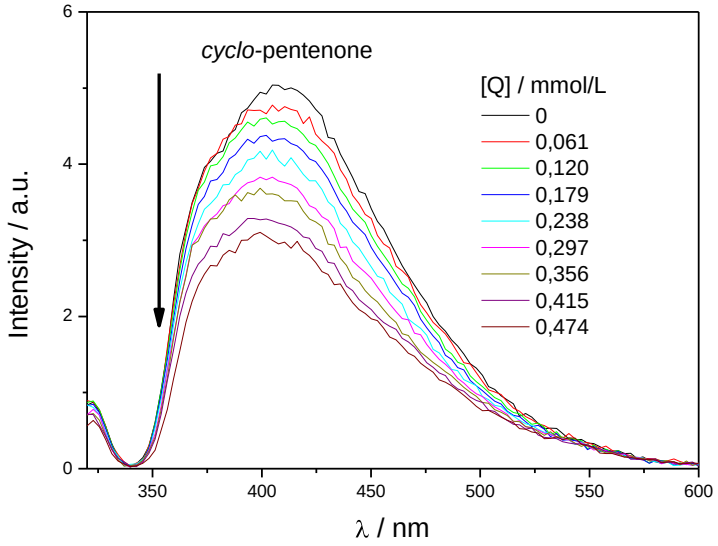

Figure 44: Fluorescence quenching of TC with *cyclo*-pentenone.

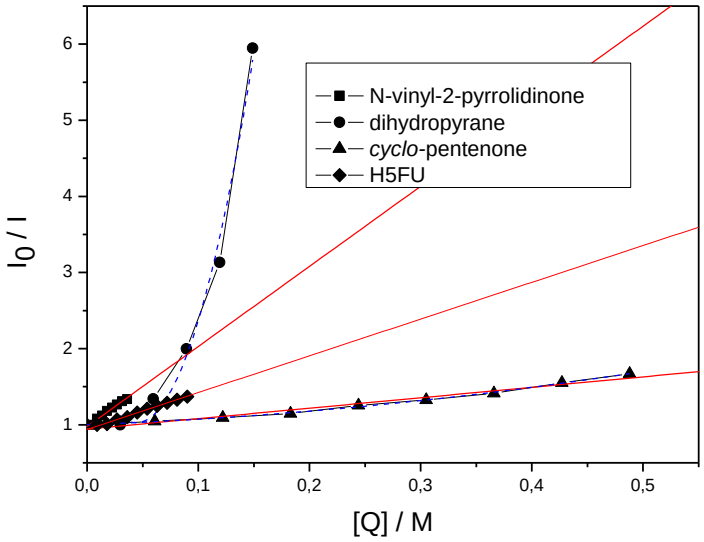

Figure 45: *Stern-Volmer* plot of fluorescence intensity. (static: red; static+dynamic: blue dash)

substance	**H5FU**	***N*-vinyl-2-pyrrolidinone**	**dihydropyrane**	***cyclo*-pentenone**
slope	4.8	10.5	-	1.4
k_q / (mol/L·s)$^{-1}$	$9.6 \cdot 10^9$	$2.1 \cdot 10^9$	-	$2.8 \cdot 10^8$
a	-	-	204.9	1.7
b	-	-	6.7	0.5
k_q / (mol/L·s)$^{-1}$	-	-	$9.5 \cdot 10^9$	$2.2 \cdot 10^8$
k_{Eq} (mol/L)$^{-1}$	-	-	9.2	1.6

Table 14: *Stern-Volmer* values for τ_0(7-hydroxycoumarin) = 5 ns.

The *cyclo*-pentenone addition can be evaluated in both the dynamic and the static+dynamic way. For the lifetime the literature value for 7-hydroxycoumarin of 5 ns is used.[106] This often times difficult to get value can also be taken from the devision of 1/1. *Einstein* coefficient which can be derived from the IAC, as seen in chapter 2.2.3. The calculated value is τ(TC) = 3.5 ns. The slope values for coumarin quenching are in the same range as literture ones of ~ 10.[41] For the dihydropyrane the *Perrin* plot can be made, showing a small radius of 15 Å (Figure 46).

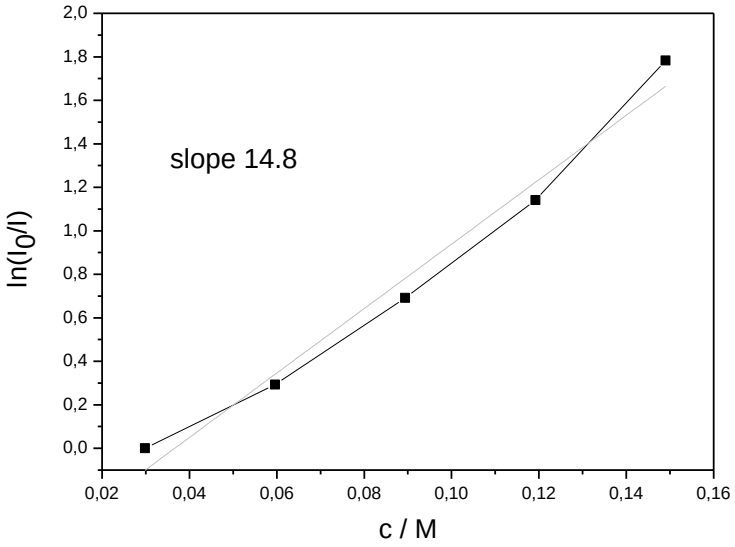

Figure 46: *Perrin* plot for TC with dihydropyrane.

c) Phosphorescence

Even the phosphorescence can be made visible in solution when a complex of the TC and the heavy atom containing molecule dibromoethane inside a cyclodextrin is formed.[107] Thereby, the collision quenching of the molecule´s triplet state, which was stimulated by the heavy atom containing molecule, is inhibited. The concomitantly increased intersystem crossing allows the recording of a phosphorescence spectrum in solution. The quantum yield is not the natural, uninfluenced one, but the energy of the triplet level can be established. For TC the β-cyclodextrin with an intermediate internal cavity of about 6 Å is used. The spectra are shown in Figure 47. The phosphorescence is at 460 nm and the energy of the T-state is E_{ph} = 265 kJ/mol (~60 kcacl/mol) which fits well with the 455 nm in the literature.[106]

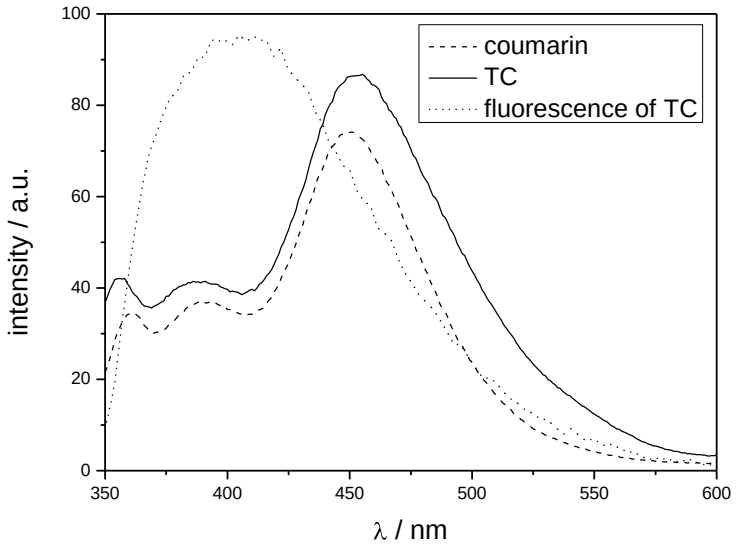

Figure 47: Phosphorescence of TC in solution.

2.3.3. Singlet or Triplet reaction

There was a long term discussion about the nature of the [2+2]-cycloaddition reaction and whether they employ mainly S- and/or T-states. Coumarin especially was thought to have two different reaction mechanisms for its four stereoisomers. Two of them stemming from a S-state and two from a T-state. However, the empiric result shows that a lot of factors such as the solvent or any kind of additives like sensitizers, *Lewis* acids, or a metal salts will change the stereoisomer distribution. The T-state thus seems more important, because it has a much longer lifetime than the S-state. Within this lifetime it can form all four isomers via rearrangement into a stable intermediate and moreover it can diffuse over longer distances in solution. After all, the intermolecular cycloaddition reaction in solution is diffusion controlled and the number of collisions is crucial. Even though, the inter-system-crossing quantum yield from S- to T- state is about a few percent,[108,109] the S-state can also be depopularized by fluorescence whereas the T-state does not present any phosphorescence in solution. Generally, a photoreaction occurs from the lingering T-state and only does so when the activation energy is below 20 kcal/mol. The S-state on the other hand cannot outcompete the fluorescence, if the activation energy is above 10 kcal/mol. So the energy and population of the T-state are most relevant. Table 15 gives an overview of some general characteristics for each state.

singlet	triplet
short lived (ns)	long lifetime (µs)
zwitterionic character	biradical character
fast, concerted reaction	stepwise reaction
stereospecific	non stereospecific
competing with fluorescence	followed by termination reaction
examples: electrocyclic rearrangements, sigmatropic rearrangements, concerted cycloadditions	examples: H-abstraction, radical rearrangements, homolytic rearrangement/fragmentation

Table 15: S- , T-state characteristics.

To confirm the biradical character of the excited coumarin, TC was irradiated with the radical catchers AIBN at 75 °C and another time together with TEMPO at room temperature. Several new peaks are found in the HPLC which reveal adducts in the LC-MS. The AIBN reaction shows both the single and double adduct with M^+= 344, 412 g/mol. The TEMPO reaction shows singular addition with M^+= 432 g/mol. In case butadiene is added to the TC solution during the photoreaction the cycloaddition reaction is suppressed by this radical catcher. EPR measurements confirm the biradical character of excited coumarin.[110,111]

2.3.4. Kinetics

The velocity of a reaction is an important part in understanding relationships between substrate and solvent, as well as lifetimes and the mechanism. It is vital to be able to quantitatively compare the photolinkers reactivity. Within this parameter there is the absorption process or excitation of a substrate S to an activated form S* which has to diffuse towards a reaction partner. At any point before, during, or shortly after both molecules meet there can be some sort of intermediate I. This in-between state is then responsible for the build up of different products P and or stereoisomers. With the last step of product formation often times radical or ion chemistry is involved. Figure 48 gives an overview over a typical photoreaction.

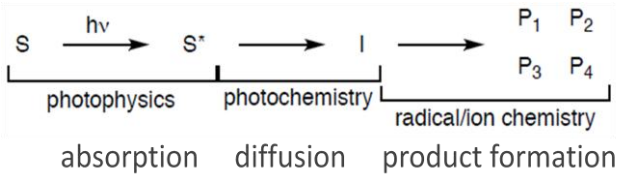

Figure 48: Generic photochemical reaction.

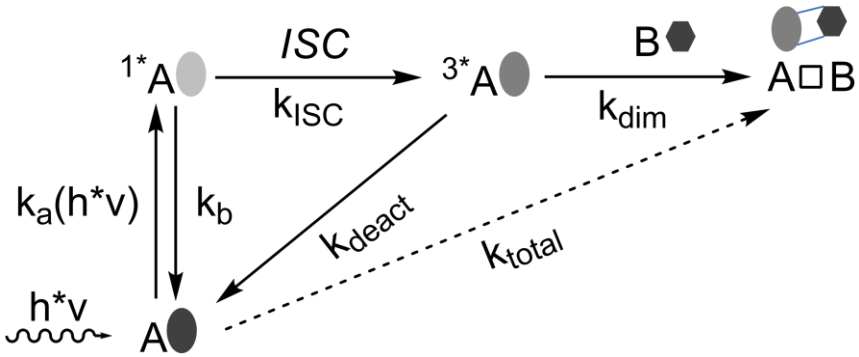

Figure 49: Overview of kinetic constants, which all are included in the total reaction constant k_{total}.

More specific for my reaction is Figure 49. The excitable substrate A absorbs the photons, performs intersystem crossing and reacts via diffusion dependent collision quenching with B to form some sort of dimer, preferably a crossdimer. Everything, from the absorption speed/probability k_a the quenching of the ^{1}S-state k_b, the deactivation of the reacting ^{3}T-state k_{deact}, and the dimerization velocity k_{dim} is part of the total reaction constant k_{total}.

This number therefore stands for a complete reaction from start to finished crossdimer product and can be compared to values of other photo-reactive combinations. To compare photo-linker and different reaction partners with each other would be too much and is very complicated. Instead it is easier to only work with linker molecules and keep H5FU as a B component constant. After all, for each linker there still remains the homo- and heterodimerization with 4 stereoisomers respectively.

For the interpretation of the kinetic measurements the *initial reaction velocity* method is used. Therefore, the reaction is simplified to being pseudo first order with regard to the TC species at the beginning. So the simple measurement of the declining TC during the irradiation can be consulted to determine the total reaction constant. With a 1:1 ratio of A:B this simplification is definitely questionable, but at 10:1 or greater pseudo first order is guaranteed. A better kinetic would be to include the photon as a separate reaction partner, too, but such a perspective would be daring and is not comparable with literature, because it has never been done. An idea of how important the photon-number is has been given in the previous part (chapter 2.2.5). The reaction velocity v can be seen as change in the concentration of A:

$$v = \frac{d\ A}{dt} = -k\ A \tag{12}$$

Separating the variables, results in the following integral with the initial concentration at the beginning at a time t. Through integration the final form is gained:

$$\int_{A_0}^{A_t} \frac{1}{A} d\ A = -k \int_{t_0}^{t} dt \tag{13}$$

$$\rightarrow \ln \frac{A_0}{A_t} = kt \tag{14}$$

With the *Lambert Beer* law the concentrations can be calculated and with plotting the natural logarithm of the concentration ratio against the reaction time the slope becomes k. These reactions will start with a linear rise and later on flatten towards a constant value. For this method, it is important to only appraise the initial, linear part.

Table 16 gives an overview of all the photo-linkers that were investigated for kinetic measurements. (IR-spectra of them can be found in the Supplement section) The top four consist of a coumarin structure but represent different derivatives. Position 3´ and 4´ are substituted with either an electron withdrawing or donating group. Another ring is annulated or the protective group is changed. Together they represent a compact variety of what can be changed. The chalcone is an example for an open chain linker and the synthesized benzindenone stands for a small, compact, and highly conjugated linker. Figure 50 shows the UV-Vis spectra of the used substances.

name / structure	**ε(main Abs.); ε(355nm); FWHM (355 nm); M; ε(355nm)/M**
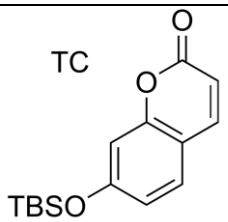	ε(317 nm) = 12500 L·mol^{-1}cm^{-1} ε(355nm) = 990 L·mol^{-1}cm^{-1} FWHM = 60 nm M = 276 g/mol ε/M = 3.6
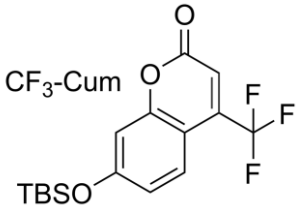	ε(328 nm) = 10500 L·mol^{-1}cm^{-1} ε(355 nm) = 3880 L·mol^{-1}cm^{-1} FWHM = 60 nm M = 344 g/mol ε/M = 11.3
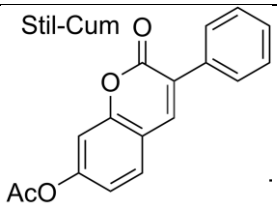	ε(324 nm) = 18300 L·mol^{-1}cm^{-1} ε(355 nm) = 4600 L·mol^{-1}cm^{-1} FWHM = 70 nm M = 280 g/mol ε/M = 16.4
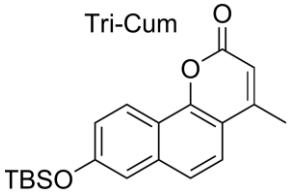	ε(330 nm) = 9600 L·mol^{-1}cm^{-1} ε(355 nm) = 8800 L·mol^{-1}cm^{-1} FWHM = 70 nm M = 340 g/mol ε/M = 25.9
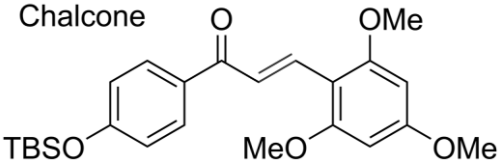	ε(315 nm) = 22050 L·mol^{-1}cm^{-1} ε(355 nm) = 2850 L·mol^{-1}cm^{-1} FWHM = 60 nm M = 429 g/mol ε/M = 6.6

name / structure	ε(main Abs.); ε(355nm); FWHM (355 nm); M; ε(355nm)/M
benzindenone 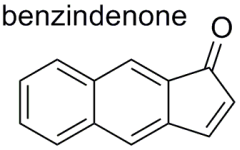	ε(400 nm) = 820 L·mol^{-1}cm^{-1} ε(355 nm) = 590 L·mol^{-1}cm^{-1} FWHM = 100 nm M = 180 g/mol ε/M = 3.3

Table 16: Different photo-linkers.

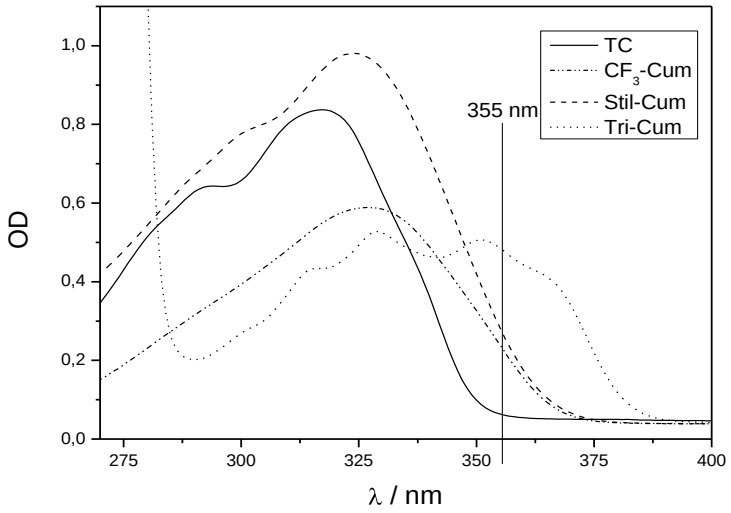

Figure 50: UV-Vis spectra of studied substances.

Preliminary test are made with 2 mL solutions of pure linker and 1:1, 10:1 mixtures with H5FU concentrations of 20 and 200 mmol/L which are irradiated for 20 min with 355 nm laser light at 66 µJ/pulse. The irradiated reaction mixtures are analyzed by HPLC with regards to number of stereoisomers and CD/HD ratio.

substance	dimerization	dimer yield / %	homodimer isomers	crossdimer isomers	CD/HD
TC	homo	54	3	-	-
	cross 1:1	63	3	3	0.4
	cross 10:1	95	3	3	2.9
CF_3-Cum	homo	60	1	-	-
	cross 1:1	68	1	1	0.05
	cross 10:1	89	1	1	0.4
Stil-Cum	homo	89	2	-	-
	cross 1:1	96	2	0	-
	cross 10:1	100	2	2	0.5
Tri-Cum	homo	-	0	-	-
	cross 1:1	55	0	1	-
	cross 10:1	100	0	3	-

Table 17: Preliminary laser irradiations.

Table 17 summarizes the laser illuminations. Only the TC reaction has complete turnover. TC is best adapted for the conditions (concentration and laser power), because it was the foundation for the laser synthesis. The Tri-Cum seems to be very slow reacting and almost no isomers are found under these conditions. Only TC produces crossdimer excess if only with a 10 fold H5FU overhead. The coumarin based molecules are all very likely to favor the homodimerization reaction. The benzindenone already absorbs in the visible region and therefore is of no use for a selective photolinker application. The chalcone exhibits lots of side products and low reactivity due to the *E,Z*-isomerization which is the preferred energy utilization of open chain compounds. Merely the coumarin derivatives are useful.

As a control experiment the homo- and crossdimerization at 10:1 is run for 72 h in the *Rayonet* reactor until completion. All the homodimers have gained one more peak, which in some cases is lactone opened, but in general more side products are visible. The Tri-coumarin has degraded to a great extend, unlike with the laser (Table 18).

substance	**dimerization**	**dimer yield / %**	**homodimer isomers**	**crossdimer isomers**	**CD/HD**
TC	homo	74	4	-	-
	cross 10:1	89	4	3	3.0
CF_3-Cum	homo	68	2	-	-
	cross 10:1	85	2	1	1.2
Stil-Cum	homo	88	3	-	-
	cross 10:1	94	3	2	2.0
Tri-Cum	homo	-	0	-	-
	cross 10:1	92	0	0	-

Table 18: Preliminary *Rayonet* reactor irradiation.

The kinetic measurement will depend on the ratio of photons to molecules and after excitation on the ratio of excited molecules to ground state reaction partners. As options, there is the variation of the cuvette thickness, the laser intensity, or the concentration. For comparability there are two different methods. Either the same concentration can be used for each substance which will result in completely different starting optical densities (OD), or the same starting OD can be collimated which will mean different concentrations. To be clear, whichever parameter is tuned, the initial ratio of TC and H5FU will always be 10:1.

a) Constant concentration

First, a 1 cm thick cuvette is filled with 2 mL reaction mixture with a set 0.1 mmol/L concentration. This guarantees that all OD_{355} are below the value of 1 for linear absorption. The next Figures 51, 52 display all spectra and the evaluation graphs for the homo- and crossdimerization reactions.

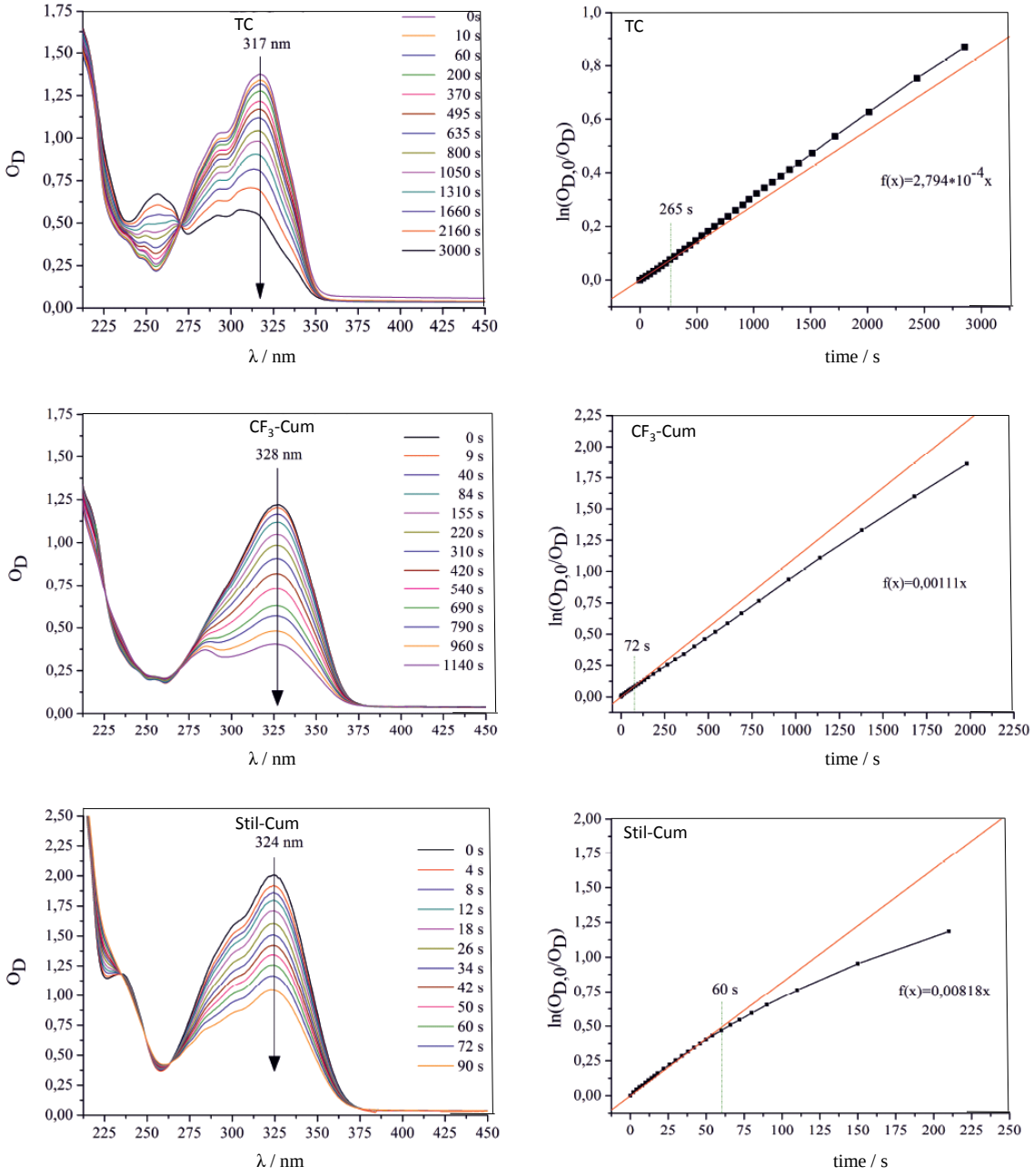

Figure 51: Kinetic of homodimerization; 10 mm cuvette.

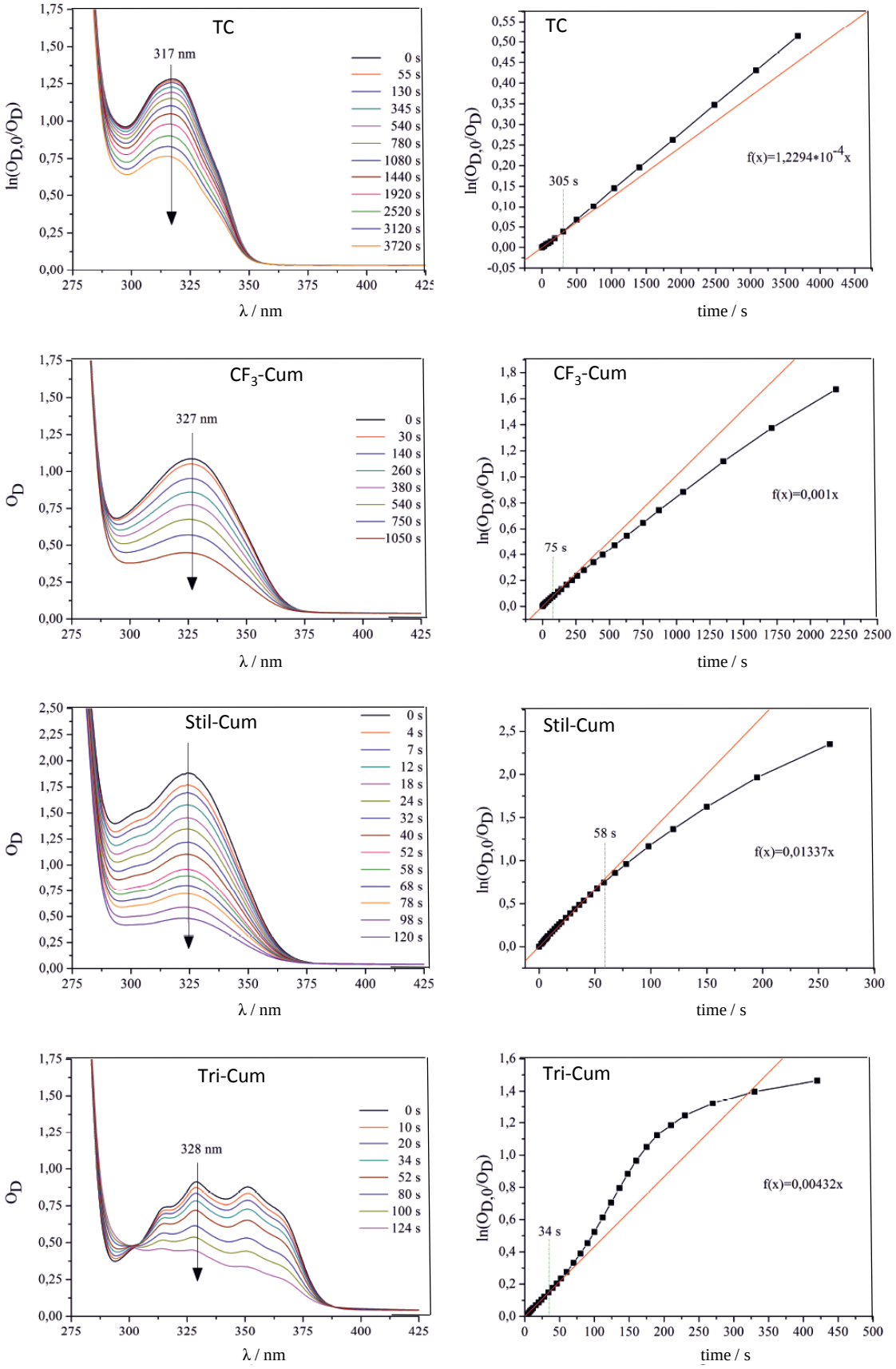

Figure 52: Kinetic spectra from 10:1 crossdimerization; 10 mm cuvette.

The number of points of the linear fit for every kinetic is deliberately chosen to guarantee that all mixtures have absorbed the same energy with t·ε = constant. The guideline for this constant is the fastest reaction of Stil-Cum. The reaction velocity declines from the Tri-Cum over the CF_3-Cum to the slowest the TC. Curiously, the homo- and crossdimerization speeds do not vary from each other with each photo-linker. Here, I can use the diffusion to explain the situation. Calculation of the diffusion distance and the possible to reach reaction partners show that an excited molecule has only 12 similar and 120 crosspartners available. So the reaction is less statistics than merely luck to occur. The TC reactions even show the homodimerization dominance which causes the homoreaction to be the faster one (Table 19).

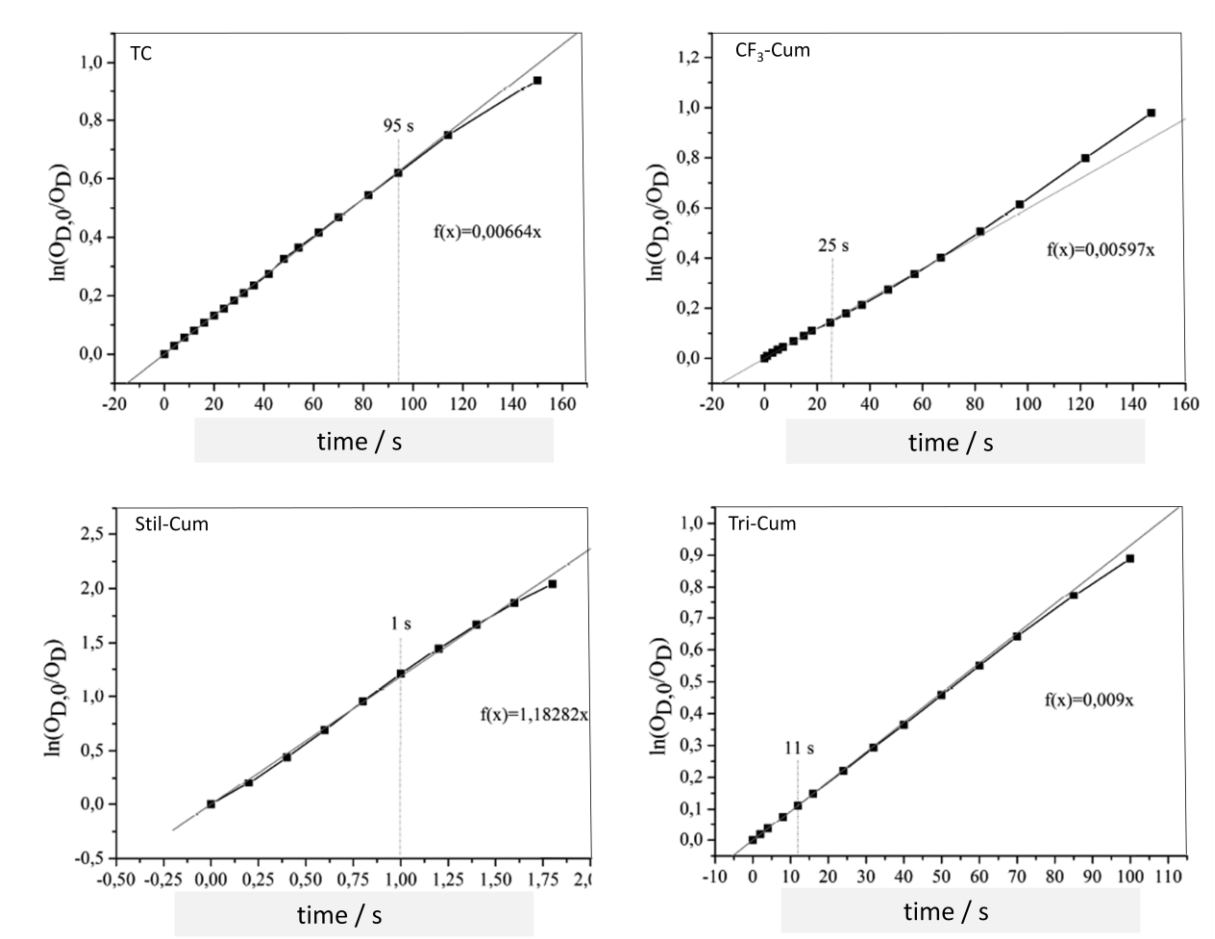

Figure 53: Kinetic of 150:1 crossdimerization; 10 mm cuvette.

substance	dimerization	k_{total} / s^{-1}	k_{total} (cross/homo)
TC	homo	$2.8 \cdot 10^{-4}$	
	cross 10:1	$1.2 \cdot 10^{-4}$	~ 0.5
	cross 1500:1	0.007	~ 25
CF_3-Cum	homo	0.001	
	cross 10:1	0.001	1
	cross 1500:1	0.006	6
Stil-Cum	homo	0.008	
	cross 10:1	0.013	~ 1.5
	cross 1500:1	1.2	~ 150
Tri-Cum	homo	-	
	cross 10:1	0.004	-
	cross 1500:1	0.009	

Table 19: Results of kinetic study.

To clear up the results, the concentrations of the coumarin component is raised to $1.25 \cdot 10^{-4}$ mol/L and a 1500 fold excess of H5FU is used to eradicate all doubts about collision quenching failure. Now, there are 24000 collision partners. The evaluation graphs are shown in Figure 53 and all results are summarized in Table 19. After increasing the H5FU concentrations the ratios of cross- to homodimerization have changed. Again, it is clear to see that the homodimerization is the destined reaction. Only with Stil-Cum can a direct 150 times increase be seen. For all the other reactions, the low concentration of reaction partners meant to little ground state molecules in their grasp. The constant concentration kinetics in a thick cuvette are not that clear cut. A thinner cuvette and constant OD should clarify the results.

b) Constant absorption (OD)

The path length of the light is shortened from 10 to 2 mm and an initial OD of about 1 is used. The graphs can be seen below (Figure 54, 55) and Table 20 collects all results. The fits are all made to have the same change in OD. The TC molecule now is a lot better with the crossreaction which might indicate that the homodimerization is below the diffusion limit at these low concentrations. The CF_3-Cum is faster than the TC and exhibits the 10:1 ratio. Stil-Cum is again the fastest, but the difference for cross- and homodimerization has completely vanished. So we see, that the previous kinetic did fall short of the critical diffusion controlled concentration. The Tri-Cum again holds the second fastest velocity, but this time the values for cross- and homodimerization are much more in balance. The smaller cuvette with higher initial concentrations suits a laser driven kinetic better.

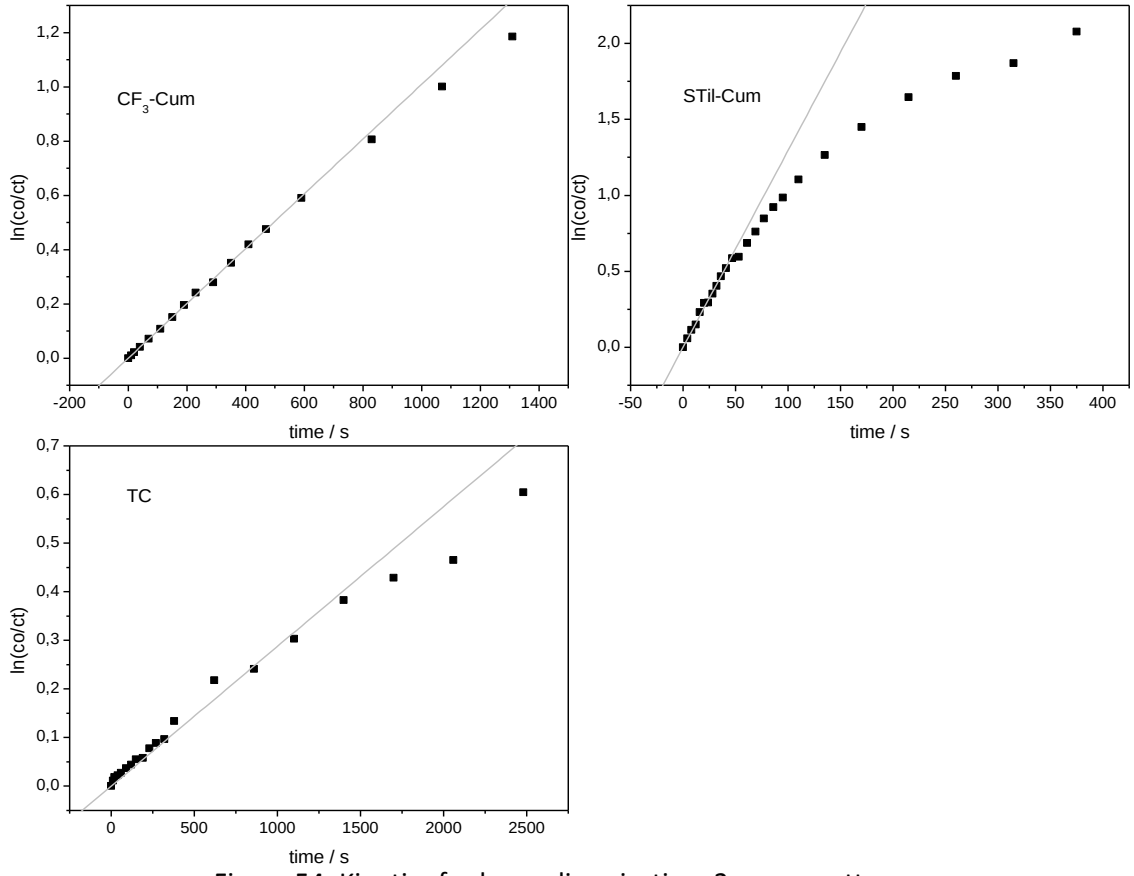

Figure 54: Kinetics for homodimerization; 2 mm cuvette.

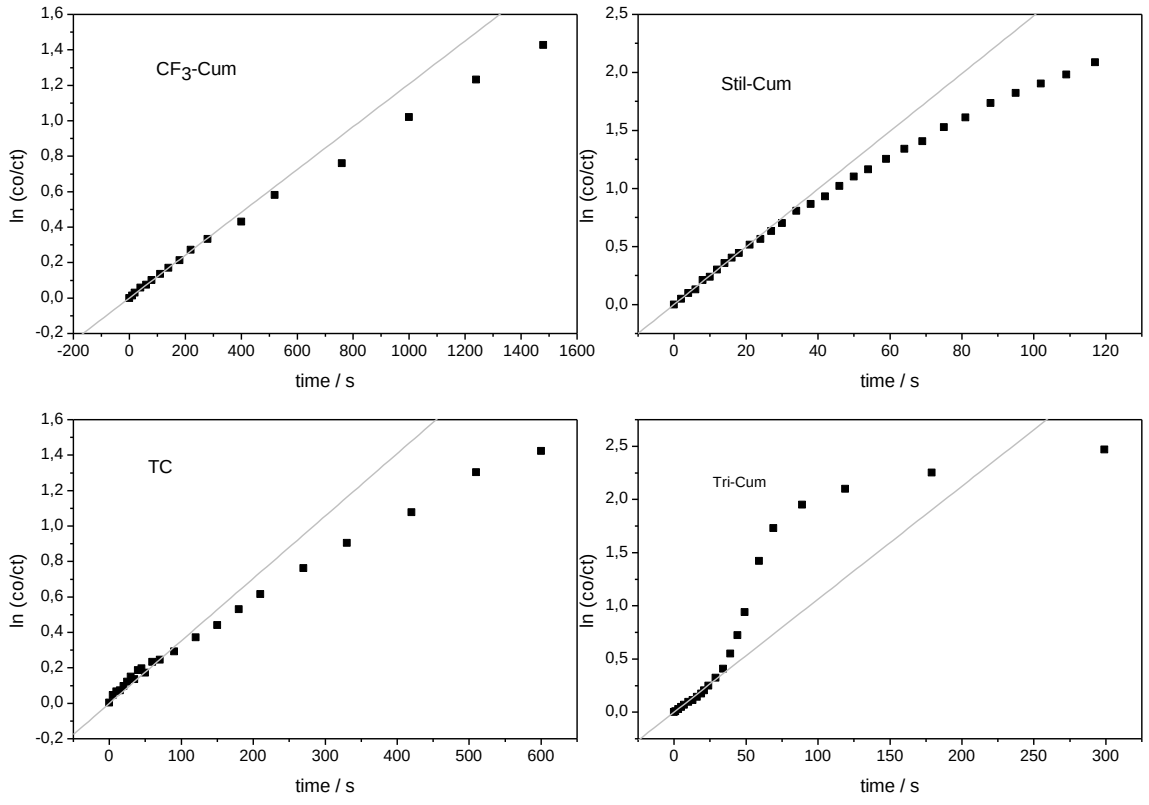

Figure 55: Kinetics of crossdimerization 10:1; 2mm cuvette.

substance	dimerization	k_{total} / s^{-1}	crossdim./homodim.
TC	homo	$2.4 \cdot 10^{-4}$	
	cross 10:1	$3.9 \cdot 10^{-3}$	~ 16
CF_3-Cum	homo	$9.7 \cdot 10^{-5}$	
	cross 10:1	$9.3 \cdot 10^{-4}$	~ 10
Stil-Cum	homo	$8.8 \cdot 10^{-3}$	
	cross 10:1	0.018	~ 2
Tri-Cum	homo	-	
	cross 10:1	0.011 (0.2 for 65s)	-

Table 20: Kinetic results for constant OD.

Another possible way to measure the kinetics is to record the transmission intensity. Within the smaller 2 mm cuvette not all photons are absorbed and a good fraction of them is transmitted. As the reaction proceeds, more and more coumarin is turned over and the transmission increases. The change in transmitted intensity I, according to *Lambert Beer*, is proportional to the TC decrement dc/dt. Parallel HPLC measurements deliver the concentration of the product of TC and H5FU which can also be used to determine k. The kinetic constant turns out to be k_{total} = 0.0028 which is close to the precisely determined one above (TC cross 10:1). Figure 56 shows the measurements.

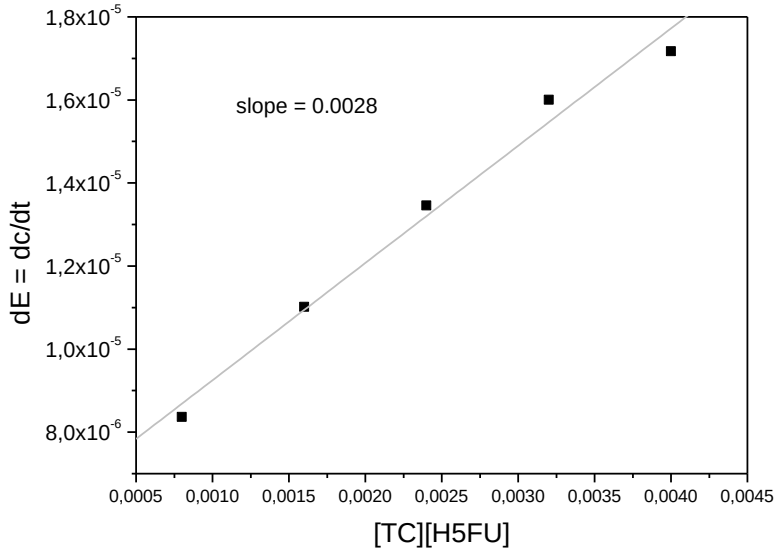

Figure 56: Kinetic transmission measurements.

All these molecules are very different in structure and then probably in their excited state lifetime. However, there are some trends to be deduced from the kinetic studies. TC has a free accessible double bond whereas all the other three are substituted. The phenyl-group has proven, with the second kinetic series, to be inconsequential. The methyl- or trifluoromethyl-group are more of a steric hindrance. Especially, the Tri-Cum does not seem to form homodimers very well. When extreme conditions are chosen, together with long reaction times, the Tri-Cum and methylcoumarin both also form homodimers, but with the conditions from above nothing is happening. When compared, it turns out that the -CF_3 is bigger in volume than the -CH_3. The steric hindrance therefore does have impact but is no sufficient answer to a varying reactivity (Figure 57).

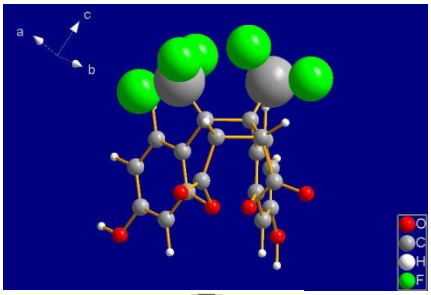

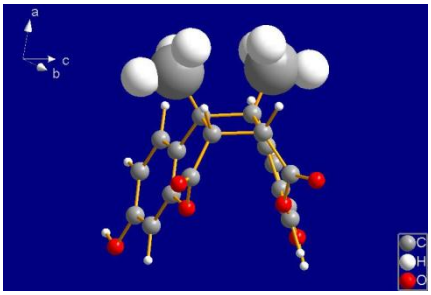

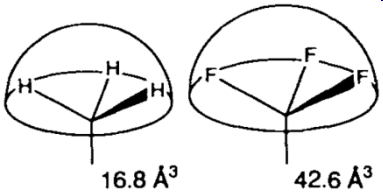

substituent	vdW radius / Å	vdW volume / Å³
CH_3	1.6	16.8
CF_3	2.7	42.6

Figure 57: -CH_3, -CF_3 -coumarin comparison.

(Values from [112], 3D-model made in *Diamond*)

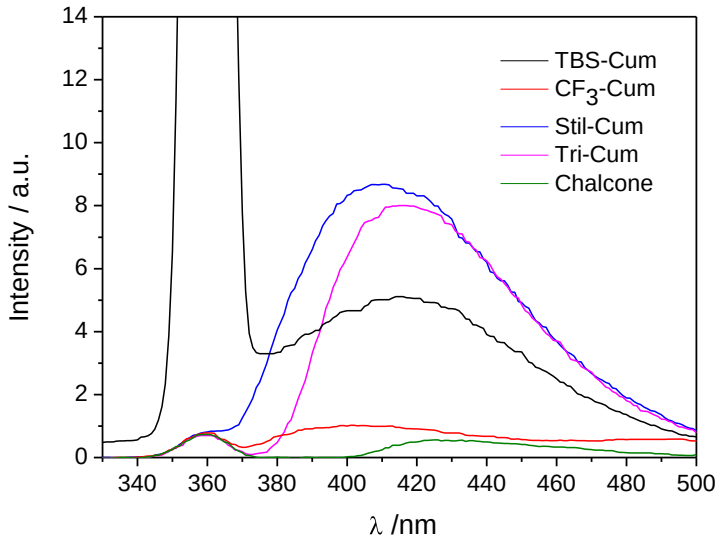

Figure 58: Fluorescence of kinetic substrates.

To find out about the lifetimes, fluorescence measurements with equal concentrations are made (Figure 58). An excited molecule can do intersystem crossing, fluoresce, or lose its energy via internal conversion. The longer the lifetime of the excited state is the better the fluorescence should be because the ISC is generally only a few %. A general overview of time frames is presented in Table 21.

process	transition	timescale / s
internal conversion	$S_n \rightarrow S_1$	10^{-14} to 10^{-11}
vibrational relaxation	$S_n^* \rightarrow S_n$	10^{-12} to 10^{-10}
intersystem crossing	$S_1 \rightarrow T_1$	10^{-11} to 10^{-6}
fluorescence	$S_1 \rightarrow S_0$	10^{-9} to 10^{-6}
phosphorescence	$T_1 \rightarrow S_0$	10^{-3} to 100
non-radiative decay	$S_1 \rightarrow S_0$	10^{-7} to 10^{-5}

Table 21: Time scale for transitions.

In section 2.2.3 it is illustrated how the lifetime of the excited state can be measured by the integrated absorption coefficient IAC. In essence: the bigger the IAC the longer is the lifetime. In Figure 58 it is clear to see that the Tri-Cum, even though it has by far the biggest absorption cross section for 355 nm, has only the second highest fluorescence peak. The winner again is the Stil-Cum. Hence, a possible explanation for the Tri-Cum result might be a short excited state lifetime. The chalcone is at the bottom of the graph and again shows its miserable energy utilization.

So far, I have mentioned the substitution and the lifetime as important for the reaction speed but the third and most variable factor is the molecular weight. Because the diffusion is such a great part of the reaction, the movement is critical. To visualize this relationship, hydroxycoumarin was also protected with an acetyl protective group instead of the TBS one in TC. Unfortunately, the new group shifted the absorption too far hypsochrom for 355 nm to have any kind of absorption (Figure 59).

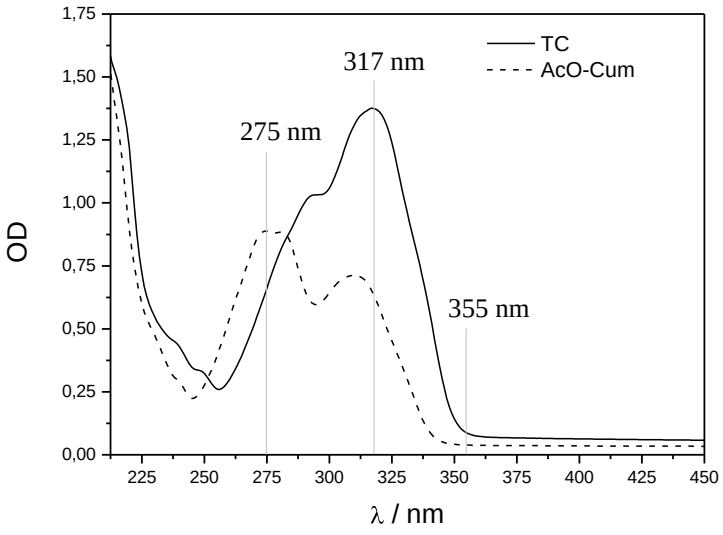

Figure 59: Acetyl protected hydroxycoumarin.

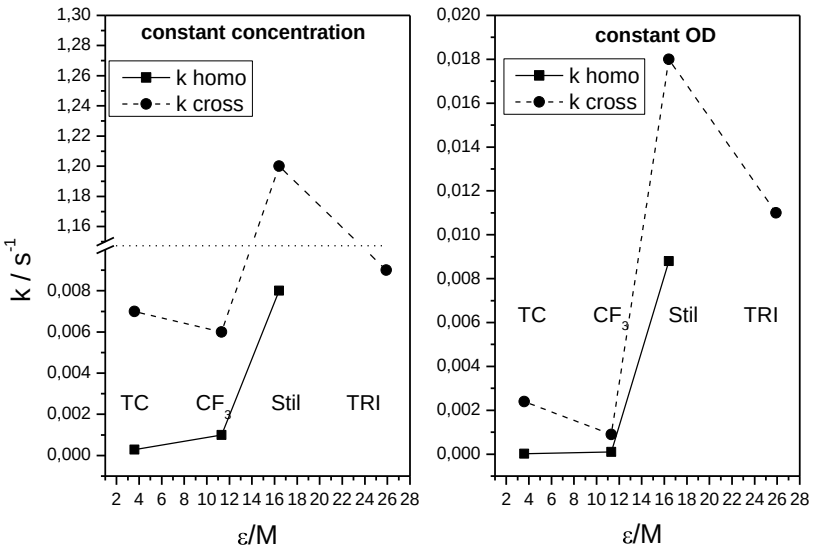

Figure 60: Reaction constants depending upon absorption/mass quotient.

It is clear from the kinetic measurements that the smaller, lighter substrates are reacting faster than the larger ones. Therefore, the quotient of the absorption coefficient ε_{355} divided by the molar mass M is plotted against the kinetic constant k (Figure 60). Both kinetics result in the same message. The Stil-Cum is the fastest to react and a mid ratio of absorption to mass is good. Obviously a smaller mass would be better, but a certain amount of conjugation needs some functional groups. Conclusively, it is very important to realize that a high absorption at the laser wavelength, at high (~mmol/L) concentrations does not provide the fastest dimerization reaction! For an efficient reaction, the concentration has to be collimated with the light intensity. To do so a kinetic measurement can help to find the right balance.

c) Reaction rates

Kinetic measurements are great to gain more insight into the reaction. On the downside, they are time consuming and labor intensive. To just find out whether a linker, a reaction, or a set up works it is easier to determine the starting reaction rate. For TC reactions it is best to simply monitor the decline in TC concentration with HPLC measurements at different time spans during the reaction. Again, the exemplary reaction of TC + 10 H5FU is used with equal laser intensity and equal concentrations in three different set ups. All setups can be seen in the corresponding section 2.2.4. There is the most simple and effective direct irradiation, the standard 2 mm cuvette, and the high volume flow cell. To compare these completely different systems a constant is created again to make

all three experiments comparable. The ratio of irradiation time divided by the reaction volume is to stay fixed around 800 s/mL (Figure 61). Table 22 displays the reaction rates. In whichever set up, the laser is fast in delivering product and because of the flow cell, the laser is also scalable.

system	reaction rate R / nmol/s
direct irradiation	12.9
2 mm cuvette	19.8
flow cell	12.6

Table 22: Reaction rates.

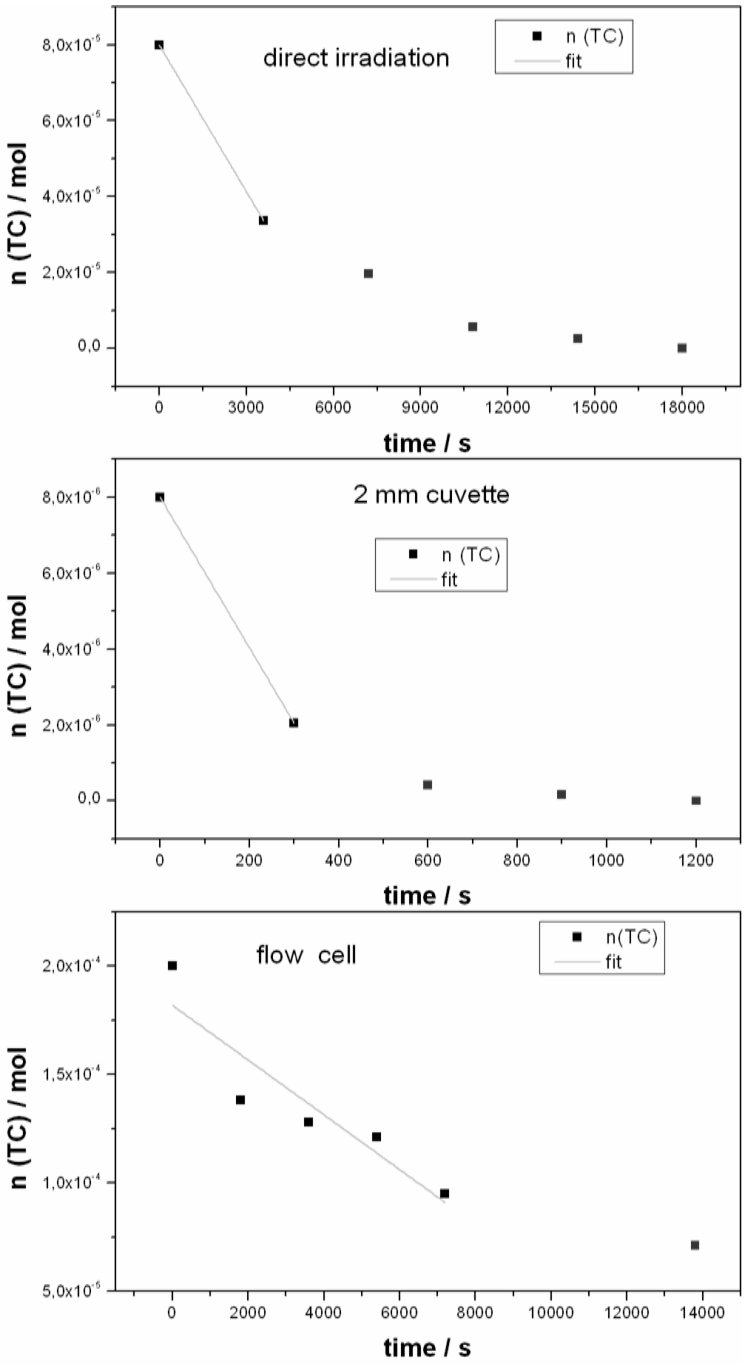

Figure 61: Reaction rates R.

When the laser is compared to the *Rayonet* reactor, the concentration based reaction rates for the laser R_L = $3.0 \cdot 10^{-3}$ mol·L^{-1}·min^{-1} and the *Rayonet* reactor R_{RR} = $1.3 \cdot 10^{-5}$ mol·L^{-1}·min^{-1} seam very different, but are actually close when the volume is factored in.

d) Quantum yield

In general, photoreactions are compared by their quantum yield. This value quantifies the number of products formed for every absorbed photon. The *Rayonet* reactor has an average power of 4.71 W. Its main emission is at 350 nm which means that every photon ph carries the energy of ph_{350} = $5.676 \cdot 10^{-19}$ J. The number of photons per second and square centimeter is n_{RR} = $8.29 \cdot 10^{15}$ s^{-1}cm^{-2}. The laser on the other side has a monochromatic emission at 355 nm with every photon having ph_{355} = $5.596 \cdot 10^{-19}$ J. Its beam diameter can be varied, so no area dependence is needed. The mainly used power at the cuvette is 0.66 W which is a number of photons of n_L = $1.18 \cdot 10^{18}$s^{-1}. To completely dimerize 1 mL of 0.02 mmol/L TC solution with n_{TC} = $1.20 \cdot 10^{19}$ molecules and 0.2 mmol/L H5FU the *Rayonet* reactor needs 48 h and the laser 20 min. With an area of A = 4 cm² per mL in the quartz tubes the quantum yield for the *Rayonet* reactor is:

$$\Phi_{RR} = \frac{n_{TC}}{n_{RR} \cdot A \cdot t} = \frac{1.20 \cdot 10^{19}}{8.29 \cdot 10^{15}\,\mathrm{s}^{-1}\,cm^{-2} \cdot 4cm^{2} \cdot 172800\,\mathrm{s}} = 2.1 \cdot 10^{-3} \qquad (15)$$

The quantum yield for the laser is:

$$\Phi_{L} = \frac{n_{TC}}{n_{L} \cdot t} = \frac{1.20 \cdot 10^{19}}{1.18 \cdot 10^{18}\,\mathrm{s}^{-1} \cdot 1200\,\mathrm{s}} = 8.5 \cdot 10^{-3} \qquad (16)$$

Compared to literature values for quantum yields of $1 \cdot 10^{-3}$ in DCM and $9 \cdot 10^{-4}$ in ACN for the homodimerization of the lighter non-substituted coumarin, these values are a little better.[109] But the literature fails to describe how these values were measured or calculated. Considering the complexity of this diffusion controlled reaction and more weight, due to the protective group, I think of these quantum yields as high.

2.4. Reversibility

The [2+2]-photocycloaddition so far proofed to be a reliable tool for the build up of crossdimers. Even better is the reversibility of this reaction. Due to the loss of conjugation of the two parent molecules the created dimer will have a hypsochrom shifted absorption of at least 20 nm. For coumarin molecules the cyclobutane cleavage wavelength is below 300 nm and other dimers tend to require the same range. This reversibility then completes the functionality of dimeric structures, so that they can be used as photo-linkers. Through irradiation with light of two different wavelengths dimers can be formed or cleaved. Applications range from drug delivery and diffractive index tuning to polymer coupling.[113,114] The cycloreversion reaction in general regenerates the two starting molecules in a symmetric cleavage. As a side reaction the ring opening can also occur asymmetric, producing new molecules.[81-84] (s. 2.3.1) Fortunately this happens seldom. Light is the best controllable cleavage tool for cylcobutanes, but some dimers have shown to be cleaved thermally or through shear on chromatography columns.

2.4.1. Single photon absorption (SPA)

To determine the quantum efficiency of the single photon absorption (SPA), solutions of the isolated stereoisomers of the dimers are irradiated under stirring with 266 nm at room temperature in a d = 1 cm quartz cuvette. The rate is measured with the increasing absorption of released TC at 316 nm. From the *Lambert Beer* law the concentration can be calculated with the absorption coefficient of TC ε_{316} (TC) = 12907 $L \cdot mol^{-1} \cdot cm^{-1}$ and the optical density.

$$c = \frac{OD}{\varepsilon_{316} \cdot d} \tag{17}$$

c = concentration of TC

A plot of the concentration against the irradiation time delivers with its slope the initial reaction velocity v_0 of the cycloreversion reaction.

$$\Delta v_0 = \frac{\Delta c}{\Delta d} \tag{18}$$

Therefrom, the number of cleaved molecules per second n_m can be calculated with the volume V and the *Avogadro* constant N_A.

$$n_m = \frac{\Delta c}{\Delta t} \cdot V \cdot N_A \tag{19}$$

To figure out the number of absorbed photons, the assumption is made, that all photons are absorbed in the solution. The energy of one photon at 266 nm is E_{266}:

$$E_{266} = h \cdot \frac{c}{\lambda} = 7.466 \cdot 10^{-19}\, J \tag{20}$$

h = *Planck* constant, c = velocity of light;

The number of absorbed photons per second n_P then can be determined from the power of the light source P.

$$n_P = \frac{P}{E_{266}} = \frac{5{,}33 \cdot 10^{-4} W}{7.466 \cdot 10^{-19}\, J} = 7.14 \cdot 10^{14}\, s^{-1} \tag{21}$$

The quantum efficiency for the SPA process Φ_{SPA} is:

$$\Phi_{SPA} = \frac{n_m}{n_P} \tag{22}$$

The following Figures 62-65 show the absorption spectra, the reaction velocity determinations, and the values for each experiment, as well as the absorption cross sections at 266 nm for SPA σ_{SPA}.

$$\sigma_{SPA} = 1000 \cdot \ln(10) \cdot \frac{\varepsilon}{N_A} \tag{23}$$

a) TC-homodimer; syn, head to head

V= 2.5 mL

c_0= 0.49 mmol/L

v_0= $1.76 \cdot 10^{-7}$ mol·L^{-1}·s^{-1}

n_m= $1.33 \cdot 10^{14}$ s^{-1}

Φ_{SPA}=0.186

ε_{266}=2210 L·mol^{-1}·cm^{-1}

σ_{SPA}=$8.45 \cdot 10^{-18}$ cm²

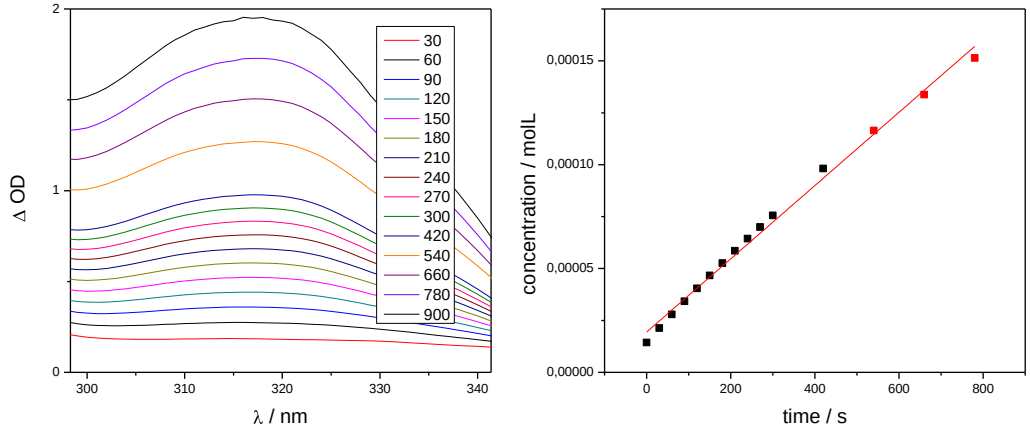

Figure 62: SPA of syn-hh HD.

For every homodimer cleaved there are two TCs generated which has to be factored into the calculation.

b) TC-H5FU-dimer; syn, head to tail; 1. CD

V= 2.5 mL

c_0= 0.99 mmol/L

v_0= $4.36 \cdot 10^{-8}$ mol·L^{-1}·s^{-1}

n_m= $6.57 \cdot 10^{13}$ s^{-1}

Φ_{SPA}=0.092

ε_{266}=1990 L·mol^{-1}·cm^{-1}

σ_{SPA}=$7.61 \cdot 10^{-18}$ cm^2

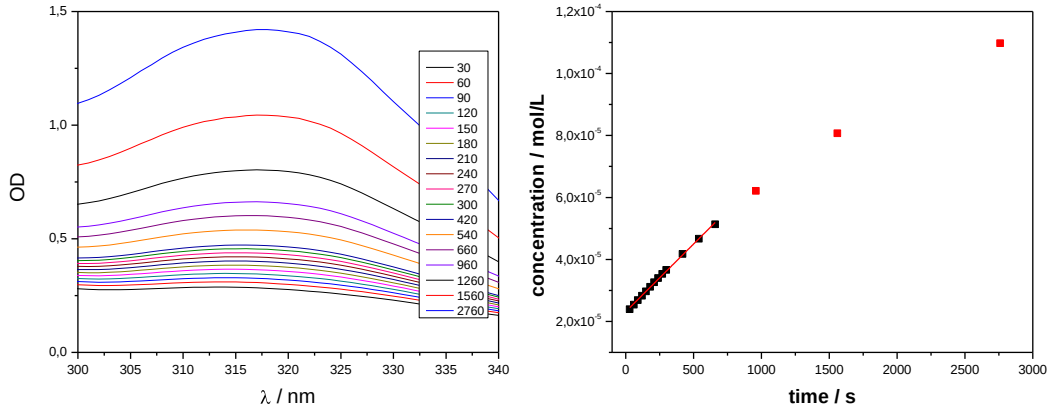

Figure 63: SPA of 1. CD.

c) TC-H5FU-dimer; syn, head to head; 2. CD

V= 2.5 mL

c_0= 0.99 mmol/L

v_0= $8.98 \cdot 10^{-8}$ mol·L^{-1}·s^{-1}

n_m= $1.35 \cdot 10^{14}$ s^{-1}

Φ_{SPA}=0.189

ε_{266}=2120 L·mol^{-1}·cm^{-1}

σ_{SPA}=$8.11 \cdot 10^{-18}$ cm^2

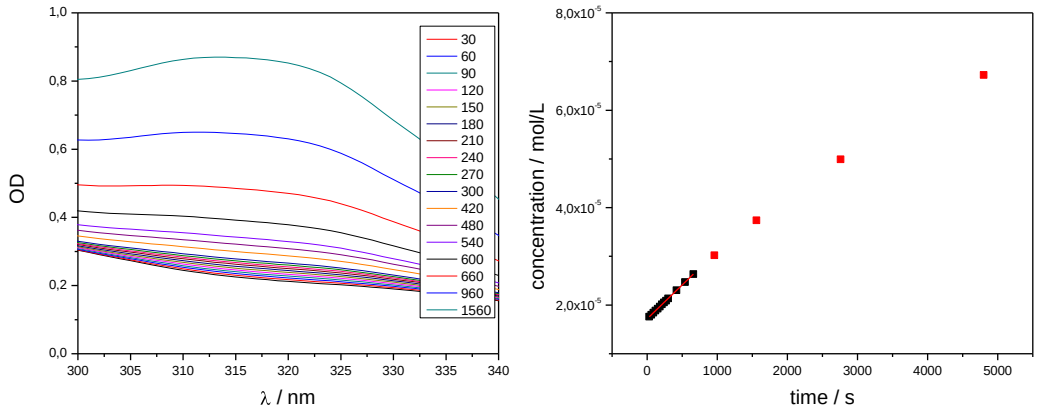

Figure 64: SPA of 2. CD.

d) TC-H5FU-dimer; anti, head to tail; 3. CD

V= 2.5 mL

c_0= 1.00 mmol/L

v_0= $1.39 \cdot 10^{-8}$ mol·L^{-1}·s^{-1}

n_m= $2.09 \cdot 10^{14}$ s^{-1}

Φ_{SPA}=0.029

ε_{266}=1070 L·mol^{-1}·cm^{-1}

σ_{SPA}=$4.09 \cdot 10^{-18}$ cm^2

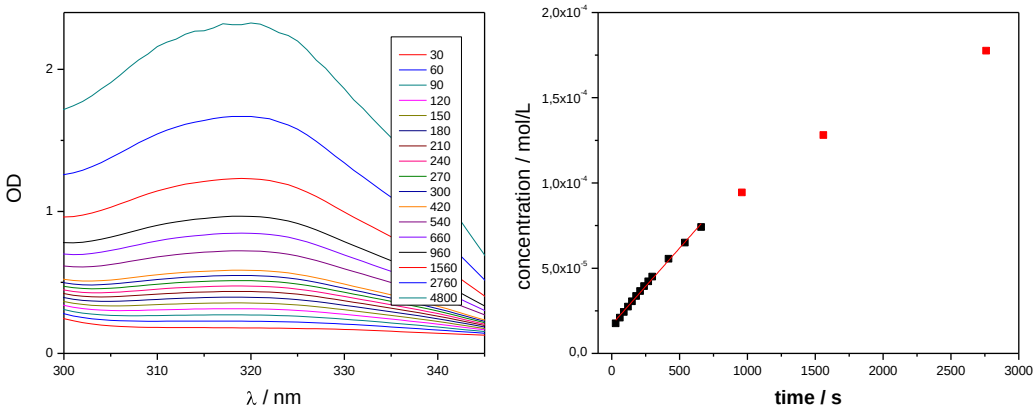

Figure 65: SPA of 2. CD.

stereoisomer	$\varepsilon_{266\,nm}$ / L/mol^{-1}·cm^{-1}	dipole moment / D	σ_{SPA} / cm^2	ratio σ_{SPA}	Φ_{SPA}	ratio Φ_{SPA}
TC-homodimer syn hh	2210 ± 55	6.7	$8.45 \cdot 10^{-18}$	2.07	0.186 ± 0.03	6.4
1. CD: TC-H5FU syn ht	1990 ± 43	4.9	$7.61 \cdot 10^{-18}$	1.86	0.092 ± 0.01	3.2
2. CD: TC-H5FU syn hh	2120 ± 53	5.8	$8.11 \cdot 10^{-18}$	1.98	0.189 ± 0.02	6.5
3. CD: TC-H5FU anti ht	1070 ± 22	3.7	$4.09 \cdot 10^{-18}$	1.0	0.029 ± 0.02	1.0

Table 23: SPA values.

The results are summarized in Table 23, with the nomination of 1., 2., and 3. CD from the HPLC chromatogram. If anything, these SPA values are a little too small because the generated TC can also absorb the cleavage wavelength. This divergence is deemed negligible within initial part of the reversion reaction which is why only the initial velocity is used to determine the quantum efficiency. The SPA values correspond well with the absorption coefficients, so the better the molecule absorbs 266 nm light, the better the cycloreversion works. At this point, I am not able to differentiate the absorption from any kind of thermodynamic stabilization effect on the cleavage, which might also come into play. The absorption cross sections do correlate well with calculated dipole moments, emphasizing the interaction of the photons with the polarity of the dimers. Interesting to notice is the syn-hh crossdimer which is in the range of the bigger homodimer. The crossdimer isomers differ in cleavage efficiency by a significant factor greater than 6. This distinction could be used in raising the efficiency of photo-switchable materials or drug release.

2.4.2. Two photon absorption (TPA)

To determine the two photon cross section, solutions of the stereoisomers in a 1 cm stirred quartz cuvette, at room temperature, were irradiated with 532 nm laser pulses. The velocity of the cleavage reaction is measured analogous to the SPA reaction by the absorption of TC. Because this reaction is more sensitive, the irradiated volume V_b needs to be calculated from the thickness of the cuvette d = 1 cm times the cross section area of the laser beam A = 0.138 cm ²

$$V_b = A \cdot d = 1.38 \cdot 10^{-4} L \tag{24}$$

With this irradiated volume the concentration of the effective cleaved molecules c_{eff} can be calculated:

$$c_{eff} = \frac{\Delta c \cdot V}{\Delta t \cdot V_b} \tag{25}$$

The number of photons per second can be derived from the pulse energy E_P, the pulse length t_P = 3 ns, and the energy of one photon at 532 nm $E_{532} = 3.73 \cdot 10^{-19}$ J:

$$n_P = \frac{E_P}{t_P \cdot E_{532}} \tag{26}$$

The photon flux can be gained by dividing n_P by A:

$$F = \frac{n_P}{A} \tag{27}$$

The two photon cross section δ_{TPA} then is:

$$\delta_{TPA} = \frac{c_{eff}}{\Phi_{SPA} \cdot F^2 \cdot c_0} \tag{28}$$

c_0 = starting concentration

Hereby, the assumption is made that the TPA quantum efficiency Φ_{TPA} is equal to the SPA quantum efficiency.[115] The following Figures 66-75 show the difference spectra and velocities together with the TPA values. Each isomer was irradiated with two different pulse intensities. HPLC measurements confirm the cleavage of the dimers into the substrates. The verification for a two photon process is made with a double logarithmic plot of the pulse intensity against the initial velocity. The ideal slope for this graph is 2, which can be deduced from the following formula:

$$\ln v_0 = \ln k + 2 \ln I \tag{29}$$

k = constant, I = intensity.

a) TC-homodimer; syn, head to head

V= 2.0 mL

c_0= 4.91 mmol/L

E_p= 52 mJ

v_0= $7.79 \cdot 10^{-11}$ mol·L^{-1}·s^{-1}

ceff= 0.565 mol·L^{-1}·s^{-1}

F= $3.36 \cdot 10^{26}$ s^{-1}·cm^{-2}

Φ_{SPA}= 0.029

δ_{TPA}= 0.55 GM

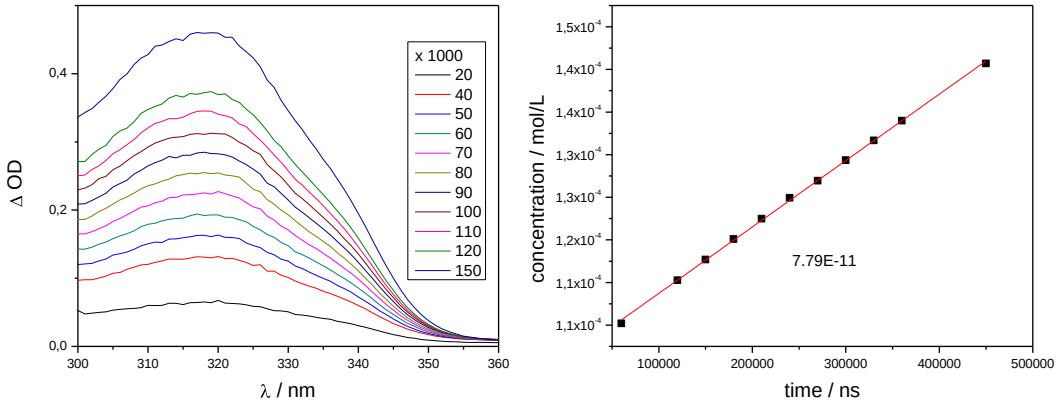

Figure 66: TPA of syn-hh TC homodimer.

b) 1. TC-H5FU-dimer; syn, head to tail; 1. CD

V= 2.0 mL

c_0= 4.96 mmol/L

Φ_{SPA}= 0.092

1. E_p= 58.4 mJ

F= $3.78 \cdot 10^{26}$ s^{-1}·cm^{-2}

δ_{TPA}= 0.51 GM

v_0= $2.30 \cdot 10^{-11}$ mol·L^{-1}·s^{-1}

c_{eff}= 0.340 mol·L^{-1}·s^{-1}

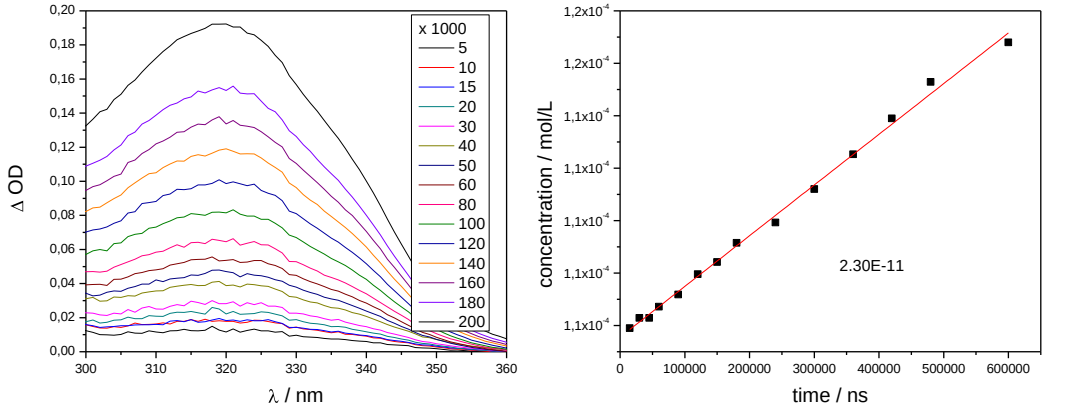

Figure 67: TPA of 1. CD at E_p= 58.4 mJ.

2. E_p= 72 mJ

v_0= $3.17 \cdot 10^{-11}$ mol·L^{-1}·s^{-1}

F= $4.66 \cdot 10^{26}$ s^{-1}·cm^{-2}

c_{eff}= 0.459 mol·L^{-1}·s^{-1}

δ_{TPA}= 0.46 GM

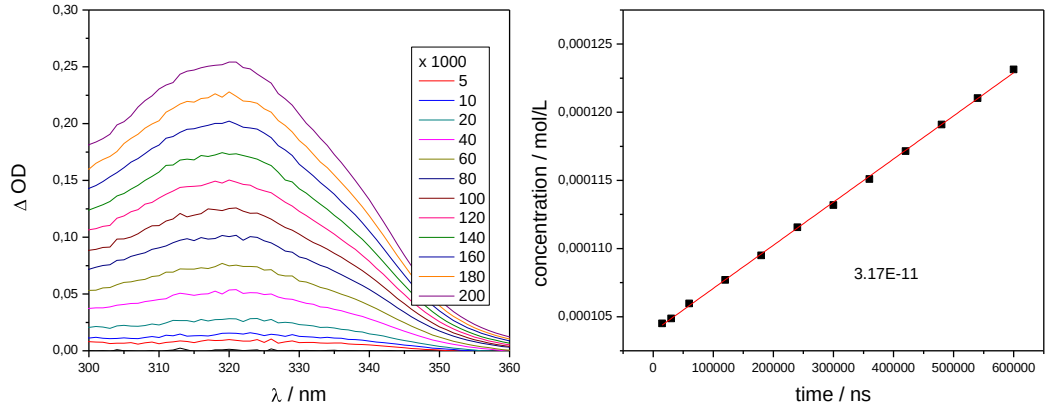

Figure 68: TPA of 1. CD at E_p= 72 mJ.

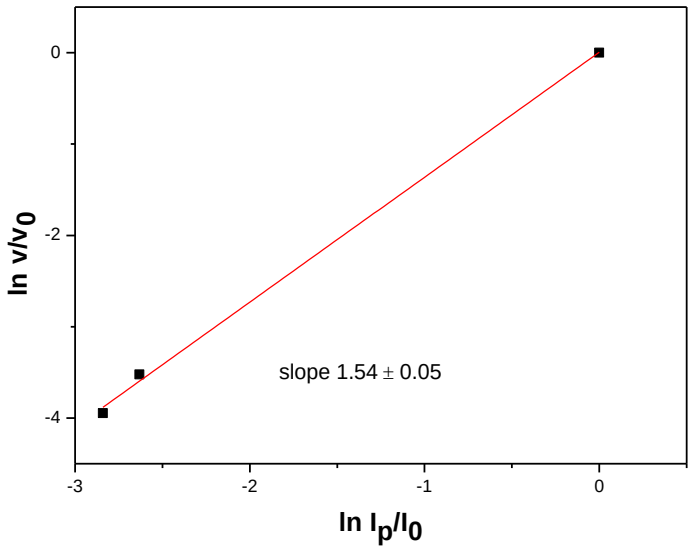

Figure 69: Double logarithmic plot of initial velocity and Intensity of syn,ht crossdimer.

The linear regression shows a slope of 1.54 ± 0.05, indicating a two photon process. The deviation from the expected value of two stems from non linear absorption of the created TC molecules and possible absorption of the excited dimer.

c) 2. TC-H5FU-dimer; syn, head to head; 2. CD

V= 2.0 mL

c_0= 4.97 mmol/L

Φ_{SPA}= 0.189

1. E_p= 60.5 mJ v_0= $2.58 \cdot 10^{-11}$ mol·L^{-1}·s^{-1}

F= $3.91 \cdot 10^{26}$ s^{-1}·cm^{-2} c_{eff}= 0.374 mol·L^{-1}·s^{-1}

δ_{TPA}= 0.69 GM

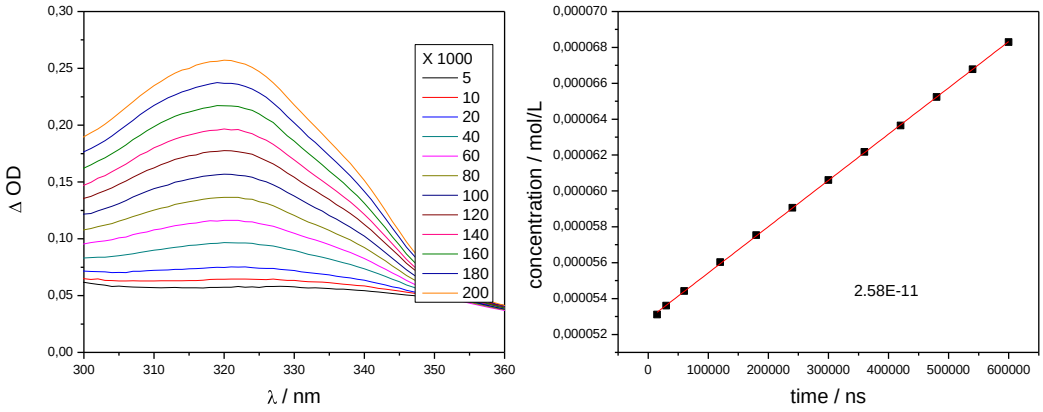

Figure 70: TPA of 2. CD at E_p= 60.5 mJ.

2. E_p= 70.6 mJ v_0= $3.65 \cdot 10^{-11}$ mol·L^{-1}·s^{-1}

F= $4.57 \cdot 10^{26}$ s^{-1}·cm^{-2} c_{eff}= 0.529 mol·L^{-1}·s^{-1}

δ_{TPA}= 0.62 GM

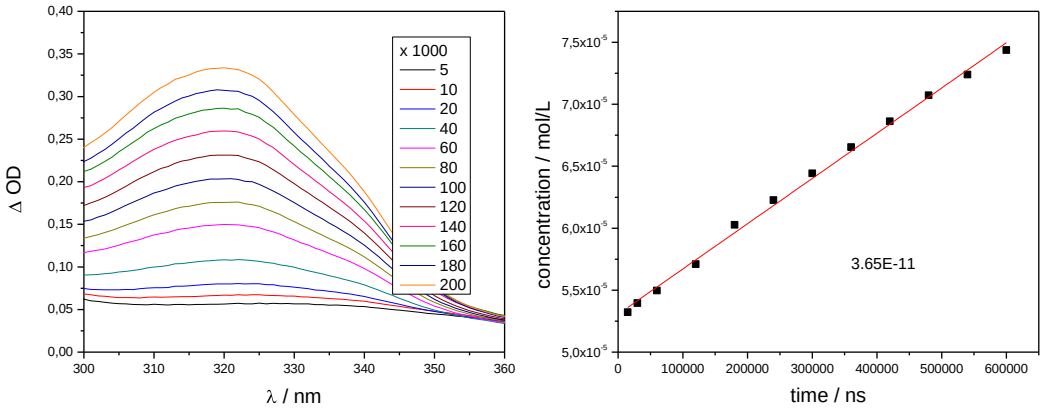

Figure 71: TPA of 2. CD at E_p= 70.6 mJ.

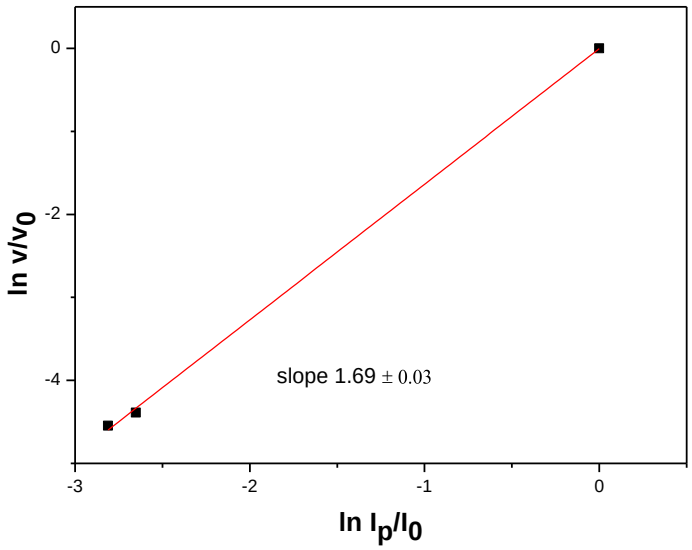

Figure 72: Double logarithmic plot for syn,hh crossdimer with slope of 1.69 ± 0.03.

d) 3. TC-H5FU-dimer; anti, head to tail; 3. CD

V= 2.0 mL

c_0= 5.0 mmol/L

Φ_{SPA}= 0.0.28

1. E_p= 60.1 mJ

v_0= $1.06 \cdot 10^{-11}$ mol·L^{-1}·s^{-1}

F= $3.89 \cdot 10^{26}$ s^{-1}·cm^{-2}

c_{eff}= 0.154 mol·L^{-1}·s^{-1}

δ_{TPA}= 0.26 GM

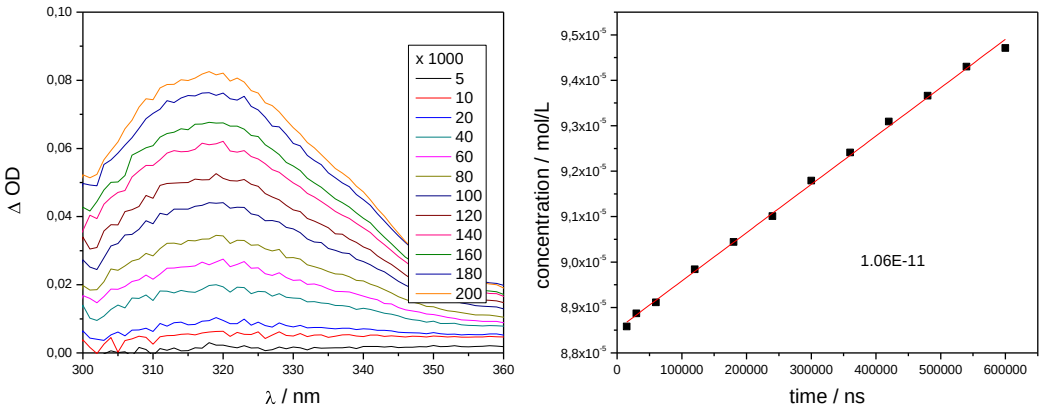

Figure 73: TPA of 3. CD at E_p= 60.1 mJ.

2. E_p= 70.5 mJ

v_0= $1.30 \cdot 10^{-11}$ mol·L^{-1}·s^{-1}

F= $4.56 \cdot 10^{26}$ s^{-1}·cm^{-2}

c_{eff}= 0.188 mol·L^{-1}·s^{-1}

δ_{TPA}= 0.27 GM

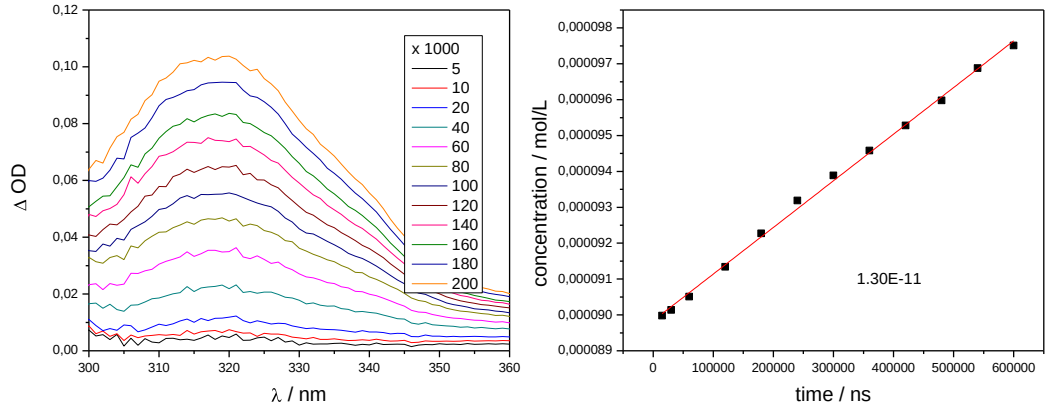

Figure 74: TPA of 3. CD at E_p= 70.5 mJ.

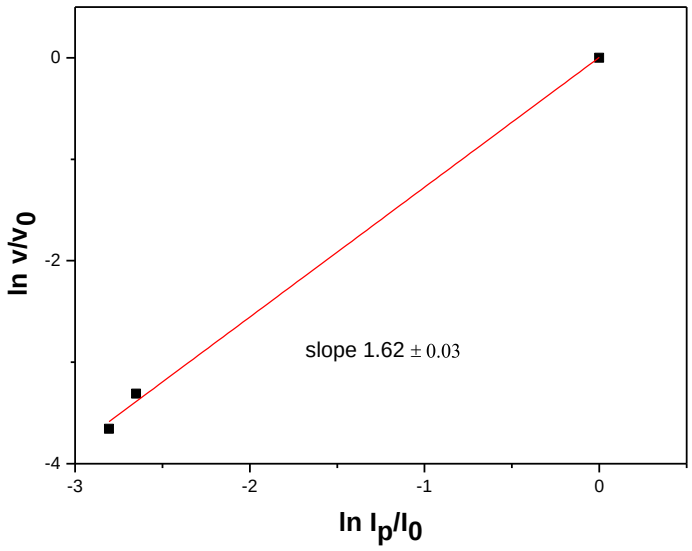

Figure 75: Double logarithmic plot for anti,ht crossdimer. The slope is 1.62 ± 0.03.

stereoisomer	Φ_{SPA}	Δ OD_{max} (316 nm)	δ_{TPA} / GM	ratio σ_{TPA}
TC-homodimer, syn ht	0.186	0.46 (2 TC) (E_p = 52 mJ)	0.55 ± 0.03	2.0
1. CD; TC-H5FU, syn ht	0.092	0.18 (E_p = 58 mJ)	0.49 ± 0.03	1.8
2. CD; TC-H5FU, syn hh	0.189	0.25 (E_p = 61 mJ)	0.66 ± 0.04	2.4
3. CD; TC-H5FU, anti ht	0.028	0.08 (E_p = 60 mJ)	0.27 ± 0.01	1.0

Table 24: Results of TPA measurements.

The ratios of the TPA cross sections are very similar to the ones of the SPA reaction, allowing their comparison (Table 24). Even though the TPA process generally has less structural dependency a difference in cleavage efficiency for the two photon reaction can be constituted. This difference is very important to lower the overall energy that needs to be induced in a two photon material for a reaction to take place.

2.4.3. Films

The cycloreversion is not only applicable in solution, but also in films the switching between covalent connected dimer and monomeric linker is possible. This feature can be used to link polymers, to change the optical density of the material, and to release drugs/molecules out of a polymer matrix.
At first, TC is dispersed in PMMA dissolved in chloroform and the mixture is spin coated onto a quartz glass window. The thickness of the films can be measured with the laser scanning microscope (LSM) because of refractive index variations at the upper and lower boundary of the film. The average thickness is about 12-14 µm (Figure 76).

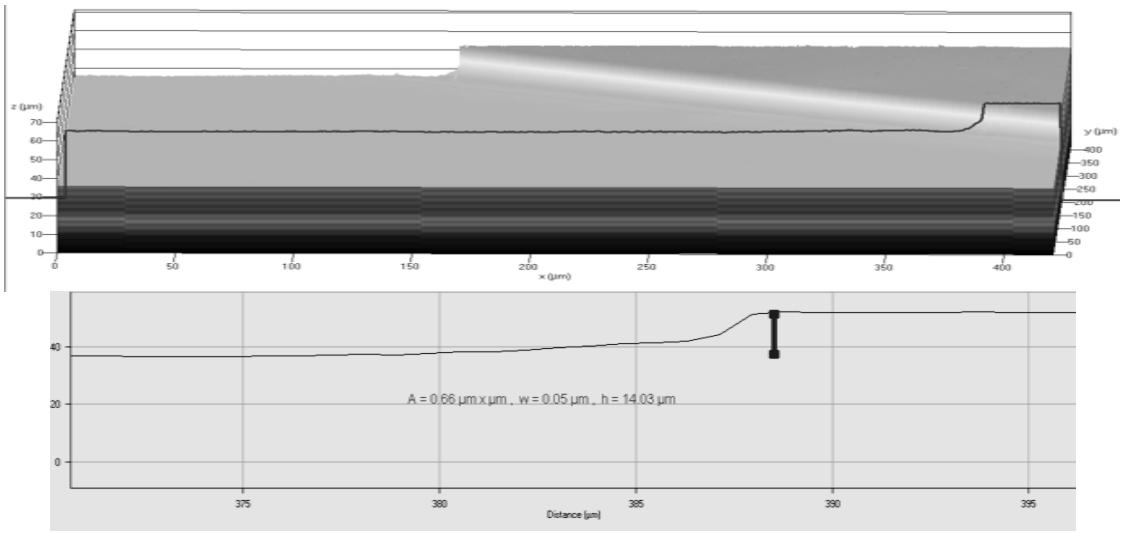

Figure 76: LSM film thickness determination.

Irradiation of the film with 355 nm laser light shows decrement of the optical density at 316 nm of TC. This dimerization reaction can be managed to a value of about 36% of the initial TC OD. Because of the rigid polymer matrix, not all TC molecules find reaction partners or they are in the wrong conformation to form dimers. Subsequent cycloreversion with 256 nm wavelength can only reestablish 74% of the initial OD. This phenomenon of uncompleted photo-switching can be explained by degradation, some minor side reactions, and equilibrium between the formation and cleavage of dimers at that wavelength.[116-118] The dimer formation requires more energy than the

cleavage because of the time it takes monomers to find each other and react together and because the 355 nm absorptivity is smaller than the 256 nm one (Figure 77).

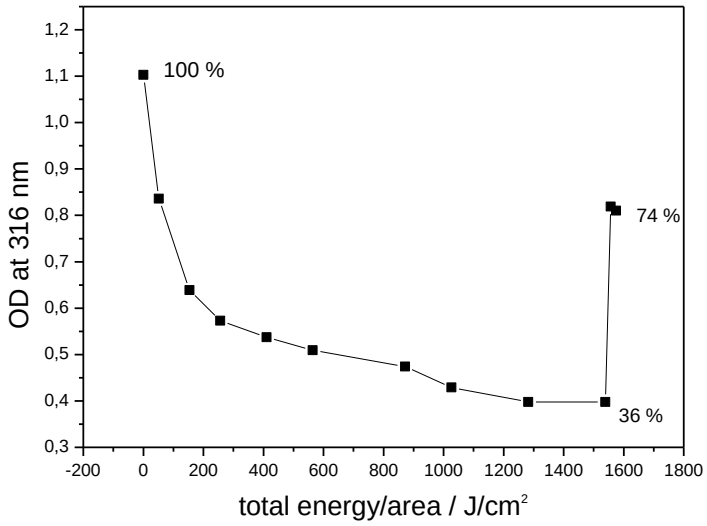

Figure 77: TC dispersed in PMMA.

Irradiation at 355 nm causes OD(TC) to drop and 256 nm increases the OD.

When TC, together with H5FU, is dispersed in the polymer, the photoswitching reaction is at least three times as fast. Due to the higher 10x H5FU concentration the TC molecules have a higher chance of forming a dimer, which needs less applied energy and results in a higher turnover of TC. Three consecutive cycles show a decreased dimerization and reversion for each cycle due to side reactions which might be caused by impeded heat distribution (Figure 78).

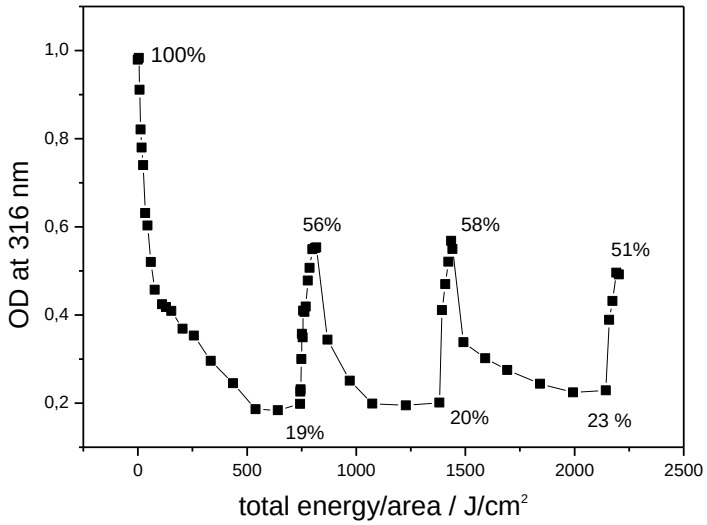

Figure 78: TC and H5FU dispersed in PMMA and irradiation at 355 and 256 nm.

2.4.4. After-treatment

When using a small cuvette, the laser powered reaction is completed within 20 min of irradiation. At that point all of the TC molecules have reacted to form dimers. Interestingly, if the irradiation is continued, then the CD/HD ratio keeps increasing. This after-treatment requires a longer time to show results but still works in favor of the dimer yield.

The majority of experiments are conducted in sealed half filled quartz cuvettes with acetonitrile (boiling point = 78 °C) as solvent. As most excited TC molecules dissipate the absorbed light energy by fluorescence and subsequent thermal dissipation the reaction solution heats up rapidly. In particular, when a pulsed laser is used as light source, the temperature inside the sample compartment reaches the boiling point of the solvent within minutes (Figure 79).

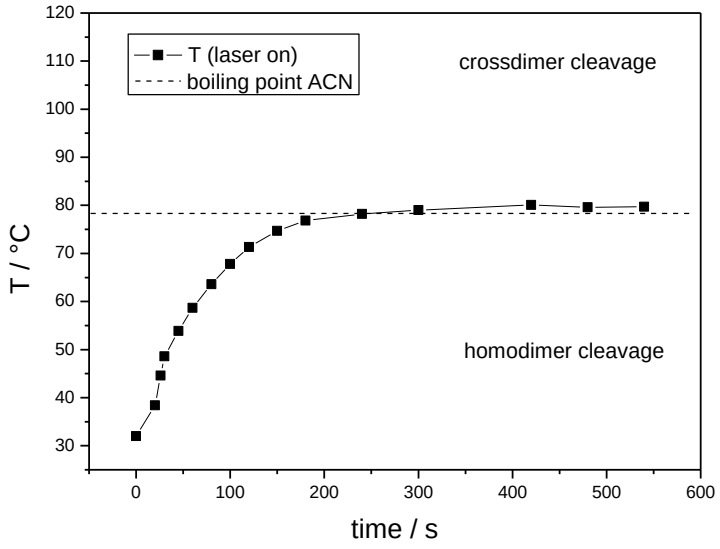

Figure 79: Temperature course inside sealed cuvette during laser-driven dimerization reaction. Temperature (■) rises until boiling point of acetonitrile (ACN) at 78 °C.

The laser thus induces heat into the reaction which can cause a thermal cycloreversion reaction. In solution, the cycloreversion reaction of other cyclobutane structures has been shown to be triggered by heat.[119-122] In this case, the TC crossdimers appear more stable towards thermal cleavage than the TC homodimers, enabling the selective cleavage of the homodimer entity by thermal treatment.

A flexible and reliable way to guarantee a constant reaction temperature within the 60 °C to 100 °C window, in which the homodimers decline and the crossdimers seem stable, is to use a solvent with a suitable boiling point.

The effect of homodimer cleavage can be seen with prolonged irradiation or with thermal treatment of the reaction mixture, before additional irradiation. Similar complex structures with a high

molecular weight and constrained rings on both sides, as compared to free moving substituents, exhibit activation barriers for the thermal cleavage of only about $E_A = 140 \pm 10$ kJ/mol (~34 kcal/mol).[123,124] It is uncertain whether the cycloreversion is a concerted or stepwise mechanism, but in both cases the *Woodward Hoffmann* rules could apply.[123]

2.4.5. Combining laser and thermal recycling

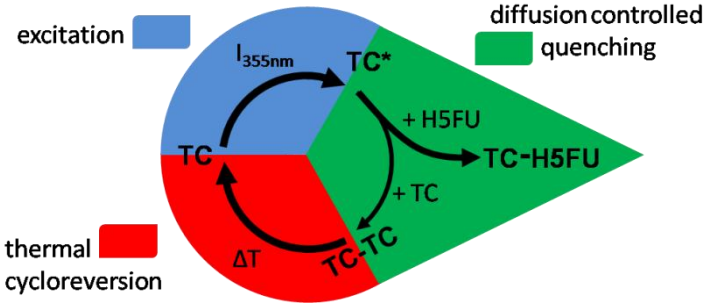

Figure 80: Combination of high intensity excitation (blue) and thermal recycling (red) helps diffusion controlled crossdimer build up (green).

Combined, the optimization of the photochemical process and the thermal recycling of homodimers describe a highly selective and versatile synthesis for intermolecular crossdimerization in solution. Figure 80 visualizes the two strategies to shift the CD/HD-ratio in strong favor of the crossdimer quantum. The first premiss is to selectively excite more molecules simultaneously, to obtain an improved CD/HD-ratio within each intense single laser pulse. This strategy was presented in chapter 2.2.5. The second one is to selectively cleave homodimers by thermal treatment and thereby improve the CD/HD-ratio. In Figure 81 the combination of both strategies for the selective preparation of crossdimers is featured as CD/HD-ratio output. Laser irradiation first creates a reasonable CD/HD-ratio with a completed reaction of TC. Heating at 90 °C then cleaves the homodimer side product while letting the crossdimer intact. Repeated laser synthesis consumes reestablished TC until almost all TC has been used up to form crossdimer with a CD/HD-ratio way beyond 30:1.

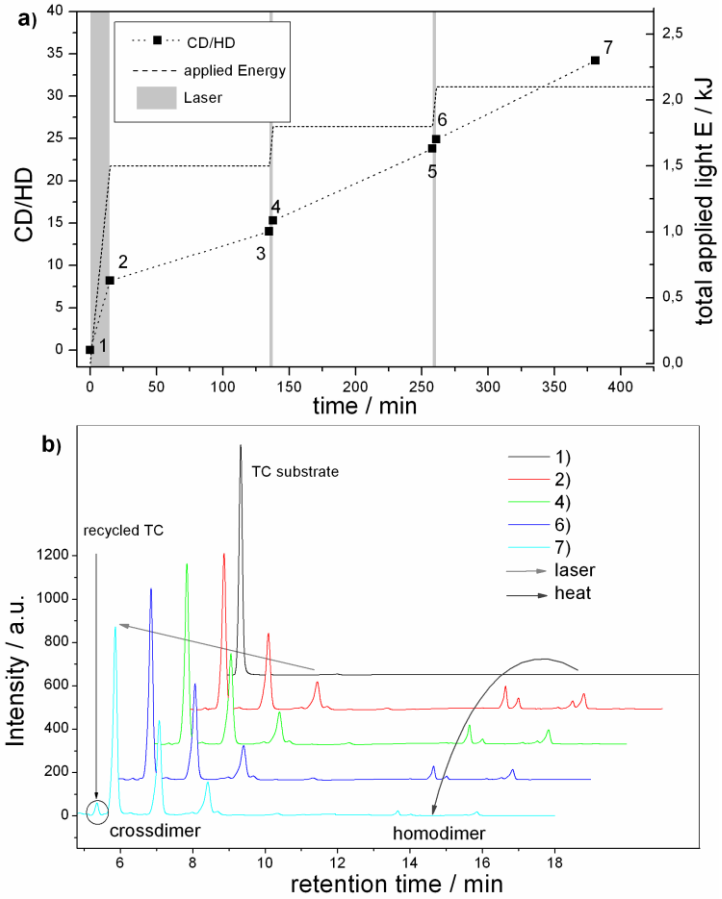

Figure 81: a) Alternating laser excitation and thermal treatment at 90 °C. The grey shaded areas represent the laser irradiation periods. b) HPLC measurements of each cycle of irradiation and thermal treatment. The numbers of the curves in b) correspond to the numbers in a).

		Start	**P**	**PTP**	**$P(TP)_2$**	**$P(TP)_2T$**
		(1)	(2)	(4)	(6)	(7)
c/mM	H5FU	200	182	181	180	180
	TC	20	-	-	-	0.22
	HD	-	2.18	1.22	0.78	0.56
	CD	-	17.4	18.2	18.4	18.4
$Yield_{CD}$ [%]		-	86.8	90.9	92.0	92.0
CD/HD-ratio		-	8.2	15.3	24.6	34.3

Table 25: Concentration of the components after several photochemical (P) and thermal (T) steps. The CD/HD-ratio describes the selectivity of the crossdimer formation.

After the initial 20 min laser step (1 → 2), heating at 90 °C for 120 min (2 → 3), followed by a second laser irradiation for 3 min (3 → 4), further thermal (4 → 5), photochemical (5 → 6) step, and a final

thermal step (6 → 7), a CD/HD-ratio of about 34 and a total crossdimer yield of 96% is obtained (Table 25). The irradiating steps are much more efficient than the thermal cleavage reaction which allows the simplification during laser irradiation to disregard cyclobutan cleavage. The reaction rate R for laser supported dimer synthesis (66 µJ/pulse) is $R = 3.0 \cdot 10^{-3}$ $mol \cdot L^{-1} \cdot min^{-1}$ measured in TC degradation. The *Rayonet* reactor is slower with $R = 1.3 \cdot 10^{-5}$ $mol \cdot L^{-1} \cdot min^{-1}$. The thermal degradation at 80 °C is 0.08 %/min which results in a half life of $t_{1/2}$ = 10.5 h. Both light driven reactions therefore are much faster than the thermal cleavage.

To check the presented concept of parallel photochemical synthesis and thermal cleavage I tested the low energy end of the scale. The sunlight intensity at wavelengths below 360 nm is low. The near IR radiation, of which about 90% is reflected by metals, may be used to heat the reaction vessel in a parabolic reflector (s. Table 8). A week of central Germany, bright, and warm summer sun produced a completed reaction with a CD/HD-ratio of 16:1 in a sealed reaction vessel with a yield of 92.2% and about 2% side products.

To sum everything up Table 26 shows the CD/HD-ratio for all the experiments with two substrate ratios 1:1 and 1:10. The combination of pulsed laser excitation and explicit thermal recycling generates a highly selective synthesis of crossdimers. These methods, the laser synthesis, and in some cases the thermal recycling, are adaptable to any kind of photochemical [2+2] dimerization reaction.

method	**TC:H5FU-ratio**	
	1:1	1:10
	CD:HD-ratio	
Rayonet reactor	0.2 ± 0.1	1.8 ± 0.2
laser, short pulse	1.1 ± 0.1	10 ± 1.4
sun + heat	2.8 ± 0.3	16.3 ± 1.5
laser + thermal	1.9 ± 0.2	34 ± 2.2

Table 26. CD/HD-ratio for two TC/H5FU substrate ratios and different reaction set-ups.

2.5. Derived reactions

The premiss so far was to learn as much as possible about photoreactions, then to understand in which way to setup a reaction, and how to influence it. Thereafter, I applied different strategies to improve the outcome and to improve upon the common methods. Lastly, I want to take two reactions and apply parts of my knowledge to them, in order to develop a concept, and to demonstrate a real life application.

2.5.1. [4+2]-heterocycloaddition

The *Schönberg-Mustafa* reaction was first discovered in 1944.[125,126] It uses plain sunlight to form a hetero *Diels-Alder* adduct. Mechanistically a 1,4-dioxane, which absorbs visible light, gets photoexcited and forms a dioxine structure via a [4+2]-cycloaddition reaction. The mechanism was originally thought to be concerted but modern literature speaks of a biradical mechanism which is depicted in Figure 82.[127]

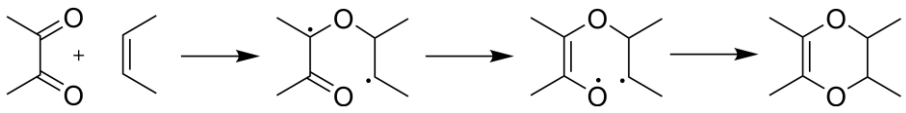

Figure 82: *Schönberg-Mustafa* reaction.

The original reaction utilized *ortho*-quinones as substrates. These molecules are willing to undergo the reaction to complete the ring aromatization. I use 2,3-butanedione as main substrate which is less reactive and needs to be activated with higher intensities for efficient product formation. The laser again is the perfect tool to excite many of these low absorbing molecules. This [4+2]-reaction, like the [2+2]-cycloaddition from above, is also an intermolecular, diffusion controlled reaction in solution. A variety of partner molecules is tested with ten-fold excess, which are listed in Table 27.

substance	reaction (info)	yield / %
tetrachloroethene	No (exciplex)	-
N-vinyl-2-pyrrolidinone	No	-
4-vinylbenzylchloride	No	-
dihydropyrane	Yes	54
2,3-methylbut-2-ene	Yes (sequential reaction)	86

Table 27: *Schönberg Mustafa*-reaction substrates.

These heteroaddition reactions seem to work well with stilbene like molecules because of their radical stabilization and electron donating group (EDG) properties.[128] I did not use stilbene, because it would also absorb the laser light at 355 nm. From Table 28 it is clear that the more electron withdrawing group (EWG) character the double bond substituents have, the less likely they are to react. On the other hand, the better the radical intermediate is stabilized, the better this reaction works. With TC, it is the same for the [2+2]-reaction as shown in 2.1.5. TC and 2,3-butanedione irradiated together form dimer as well, but both get excited, and therefore this reaction is not efficient. If 2,3-methyl-2-butene is the partner, the created molecule then has a new double bond. Under 355 nm irradiation, the 2,3-butanedione absorption at 420 nm decreases and the absorption of the generated double bond at 280 nm increases (Figure 83).

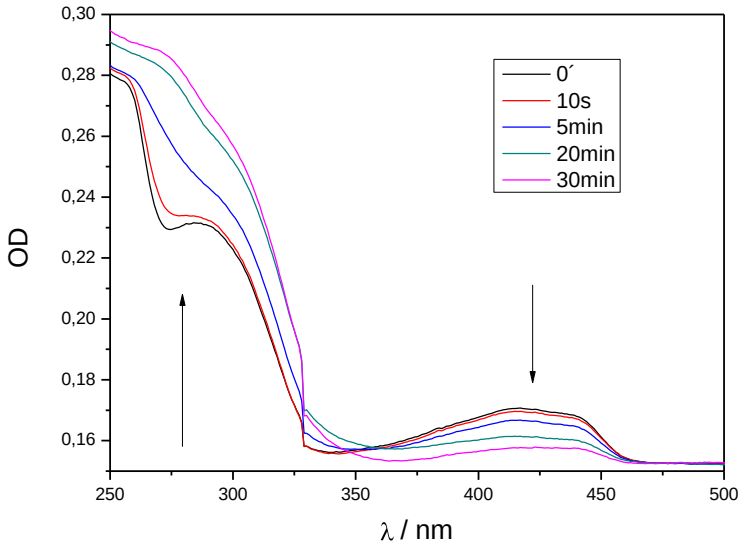

Figure 83: UV-VIS absorption of 2,3-butanedione with 2,3-methyl-2-butene [4+2]-cycloaddition during laser irradiation.

This new double bond can then be used to form a [2+2]-cycloadduct with added TC (Figure 84).

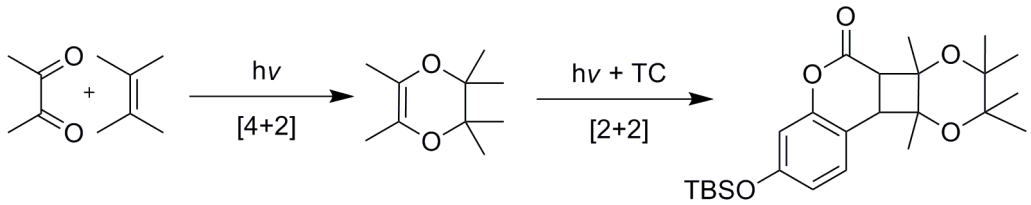

Figure 84: Sequential [4+2] and then [2+2] photoreaction.

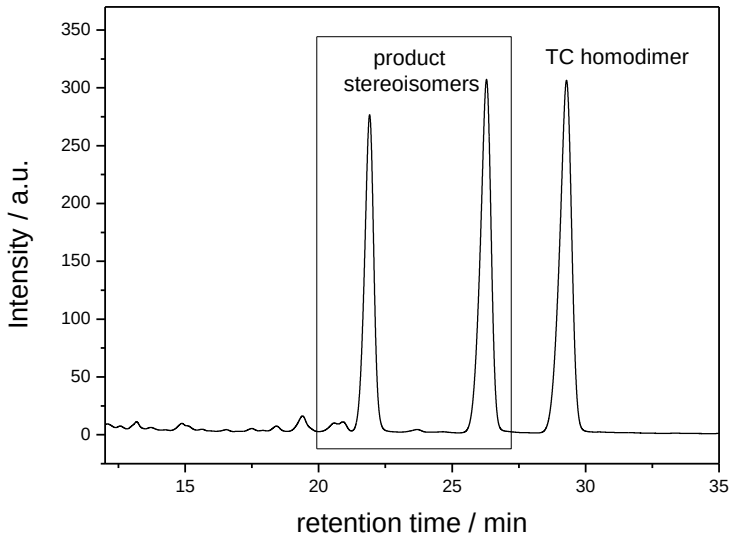

Figure 85: HPLC of sequential reaction.

In two steps, I first use the [4+2]-reaction then add TC and with successive irradiation generate a [2+2]-crossdimer. The finished product was isolated with a preparative HPLC and analyzed using HPLC (Figure 85), LCMS (M = 446 g/mol), and NMR (s. Fig. 96). To my knowledge, this is the first sequential one pot reaction with two successive photochemical steps without any kind of workup in-between. It is also an example of how to incorporate more photochemistry in synthesis. This demonstrates that I can use the advantages, like few side products, and fast reaction times, to generate novel molecules quickly and easily.

With electron donating, highly reactive molecules, the cycloaddition to 2,3-butanedione works well. If the radical stabilization decreases, then the reaction gets suspended. The TC molecule has a triplet energy of about 60 kcal/mol compared to the 55 kcal/mol of 2,3-butanedione and forms product with all molecules from Table 27. The 2,3-butanedione does not deliver enough energy but can form an energetically lower exciplex with 2,3-methyl-2-butene. This exciplex is non reactive but has a beautiful green fluorescence (Figure 86). The build up is diffusion controlled and takes about ~ 5 s during irradiation to form. In case the laser is turned on, then off, and on again the fluorescence of the exciplex can be seen in < 1 s because both molecules are still close together, simplifying reassociation. (A video of this process exists.) To proof that this emission stems from an exciplex, solvents of different polarity are used and the fluorescence is measured. The more polar the solvent is, the better this exciplex is stabilized and the emission shifts bathochrom (Figure 87). This exciplex can not be used in synthesis, however is interesting in the field of photoassociation. Exciplexes have long lifetimes and are very much structure independent, making them ideal to investigate

bimolecular interactions.[70] Even TC is argued to form a exciplex with 2,3-methyl-2-butene but no spectrum exists.[108]

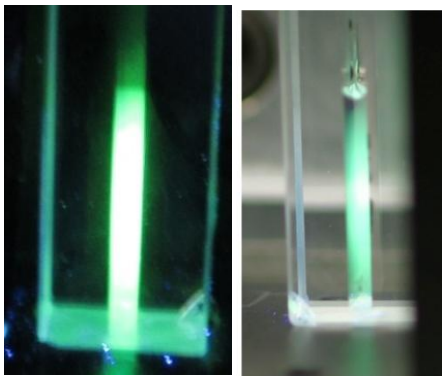

Figure 86: Green fluorescence of non reactive exciplex.

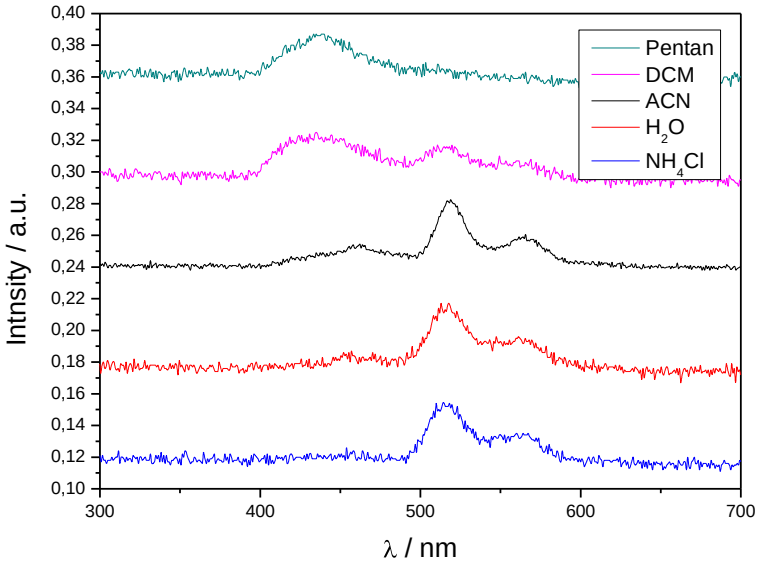

Figure 87: Fluorescence shift of exciplex in polar solvents. The initial *Stokes* shift (abs. at 420 nm to em. at 440 nm) is very small because of only few vibrational options (few sublevels).

2.5.2. Photoremovable protective group

Photoactive molecules can also be used as photoremovable protective groups (ppg). There are two prominent molecules for this purpose. A coumarin based one and a dinitrobenzyl molecule (DNB),[129-131] which are also used for two photon release (Figure 88).[132]

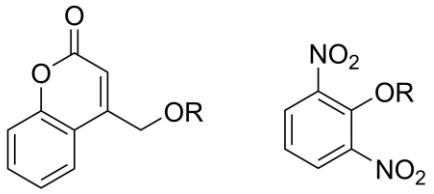

Figure 88: Photoremovable protective groups.

Since coumarin has already been extensively investigated, the nitrobenzyl group will be presented. The mechanism of the photoactivated release of the X-group in Figure 89 has been investigated thoroughly.[133-137] The mechanism incorporates an intramolecular ring closure and opening before the release of the X-group.

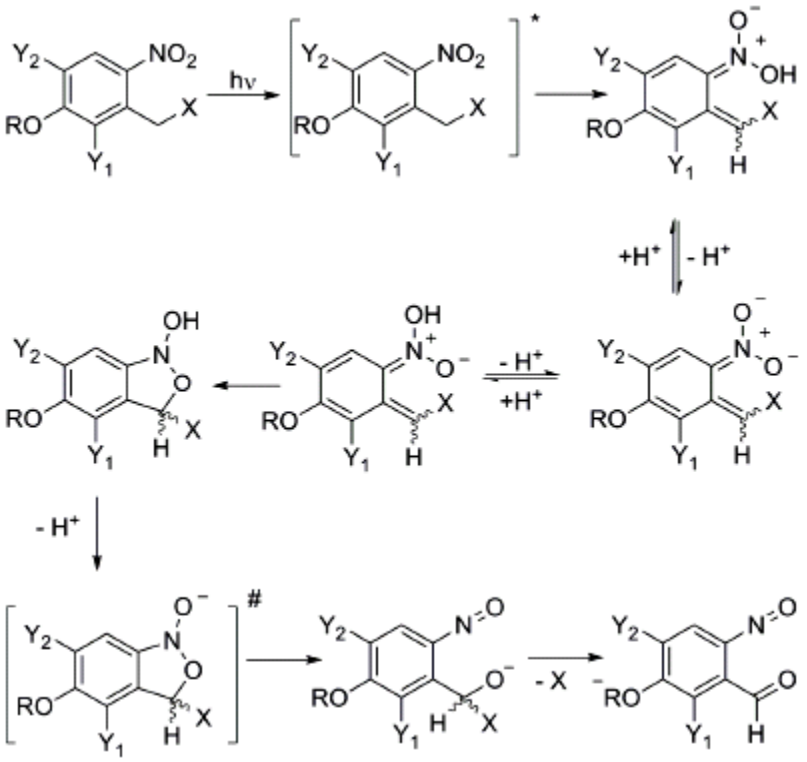

Figure 89: General mechanism of the photolysis of *ortho*-nitrobenzyl compounds: X = released compound, Y_1 = additional nitro group, Y_2 = electron donating group (e.g. OMe), OR = possible linkage.[138]

This group is used to cage the 5-fluorouracil (5FU) drug in order to selectively release it as needed. The synthesis of this protective group is composed of 5 steps and results in a good yield (Figure 90).

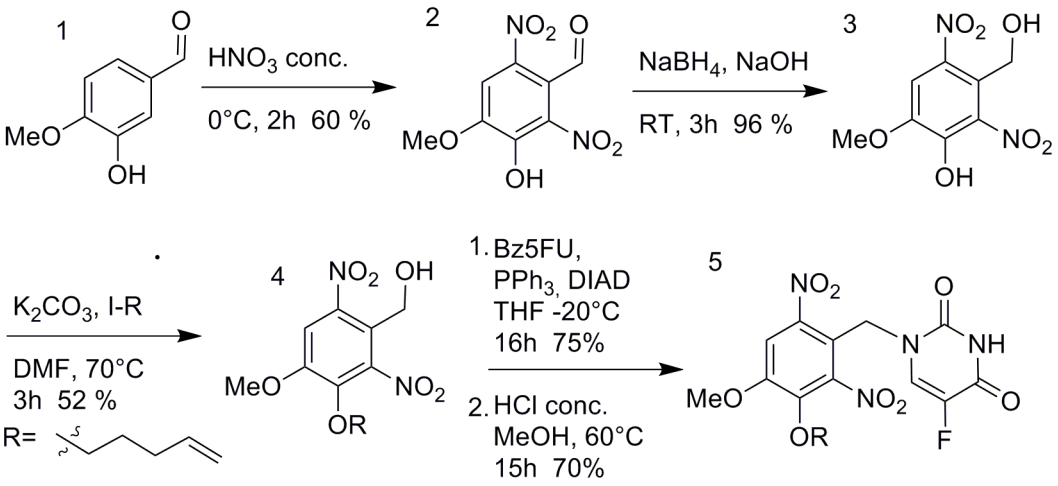

Figure 90: Synthesis of caged 5FU.

The advantage with this caging compound, in comparison to a crossdimer, is that pure 5FU in its antimetabolic form is released. The synthesis allows also every functional group that can be coupled to an alcohol to be caged.

When the caged 5FU is irradiated with UV-B light, the protective group is cleaved and the resulting benzaldehyde-derivative, as well as the 5FU, can be analyzed with HPLC (Figure 91).

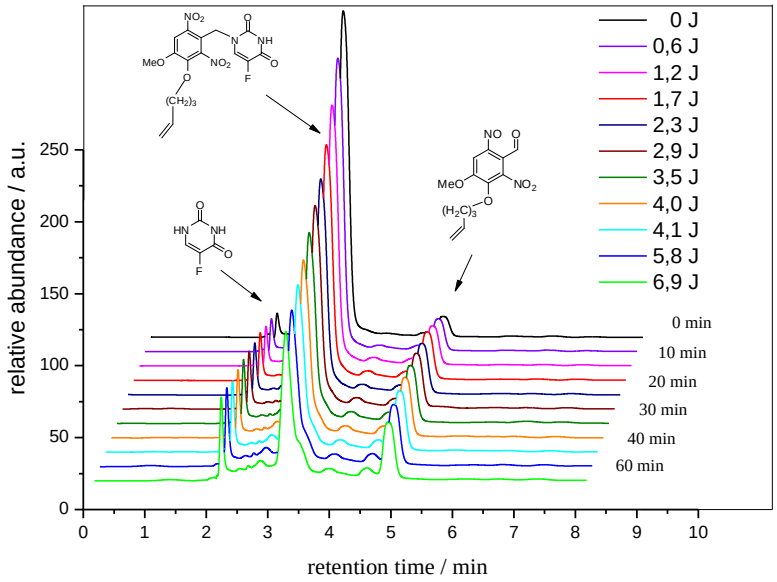

Figure 91: HPLC measurements after irradiation with 266 nm light.

Figure 92 shows the spectra for the dinitrobenzyl compound (**5** Figure 90), the products benzaldehyde-derivative, and 5FU, together with an additive spectrum of the products and the actual spectrum of the irradiated reaction mixture e).

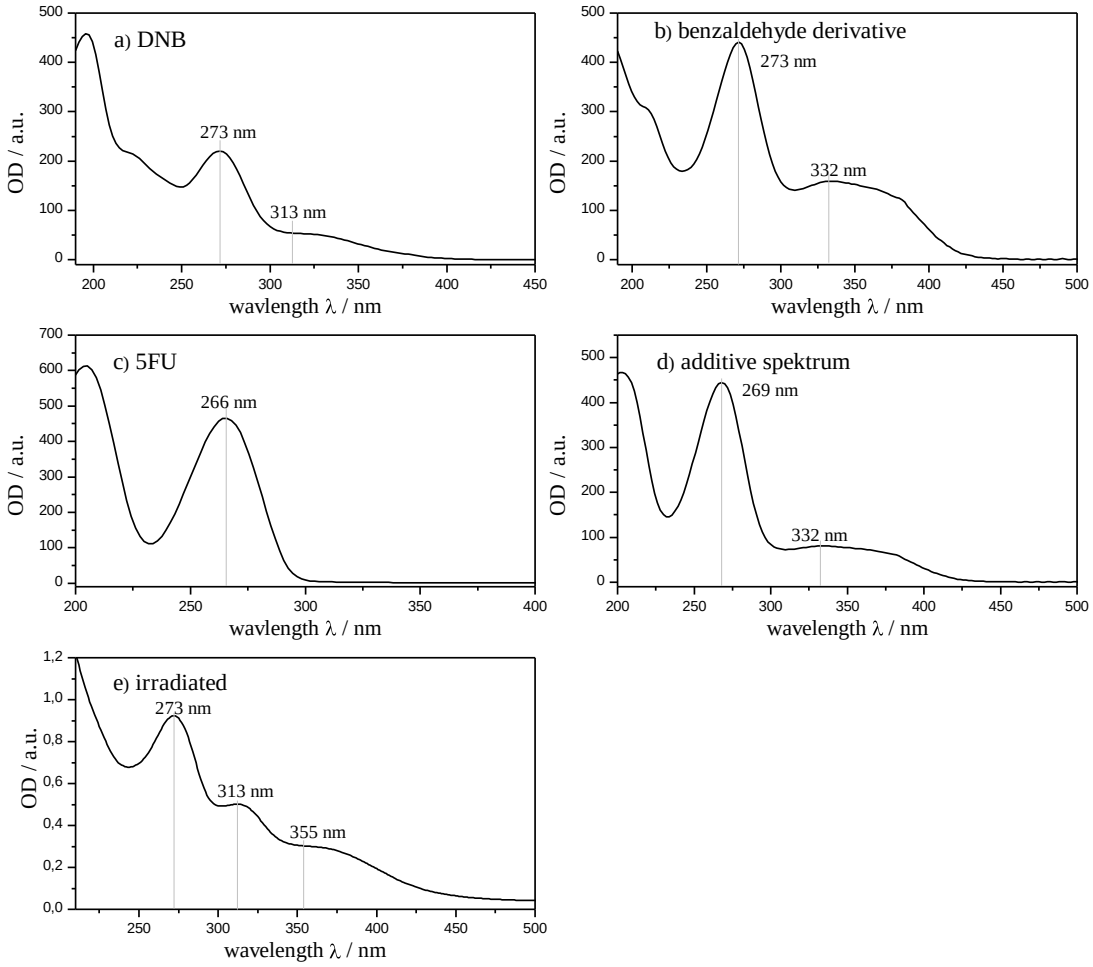

Figure 92: UV-VIS of substrate a), products b), c); additive of b) + c) = d); irradiated solution e).

The quantum yield for this uncaging reaction is ~ 25% which is in correspondence with the literature for nitrobenzyl compounds.[139] Furthermore, a TPA reaction at 532 nm in the presence of an UV-absorber is possible.[138] This allows the real life application in ACTIOL systems for the treatment of secondary cataract. The absorption cross section of the two-photon process is ~ 2, which is comparable with dimeric photoactive linker systems.

2.6. Summary and outlook

Throughout this work I have presented a variety of photolinker and reaction partner molecules for the build up of crossdimers. With kinetic measurements, UV-VIS, and HPLC measurements comparisons were made and good linker-partner combinations were identified and characterized. Important for that choice are the absorbing qualities and the mobility of the molecules in the diffusion controlled, intermolecular addition reaction in solution. An efficient energy uptake, a high photon flux, and an even photon distribution within the reaction vessel were found to be most important for the speed and quantum yield of these photoreactions. By studying possible energy dispersion passage ways, the triplet state was identified as the host for product formation. In general, photoreactions are more complicated than thermal bimolecular reactions because of the photon as a passive, third reaction partner. The spatial activation of the absorbing substrate has therefore been studied in great detail. As a novel tool for synthesis the laser was the focus in the majority of the experiments and performed superior to reactions with the *Rayonet* reactor and the sun, regarding crossdimer yield. With the high intensity laser excitation, new possibilities for the influence on photoreactions were identified. Also, less side reactions occur and additives like sensitizers and triplet promoters can be omitted. In addition, selective and well-placed excitation of one compound out of a mixture was possible. The crossdimerization reaction was improved dramatically with the tuning of concentration and set up optimization, and is now able to overcome the preferred homodimerization. By means of high turnover, the laser is able to create a difference in concentration between the illuminated volume and the surrounding. The irradiated part gets depleted of absorber and the crossdimerization of the excited species with the ground state cross component is favored. Pulsed laser excitation partially suppresses homodimerization - the higher the pulse energy the more. The intense laser light also leads to heating of the solution through the conversion of absorbing molecules. Using a solvent with a higher boiling point than the thermal cleavage temperature of the homodimer and significantly lower than any thermal decompositions of the crossdimer, is an easy and reliable way to control the thermal recycling of substrate from homodimers. Incubation of the reaction solution between light exposures at elevated temperatures contributes to increase the CD/HD-ratio to over 30:1. This procedure almost quantitatively converts the substrate into crossdimer with 92% yield.

The laser fueled reaction works like any other sourced reaction. The difference lies with the monochromaticity and the high photon flux, carrying out a more specific excitation and producing an outstanding difference between the irradiated volume and its surrounding. This allows the user to create a depletion zone scenario tailored to the generation of crossdimers, promoting the crossreaction.

Control is the key to every efficient reaction. With this intermolecular crossdimerization the number and distribution of excited molecules is the bottleneck. With low concentrations the required diffusion distances will become long or even too long for the lifetime of the reactive triplet species. High concentrations on the other side will result in short light penetration and a detrimental heat distribution. The balance of both parameters therefore is important. The difficulty therewith is that the most vital reaction parameter, absorption, is constantly changing as the reaction progresses. The logic consequence is a compromise and the realization that the quicker the reaction is, the smaller the struggle of balancing will be. The laser as a very precise and strong energy source thus is best to steer photoreactions.

The reversion of the addition reaction, with either one or two photon absorption, rounds up the versatility of photodimers. Furthermore, the individual cycloreversion of different stereoisomers was measured to show the scale of the effect in SPA and TPA. Linear absorption thereby exhibits a high conformational dependence.

With additional reactions of photoremoveable protective groups and a sequential synthesis which includes a heterocylcoaddition I have shown the versatility of photoreactions for synthesis. Photochemistry thus is fascinating because it edges both chemistry and physics and will only perform if both sciences are combined.

Further improvements in the CD/HD ratio of solution based reactions and smeltings seem possible and need to be investigated. The depletion zone photo reaction is a versatile tool, able to produce crossdimers fast, which can be better matched with their tasks. This method offers a new synthetic route to cyclobutane structures which should be compared to common recipes. The cycloreversion on the other hand has shown to vary with stereoisomers which can help to increase the cleavage efficiency of photoactive materials in the future.

3. Materials and methods:

Chemicals. All chemicals were obtained from *Sigma-Aldrich, Roth, Merck* or *Acros Scientific* and used without further purification. The solvents used were of HPLC-grade and degased.

UV-Laser. Most of the laser reactions were performed using a Q-switched frequency tripled Nd:YVO_4 diode pumped solid state laser system (*AVIA 355, Coherent*) operating at a wavelength of 355 nm. The laser parameters were 10 kHz repetition rate and 25-ns pulse duration. The intensity profile at the laser output was near-*Gaussian* and the average power, measured behind the beam expander optics, was about 0.66 J/s (66 µJ/pulse). The 6 - 9 J pulse intensities were obtained from an *Infinity 40-100* frequency tripled Nd:YAG-Laser from *Coherent*; repetition rate 100 Hz, pulse length 7 ns and flat top profile or with a *Quanta Ray* GCR-170 from *Spectra Physics* with 7 ns pulse length and 10 kHz.

Solar reactor. The solar reactor was an 18 inch polished aluminium parabolic reflector from *Edmund Optics* with a focal length of ~ 8 cm.

***Rayonet* reactor.** Built by the electronic work shop of the *Philipps-University Marburg*, the cuboid fan cooled metal box is equipped with 16 fluorescent lamps type *Eversun 40 W/79, 25X* from *Osram*. 8 quartz tubes with an individual volume of 15 mL can be mounted over 8 miniature agitators. The average power is 4.7 mW/cm², with a central wavelength at 350 nm, and a working temperature during the reaction was 35 °C.

Analytical HPLC. An *Ultimate 3000* HPLC model from *Dionex* including a quaternary low pressure gradient pump, a column oven and a diode array detector was used. Column temperature was kept constant at 40 °C. The column used was a *Prontosil C18 reversed phase* from *Bischoff.* The methods included a 23 mL/min flow, isocratic 80:20 mixture of ACN:H_2O with 100 µL/L added phosphoric acid and a gradient for crossdimer isolation (s. 3.1).

Preparative HPLC. A *P 680* HPLC model from *Dionex* including a binary gradient pump equipped with an UV-VIS-detector was used with a *Pack ODS-A* column from *YMC.* The solvent was an isocratic 80:20 mixture of ACN:H_2O, flow 23 mL/min.

UV-VIS. UV-VIS absorption spectra were recorded at room temperature on an *UVIKON 922 (Kontron Instruments)* spectrophotometer. The spectral range was from 200 to 900 nm and the scanning

speed was 480 nm/s. Cuvettes with path lengths of 2 mm, 5 mm and 10 mm were used and the maximum optical density was never over the value of 2.

NMR. Three crossdimer isomers were isolated from the laser reaction by means of the preparative HPLC. 10 mg of this crossdimer were dissolved in 0.6 mL d_6-Acetone and measured with an *Avance DRX 500* FT-NMR from *Bruker*.

LC-MS. A LC-MS model *1050* from *Agilent Technologies* comprising a quaternary low pressure gradient pump with a column oven and a diode array detector was used. Column temperature was set to 40 °C. The molecules were analyzed in the *Thermo LCQ Duo* Mass spectrometer with ESI.

Thermographic camera. IR-images were taken by a *VarioCAM hr research* from *InfraTec* in a spectral range from 7.5 - 14 µm at a resolution of 640 x 480 pixels with ± 2% temperature precision.

Fluorescence. Measurements and SPA were made with a RF-1502 spectroscope from *Shimadzu.*

Photodiode. Intensity measurements of fluorescence spectroscope, UV-C lamp and sun spectra were made with 1337-1010BQ photodiode from *Hamamatsu.*

Ultra fast photodiode. UV-Laser pulse width was measured with a FND-100Q photodiode with a suprasil window from *EG&E Judson*.

UV-C lamp. Quick SPA releases used *Philips* PL-S lamp with 9 W inside a closed metal casing.

Instaspec. Spectral measurements of *Rayonet* reactor, sun and fluorescence of laser reaction were made with an optical fiber and a CCD array *INSTASPEC (+MULTISPEC)* from *Oriel*

CCD-camera. Pictures of interference were taken with digital camera C4742-95 from *Hamamatsu* with 1000x1000 pixel resolution.

Intensity measurement. The laser intensity was measured with an air cooled *LM 80 V* sensor and a *FieldMax II TO*, both from *Coherent*.

Flow-cell. Consists of a quartz 200 µm thick flow cell, connected with fluorinated polyethylene tubes to a *REGLO-Z* pump at 5 mL/min from *Ismatec.* The minimal required volume is 7 mL.

Measurements. Parts of the measurements and synthesis were made in collaboration with students during physical chemistry traineeship. In detail these are:
Catarina Nardi-Tironi - variety of crossdimers; Kathrin Wähler - films, spatial photon distribution; Amanda Beatriz Pineda - kinetic with constant OD; Stefan Engel - kinetic with constant concentration; Thorben Badur - photoremovable protective groups; Maike Noster - reaction rates, cycloreversion of stereoisomers.

3.1. Synthesis

- 1-heptanoyl-5-fluorouracil[140]

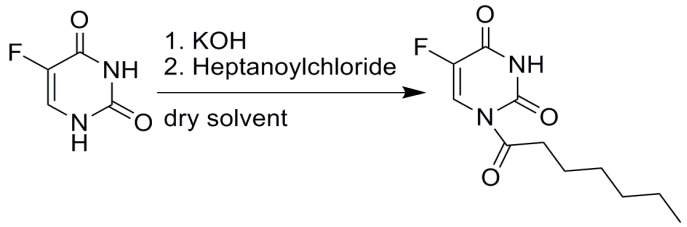

5 fluorouracil	130 g/mol	16.1 g	123 mmol	1 eq
potassium hydroxide	56 g/mol	7.1 g	125 mmol	1 eq
heptanoylchoride	148 g/mol	18.4 g	124 mmol	1 eq

A quantity of 16.1 g (123 mmol, 1.0 eq) of 5-fluorouracil, together with 7.1 g (125 mmol,~ 1 eq) potassium hydroxide in 500 mL methanol was stirred for 4 h at room temperature. Afterwards, the solvent was evaporated and the white left over solid was dried in vacuum. Then 500 mL of dried ACN (HPLC grade) were added under argon at room temperature and stirring was continued for 2h until all solids were dissolved and a white, milky solution had formed. The 18.4 g (124 mmol, ~ 1 eq) of heptanoylchloride were added dropwise under ice bath cooling and the mixture was stirred for 20 h at room temperature. After evaporation of the solvent, the remaining white solid was diluted in aceticacidethylester and impurities were removed by washing with brine. After thoroughly drying, a bright white solid was obtained. The yield was 27.2 g = 113 mmol, 90%.

UV-VIS (ACN): λ_{max}/nm (normalized absorption) = 262 (1), 214 (0.8).
IR: s. Figure 98.

^{1}H-NMR (300 MHz, acetone-D6): δ/ppm = 0.89 (t, 3H, J = 6.72 Hz, 11-H), 1.25-1.40 (m, 6H, 8-H, 9-H, 10-H), 1.67-1.74 (m, 2H, 7-H), 3.11 (t, 2H, J = 7.32 Hz, 6-H), 8.11 (s, 1H, NH), 8.30 (d, 1H, J = 6.72 Hz, 2-H).

^{13}C-NMR (75 MHz, acetone-D6): δ /ppm = 14.3 (C-11), 23.2 (C-9), 25.3 (C-10), 29.4 (C-7), 32.3 (C-8), 39.1 (C-6), 102.7 (C-3), 146.1 (C-2), 164.2 (C-1), 175.3 (C-5), 175.3 (C-4).

- TBS protected 7-hydroxycoumarin[141]

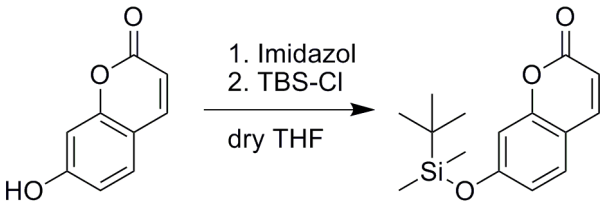

7-hydroxycoumarin	162 g/mol	10.0 g	62 mmol	1.0 eq
imidazol	68 g/mol	4.8 g	70 mmol	1.1 eq
TBS-Cl	151g/mol	11.1 g	74 mmol	1.2 eq

Under argon, 10 g (62 mmol, 1.0 eq) of 7-hydroxycoumarin were dissolved in 100 mL dry THF and 4.8 g (70 mmol, 1.1 eq) imidazol were added under stirring. This solution was allowed to react for 1 h before the 11.1 g (74 mmol, 1.2 eq) *tert.*butyldimethylsilylchloride (TBS-Cl) was added drop wise. Stirring over night was followed by quenching the mixture with brine and extracting with aceticacidethylester. The organic phase was dried over sodium sulfate and the solvent was removed under vacuum. The result was a white cristalline solid, with a yield 12.5 g = 45 mmol, 73%.

UV-VIS (ACN): λ_{max}/nm (normalized absorption) = 206 (1), 216 (0.3).
IR: s. Figure 98.

^{1}H-NMR (300 MHz, $CDCl_3$): δ /ppm = 0.25 (s, 6H, 10-H, 11-H), 1.12 (s, 9H, 12,13,14-H), 6.29 (d, 1H, J = 9.12 Hz, 2-H), 6.75 (d, 1H, J = 2.40 Hz, 8-H), 6.89 (dd, 1H J1 = 2.40 Hz, J2 = 8.37 Hz, 6-H), 7.56 (d, 1H, J = 8.37 Hz, 5-H) 7.84 (d, 1H, J = 9.12 Hz, 3-H).

^{13}C-NMR (75 MHz, $CDCl_3$): δ /ppm = -4.5 (2C, C-10, C-11), 26.0 (3C, C-13, C-14, C-15), 109.6 (C-8), 112.4 (C-2), 118.7 (C-6), 132.5 (C-5), 143.6 (C-3), 150.8 (C-1), 153.9 (C-9), 158.7 (C-7), 164.6 (C-4).

- General method for crossdimerization

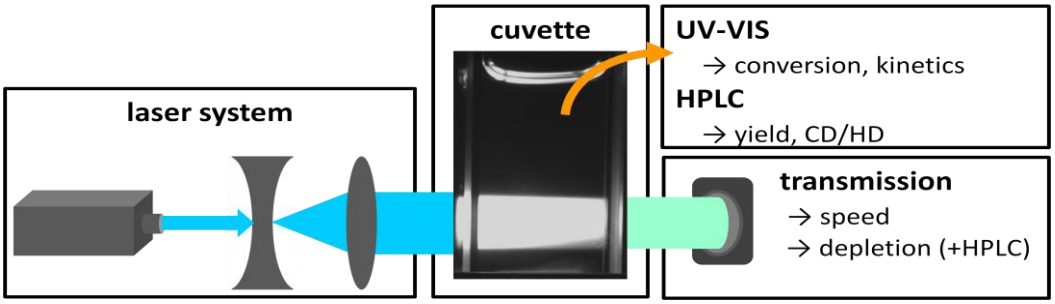

Figure 93: Standard laser synthesis setup.

Most of the experiments in this work have been performed using a standard setup with a laser beam extension to 9 mm diameter and a 1 cm wide quartz cuvette with 2 mm thickness Figure 93. The absorbing substrate (mainly TC) was dissolved and irradiated together with the non-absorbing substrate (often times H5FU) in solution for 20 min. As an example the most common crossreaction featured:

0.4 mL of a 20 mM TC and 200 mM H5FU (or crosscomponent) solution in acetonitrile purged with argon were filled in a sealed 2 mm quartz cuvette and were irradiated continuously with an expanded 355 nm laser beam. The energy density during irradiation amounts to 0.9 J / (cm^2 s) [66mJ/pulse]. After 20 min of irradiation, the solution was analyzed by HPLC.

- Synthesis of TC-H5FU crossdimer

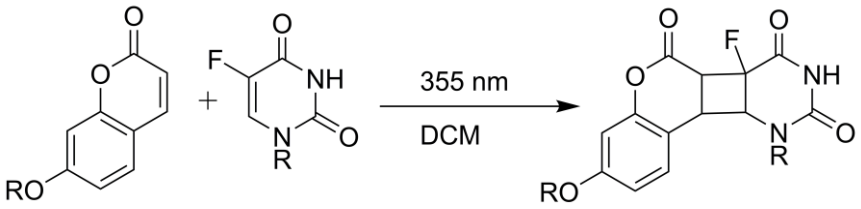

TC	276 g/mol	276 mg	1.0 mmol	1.0 eq
H5FU	242 g/mol	2.42 g	10 mmol	10 eq

The 276 mg (1.0 mmol, 1.0 eq) TC were dissolved in 50 mL DCM together with 2.42 g (10 mmol, 10 eq) H5FU. The solution was filtered and degassed with dry argon. Pumped at 5 mL/min the solution

was irradiated in the flow cell with 1.15 W laser power for 32 h. The analytical HPLC determined dimer yield is 96 % with a 4.5:1 CD/HD ratio.

Flow 0.65 mL/min; gradient: water/ACN: 0 min 18/82, 8 min 18/82 - 10 min 5/95, 15.5 min 5/95 - 16.5 min 18/82, 20 min 18/82.

The solvent was evaporated and the solid dissolved in 30 mL ACN together with 5 mL water. Stirring for 10 h at 50 °C hydrolysed the left over H5FU. The white precipitate was filtered of and the solvent was evaporated. The remains were dissolved at 300 mg/5mL in ACN and separated with the preparative HPLC. Flow 23 mL/min; gradient: water/ACN: 0 min 22/78, 25 min 20/80, 32 min 15/85, 45 min 10/90, 50 min 15/85.

There are 3 crossdimer stereoisomers with a 4:3:1 peak ratio (ACN):

MS ESI$^+$: 518, 387(-OTBS) [equal with all stereoisomers]

1. syn-ht: 108 mg, 0,2 mmol, 25%;
2. syn-hh: 59 mg, 0,1 mmol, 12,5%;
3. anti-ht: 46 mg, 0,09 mmol, 11%.

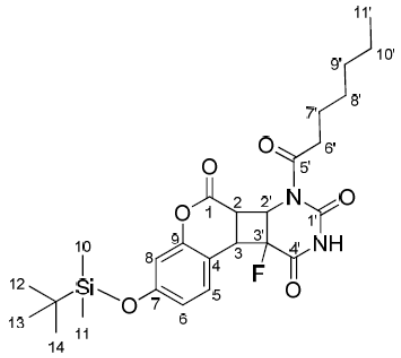

The 1 and the 4´ carbonyl-groups are designated as head and the molecule shows a syn-head-to-tail conformation.

1. stereoisomer: syn-head-to-tail, retention time 5.9 min (analytical HPLC)

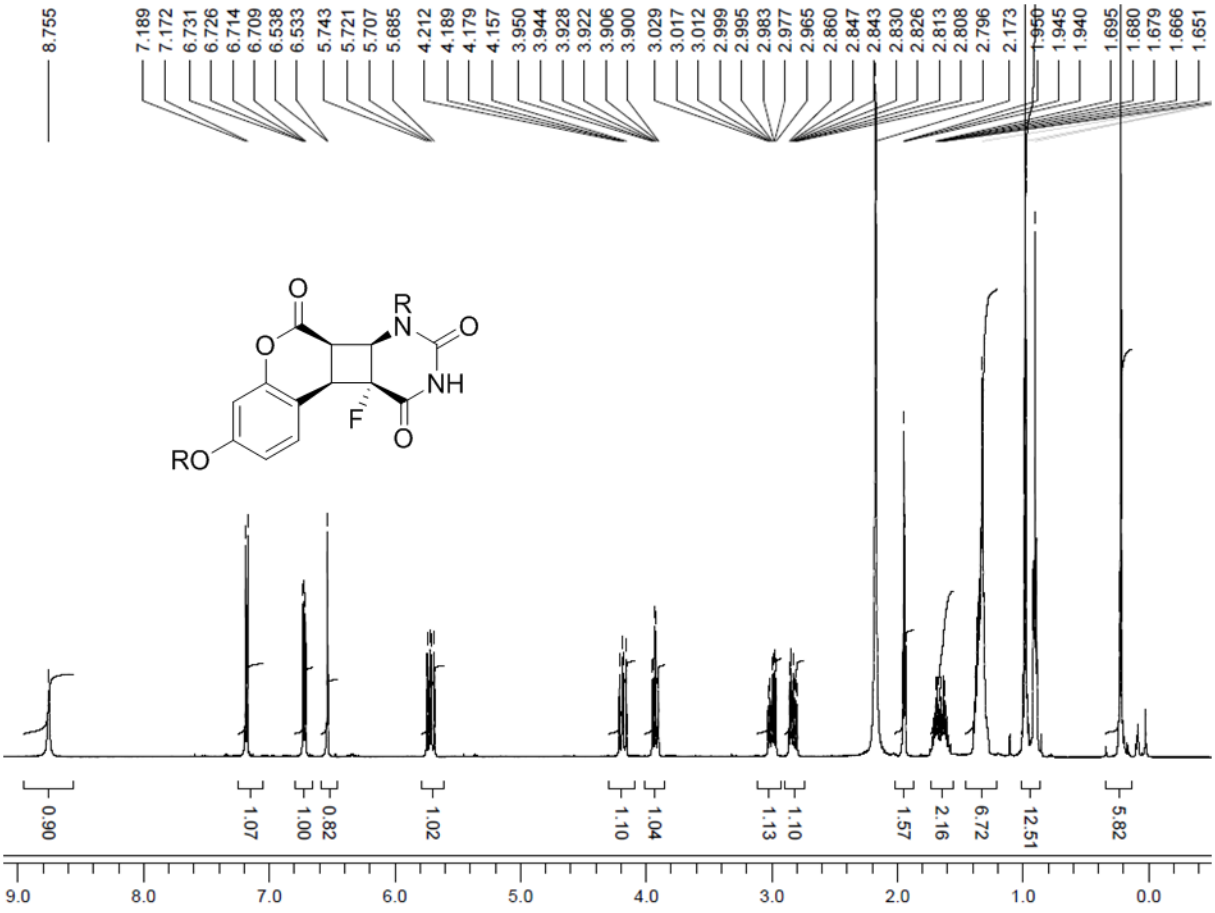

Figure 94: 1H-NMR of 1. CD.

UV-VIS (ACN): λ_{max}/nm (normalized absorption) = 207 (1).

^{1}H-NMR (500 MHz, aceton-D6):

δ /ppm = 0.21 (s, 6H, 10-H, 11-H), 0.90 (t, 2H, J = 6.92 Hz, 11'-H), 0.98 (s, 9H, 12-, 13-, 14-H), 1.20-1.40 (m, 6H, 8'-H, 9'-H, 10'-H), 1.55-1.75 (m, 2H, 7'-H), 2.91-2.85 (m, 1H, 6'-H), 2.96-3.02 (m, 1H, 6'-H), 3.92 (dt, 1H, J1 = 2.91 Hz, J2 = 11.11 Hz, 2-H), 4.18 (dd, 1H, J1 = 11.29 Hz, J2 = 16.37 Hz, 3-H), 5.71 (dd, 1H, J1 = 10.89 Hz, J2 = 18.30 Hz, 2'-H), 6.53 (d, 1H, J = 2.40 Hz, 8-H), 6.72 (dd, 1H J1 = 2.40 Hz, J2 = 8.37 Hz, 6-H), 7.18 (d, 1H, J = 8.37 Hz, 5-H), 8.75 (s, 1H, N-H).

^{13}C-NMR (125 MHz, aceton-D6):

δ /ppm = -4.41 (2C, C-10, C-11), 14.27 (C-11'), 23.19 (C-9'), 25.25 (C-10'), 25.84 (3C, C-12, C-13, C-14), 29.38 (C-7'), 32.26 (C-8'), 33.42 (C-3), 39.07 (C-6'), 41.93 (C-2), 53.07 (C-2'), 92.69 (C-3'), 109.33 (C-8), 118.00 (C-6), 131.35 (C-5), 150.22 (C-1), 153.09 (C-9), 158.03 (C-7), 163.90 (C-4), 164.21 (C-1'), 175.28 (C-5'), 175.32 (C-4'): head-to-tail conformation

2. stereoisomer: syn-head-to-head, retention time 7.1 min

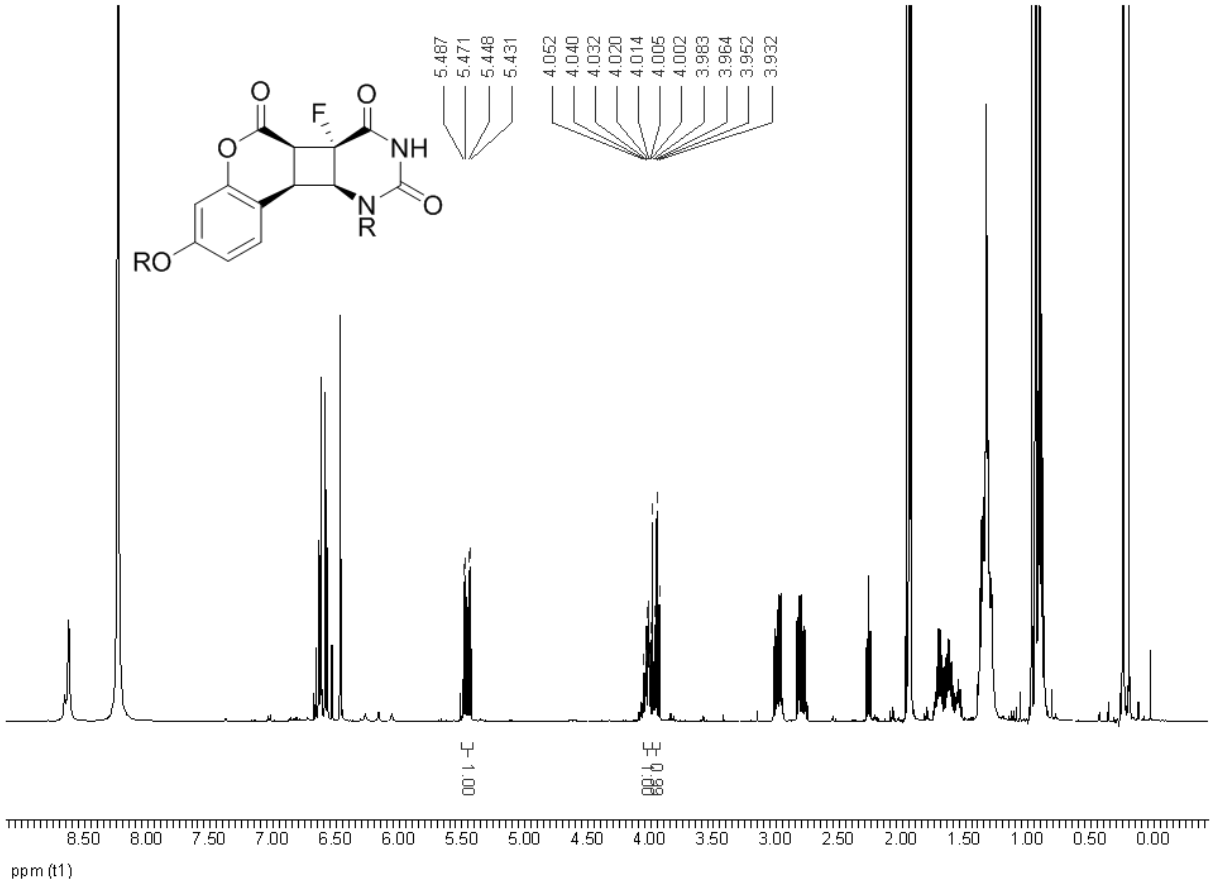

Figure 95: 1H-NMR of 2. CD.

UV-VIS (ACN): λ_{max}/nm (normalized absorption) = 218 (1).

^{1}H-NMR (500 MHz, aceton-D6):

δ /ppm = 0.21 (s, 6H, 10-H, 11-H), 0.90 (t, 2H, J = 6.92 Hz, 11'-H), 0.98 (s, 9H, 12-, 13-, 14-H), 1.20-1.40 (m, 6H, 8'-H, 9'-H, 10'-H), 1.55-1.75 (m, 2H, 7'-H), 2.91-2.85 (m, 1H, 6'-H), 2.96-3.02 (m, 1H, 6'-H), 3.96 (dt, 1H, J1 = 9.87 Hz, J2 = 15.41 Hz, 3-H), 4.03 (dd, 1H, J1 = 9.41 Hz, J2 = 3.18 Hz, 2-H), 5.46 (dd, 1H, J1 = 8.53 Hz, J2 = 19.65 Hz, 2´ -H), 6.53 (d, 1H, J = 2.40 Hz, 8-H), 6.72 (dd, 1H J1 = 2.40 Hz, J2 = 8.37 Hz, 6-H), 7.18 (d, 1H, J = 8.37 Hz, 5-H), 8.75 (s, 1H, N-H).

^{13}C-NMR (125 MHz, aceton-D6):

δ /ppm = -4.41 (2C, C-10, C-11), 14.27 (C-11'), 23.19 (C-9'), 25.25 (C-10'), 25.84 (3C, C-12, C-13, C-14), 29.38 (C-7'), 32.26 (C-8'), 39.07 (C-6'), 39.26 (C-3), 44.75 (C-2), 50.87 (C-2'), 96.63 (C-3'), 109.33 (C-8), 118.00 (C-6), 131.35 (C-5), 150.22 (C-1), 153.09 (C-9), 158.03 (C-7), 163.90 (C-4), 164.21 (C-1'), 175.28 (C-5'), 175.32 (C-4'): head-to-head conformation

3. stereoisomer: anti-head-to-tail, retention time 8.4 min

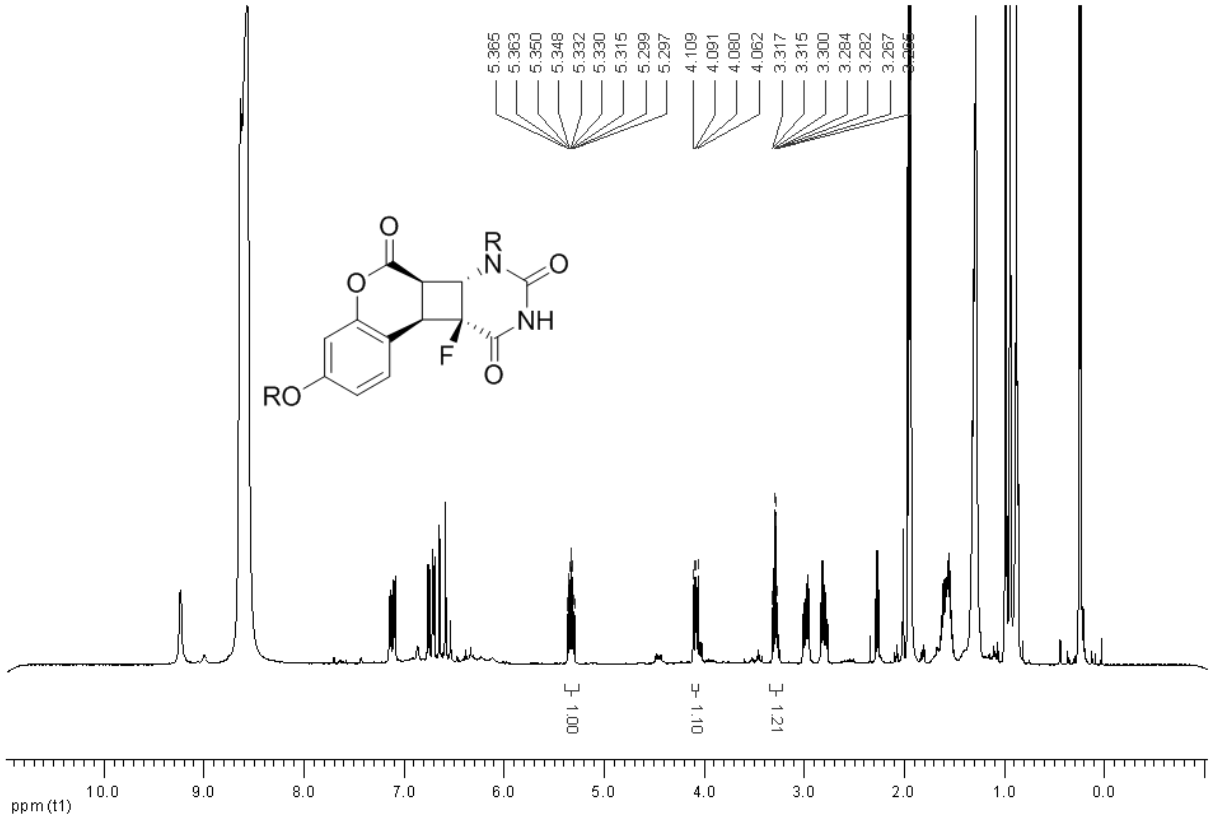

Figure 96: 1H-NMR of 3. CD.

UV-VIS (ACN): λ_{max}/nm (normalized absorption) = 198 (1).

^{1}H-NMR (500 MHz, aceton-D6):

δ /ppm = 0.21 (s, 6H, 10-H, 11-H), 0.90 (t, 2H, J = 6.92 Hz, 11'-H), 0.98 (s, 9H, 12-H, 13-, 14-H), 1.20-1.40 (m, 6H, 8'-H, 9'-H, 10'-H), 1.55-1.75 (m, 2H, 7'-H), 2.91-2.85 (m, 1H, 6'-H), 2.96-3.02 (m, 1H, 6'-H), 3.29 (dt, 1H, J1 = 8.68 Hz, J2 = 8.58 Hz, 2-H), 4.09 (dd, 1H, J1 = 8.81 Hz, J2 = 14.47 Hz, 3-H), 5.30-5.37 (m, 1H, 2´-H), 6.53 (d, 1H, J = 2.40 Hz, 8-H), 6.72 (dd, 1H J1 = 2.40 Hz, J2 = 8.37 Hz, 6-H), 7.18 (d, 1H, J = 8.37 Hz, 5-H), 8.75 (s, 1H, N-H).

^{13}C-NMR (125 MHz, aceton-D6):

δ /ppm = -4.41 (2C, C-10, C-11), 14.27 (C-11'), 23.19 (C-9'), 25.25 (C-10'), 25.84 (3C, C-12, C-13, C-14), 29.38 (C-7'), 32.26 (C-8'), 33.42 (C-3), 39.07 (C-6'), 41.93 (C-2), 53.07 (C-2'), 92.69 (C-3'), 109.33 (C-8), 118.00 (C-6), 131.35 (C-5), 150.22 (C-1), 153.09 (C-9), 158.03 (C-7), 163.90 (C-4), 164.21 (C-1'), 175.28 (C-5'), 175.32 (C-4'): head-to-tail conformation

- Synthesis of benzindan-1-one[142]

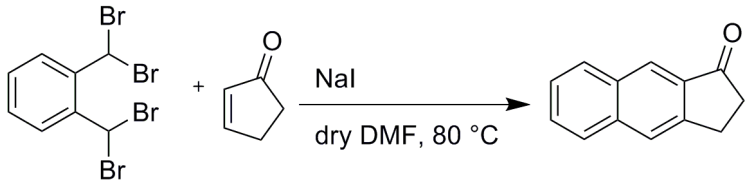

α, α, α‘,α‘-tetrabrom-o-xylol	418 g/mol	6.0 g	14 mmol	1 eq
2-cyclopenten-1-one	82 g/mol	1.2 mL	14 mmol	1 eq
sodium iodide	150 g/mol	14.0 g	94 mmol	6 eq

In 50 mL dry DMF 6 g (14 mmol, 1 eq) of tetrabrom-o-xylol and 1.2 mL (14mmol, 1eq) 2-cyclopentenone, as well as 14 g (94 mmol, 6 eq) sodium iodide were dissolved under argon as much as possible. After heating to 80 °C the dark red reaction mixture was allowed to cool. After quenching with ice water a yellow precipitation formed. Then sodium sulfite was added until the color turns from red to yellow. The precipitate was filtered of and recrystallized from ethanol. The resulting orange-brown crystals were filtered and dried under vacuum. The outcome was 0.6 g (3.29 mmol, 23%) of benzindan-1-one.

^{1}H-NMR (300 MHz, $CDCl_3$): δ /ppm = 2.79-2.83 (t, 2H, J = 7.84 Hz, 2-H), 3.31-3.35 (t, 2H, J = 7.84 Hz, 3-H), 7.47-8,33 (m, 6H, 6,8,9-H).

^{13}C-NMR (75 MHz, $CDCl_3$): δ /ppm = 30.2 (C-3), 41.7 (C-2), 126.4 (C-9), 128.6 (C-8), 131.3 (C-6), 133.6 (C-7), 135.5 (C-4), 139.1 (C-5), 208.2 (C-1).

- Synthesis of benzinden-1-one[142]

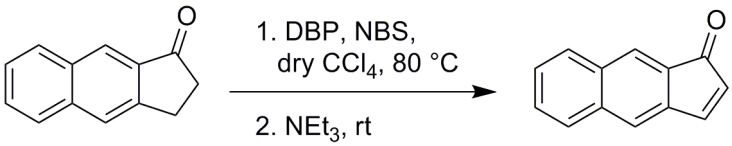

benzindan-1-on	182 g/mol	0.6 g	3.3 mmol	1 eq
NBS	68 g/mol	0.76 g	4.3 mmol	1.3 eq
DBP	186 g/mol	1.3 g	7.0 mmol	2.1 eq
triethylamine	101 g/mol	0.6 mL	4.3 mmol	1.3 eq

In 10 mL of dry carbontetrachloride 0.6 g (3.3 mmol, 1.0 eq) of benzindan-1-one were dissolved under argon as much as possible and one 1.3 g (7.0 mmol, 2.1 eq) of dibenzoylperoxide (DBP), as well

as 0.76 g (4.3 mmol, 1.3 eq) *N*-Bromsuccinimide (NBS) were added. After heating to 80 °C for 2 h under reflux the mixture turned orange and a bit of precipitation formed. After filtering, 0.6 mL (4.3 mmol, 1.3 eq) triethylamine was added drop wise under cooling in an ice bath to the yellow solution. Stirring over night delivers a yellow-brown precipitation, which was filtered out of the red solution. The precipitate was dried under vacuum and purified by flash chromatography (silica gel; pentane/EtOAc 7:1). The yield is 40 mg (0.22 mmol, 15%) of yellow benzinden-1-one.

Rf (Pentan/EtOAc 7:1): 0.49
GC-MS: m/z (%): 180 (100)

^{1}H-NMR (300 MHz, $CDCl_3$): δ /ppm = 7.22 (d, 1H, J = 9.47 Hz, 2-H), 7.35 (d, 1H J = 9.47 Hz, 3-H), 7.87-8.42 (m, 6H, 6,8,9-H).

^{13}C-NMR (75 MHz, $CDCl_3$): δ /ppm = 128.6 (C-9), 129.9 (C-8), 133.7 (C-6), 134.8 (C-2), 135.3 (C-5), 136.3 (C-4), 137.3 (C-7), 142.3 (C-3), 201.2 (C-1).

- TC-2,2,3,3,5,6-hexamethyldihydrodioxine-crossdimer

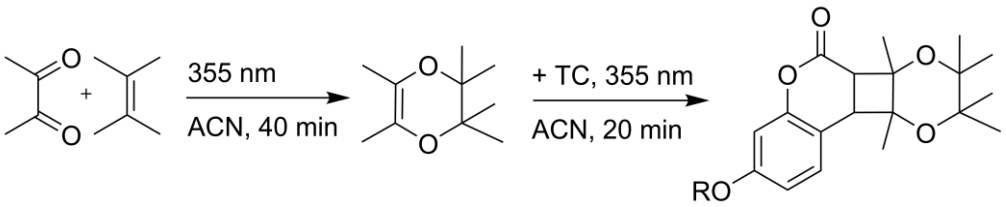

2,3-butanedione	86 g/mol	9.0 µL	0.1 mmol	1 eq
2,3-methyl-2-butene	84 g/mol	9.2 µL	0.1 mmol	1 eq
TC	276 g/mol	2.2 mg	8.0 µmol	1 eq

A volume of 400 µL of a 5 mL/20 mM mixture of 2,3-butanedione (9.0 µL, 0.1 mmol, 1 eq) and 2,3-methyl-2-butene (9.2 µL, 0.1 mmol, 1 eq) were irradiated with 355 nm laser light at 0.8 J/s for 40 min. Then TC 2.2 mg (8.0 µmol, 1 eq) was added and the solution irradiated for another 20 min. The yield is 1.1 mg (32 µmol, 32%) of *syn+anti*-stereoisomers of crossdimer. [No NOESY-NMR was used to distinguish the two forms]

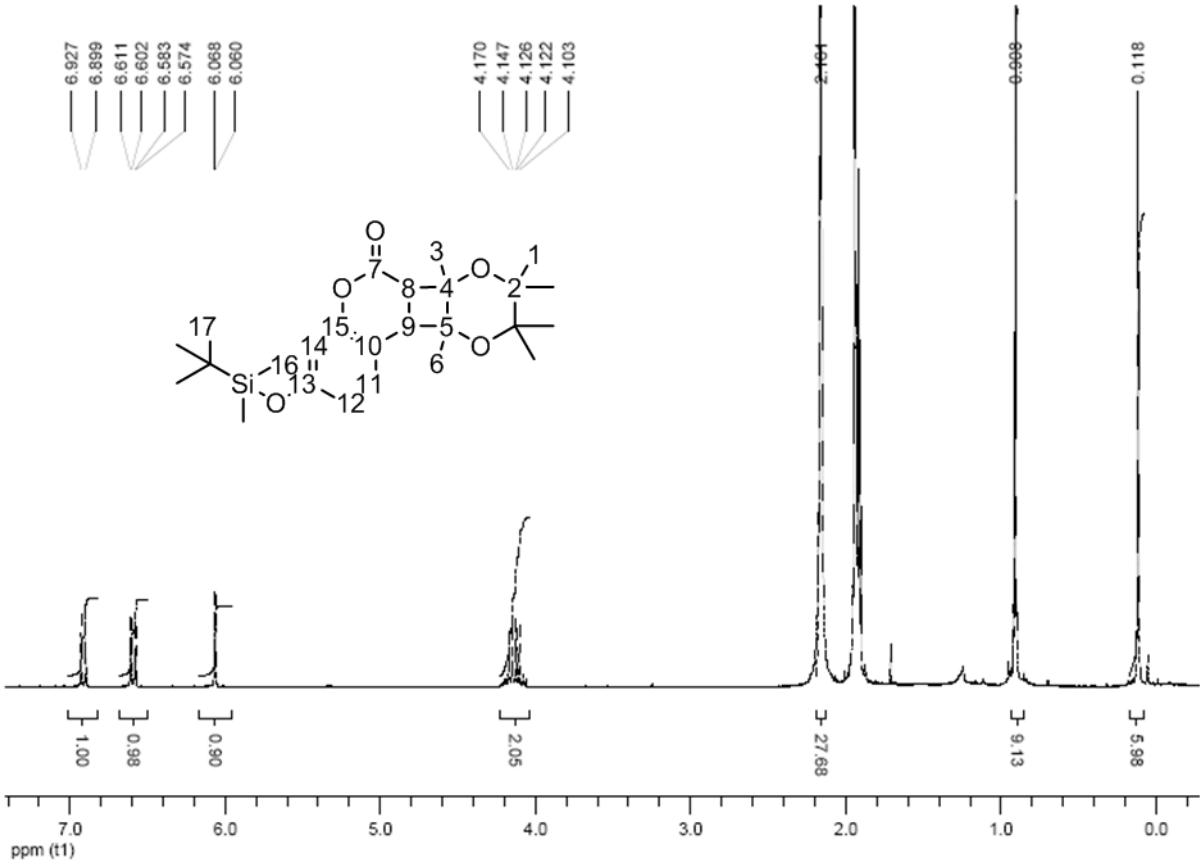

Figure 97: NMR of successive reaction.

^{1}H-NMR (300MHz, CD_3CN) δ/ppm = 0.12 (s, 6H, 16-H), 0.91 (s, 9H, 17-H), 2.16 (m, 18H, 1,3,6-H), 4.12 (d, 1H , J = 7.01 Hz, 8-H), 4.17 (d, 1H, J = 6.95 Hz, 9-H), 6.06 (d, 1H, J = 2.44 Hz, 12-H), 6.60 (dd, 1H, 1J = 2.46, 2J = 8.42 Hz, 14-H), 6.90 (d, 1H, 1J = 8.45, 11-H).

^{13}C-NMR (75 MHz, $CDCl_3$): δ /ppm = -4.5 (2C, C-16), 15.2 (2C, C-3,6), 19.2 (4C, C-1), 26.0 (3C, C-17), 40.8 (C-9), 50.6 (C-8), 85.3 (2C, C-2), 86.8 (C-4), 94.1 (C-5), 109.6 (C-14), 118.7 (C-12), 132.5 (C-11), 150.8 (C-7), 153.9 (C-15), 158.7 (C-13), 164.6 (C-10).

- Nitration of isovanelline 2[143]

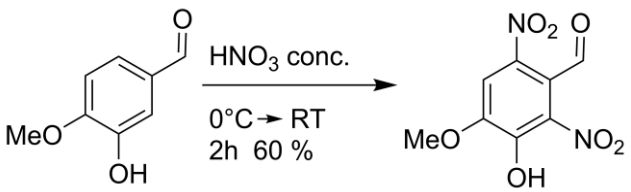

isovanilline **1**	152 g/mol	9.1 g	59.8 mmol	1 eq
HNO_3 conc.	63 g/mol	20 mL	450 mmol	7.5 eq
water	18 g/mol	8.0 mL	-	-

In 8 mL of water at room temperature 9.1 g of isovanilline (59.8 mmol, 1 eq) were dissolved and the mixture was cooled over an ice bath to 0 °C. Then 20 mL of concentrated HNO_3 (63 g/mol, 450 mmol) were added drop wise and the mixture was allowed to warm to root temperature, at which it was stirred for 2 h. After the addition of 100 mL of ice water the precipitate was filtered with a porcelain filter. The resulting solids are recrystallized from water and dried under high vacuum. The yield was 8.9 g (36.5 mmol, 60%).

MS (EI):*m/z* (%): 244 (9), 209 (26), 192 (43), 179 (12), 166 (37), 149 (23), 138 (33), 122 (37), 107 (37), 93 (32), 79 (72), 69 (85), 53 (100).

^{1}H-NMR (300 MHz, CD_3CN): δ/ppm = 10.18 (s, Ph-CHO, 1H), 7.82 (s, CHarom:, 1H), 4.06 (s, Ph-OCH3, 3H).

^{13}C-NMR (75 MHz, CD_3CN): δ/ppm = 192.4, 160.3, 145.5, 144.5, 142.0, 121.3, 115.4, 56.3.

- Reduction of 2,6-dinitro-4-methoxy-3-hydroxybenzaldehyde 3[143]

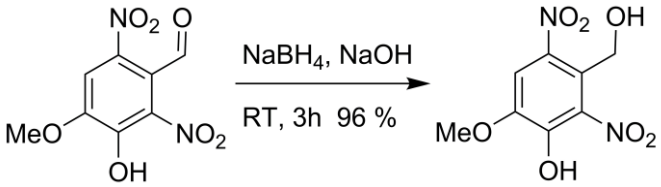

dinitrobenzaldehyde **2**	242 g/mol	7.0 g	29 mmol	1 eq
sodium hydroxide	40 g/mol	1.4 g	35 mmol	1.2 eq
sodium borohydride	38 g/mol	0.85 g	22.5 mmol	0.8 eq

The 7.0 g of 2,6-dinitro-4-methoxy-3-hydroxybenzaldehyde (29mmol, 1 eq) were dissolved in 100 mL of water and 1.4 g (35 mmol, 1.2 eq) of sodium hydroxide was added under stirring. After about 10 min the solution had turned from yellow to red in color and 0.85 g (22.5 mmol, 0.8 eq) of sodium borohydride were added which turned the mixture dark. After stirring for 3 h at room temperature the mixture was diluted with 50 mL of water, neutralized with 4N HCl and extracted multiple times with ethylacetate. The combined organic phases are washed with ~ 200 mL of brine and dried over $MgSO_4$. Drying under high vacuum resulted in a red-brown solid. For further purification a flash column (silica gel; acetone) was used. The yield of 3-(hydroxymethyl)-6-methoxy-2,4-dinitrophenole was 96% (6.78 g, 27.8 mmol)

Rf (acetone): 0.85

UV/Vis (ACN): λ_{max}/nm (normalized absorption) = 273(1), 332 (0.3)

GC-MS: m/z (%): 244 (84), 213 (-OMe; 16)

^{1}H-NMR (300 MHz, CD_3CN): δ/ppm =7.66 (s, CHarom:, 1H), 4.72 (s, Ph-CHOH, 2H), 3.97 (s, Ph-OCH3, 3H).

^{13}C-NMR (75 MHz, CD_3CN): δ/ppm = 152.46, 144.62, 121.27, 110.28, 75.48, 62.92, 57.07, 56.84, 32.32, 29.61, 25.94, 25.62, 21.83, 18.33, 1.00, -5.31.

- Synthesis of 3-(hydroxymethyl)-pent-4-enyloxy-6-methoxy-2,4-dinitrophenol 4[138]

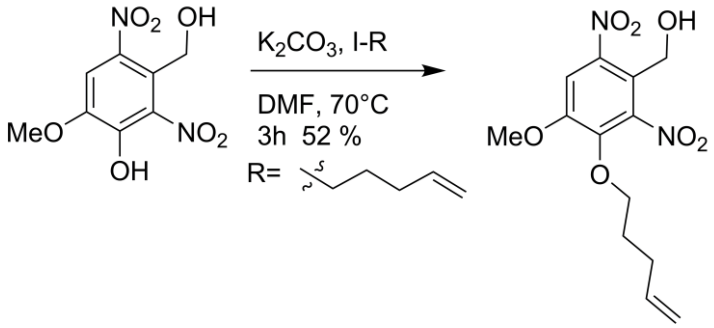

dinitrobenzalcohol **3**	244 g/mol	3.6 g	15 mmol	1 eq
potassium carbonate	144 g/mol	10.2 g	75 mmol	5 eq
alkylhalide	196 g/mol	3.0 g	16.5 mmol	1.1 eq

3.6 g (15 mmol; 1 eq) of the 2,6-dinitro-4-methoxy-3-hydroxybenzalcohol **3** and 10.2 g (75 mmol, 5 eq) of potassium carbonate were suspended in 150 mL of *N,N*-dimethylformamide (DMF). After addition of 3.0 g (16.5 mmol, 1.1 eq) of the alcylhalide (4-pentenebromide) the suspension was heated to 70 °C for 3 h. After cooling to room temperature (RT) all insoluble salts were filtered off. The reaction solution was diluted with 400 mL of deionized water and extracted 3-times with ethyl acetate. The combined organic layers were washed with brine and dried over anhydrous sodium sulfate. Evaporation of the solvent yielded the crude product which was further purified by column chromatography on silica gel with pentane and ethyl acetate (4:1) as eluent. The yield was 52%, 3.6 g, 11.5 mmol.

UV/Vis (ACN): λ_{max}/nm (normalized absorption) = 199 (1), 273 (0.5), 313 (0.1)

HRMS (ESI): m/z = 445.2008 [M+H] Δmmu = 0.7

^{1}H-NMR (300 MHz, $CDCl_3$): δ/ppm =7.70 (s, 1H, CarH), 4.70 (d, 2H, 3J = 7.3 Hz, Car CH2 OH), 4.25 (t, 2H, 3J = 6.6 Hz, Car O CH2-R´), 3.99 (s, 3H, O CH3), 2.62 (q, 2H, 3J = 6.3 Hz, CH2–en), 1.72 (m, H, CH2 aliphatic).

^{13}C-NMR (75 MHz, $CDCl_3$): δ/ppm = 152.46, 144.62, 131.27, 115.28, 75.48, 62.92, 57.07, 56.84, 32.32, 29.61, 25.94, 25.62.

- Synthesis of 3-N-methyl-(5-fluoro-uracil)-pent-4-enyloxy-6-methoxy-2,4-dinitrophenol 5[138]

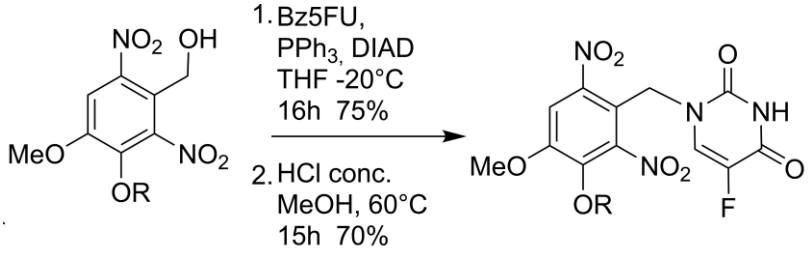

dinitrobenzalcohol´ **4**	312 g/mol	2.2 g	7 mmol	1 eq
DIAD	202 g/mol	2.8 g	14 mmol	2 eq
PPh3	262 g/mol	3.7 g	14 mmol	2 eq
1-*N*-Benzoyl-5-fluorouracil	220 g/mol	1.5 g	7 mmol	1 eq

At 0 °C 2.2 g (14 mol, 2 eq) of diisopropylazodicarboxylate (DIAD) was added slowly to a suspension of 3.7 g (14 mmol, 2 eq) of triphenylphosphine (PPh_3) in 40 mL anhydrous tetrahydrofuran (THF) and stirred for 30 min. A volume of 20 ml (7 mmol) of this beige complex suspension was added slowly to a suspension of 1.5 g (7 mmol, 1 eq) of Bz5FU and 2.2 (7 mol, 1 eq) of dinitrobenzalcohol´ in 20 mL anhydrous THF at −20 °C. The reaction mixture was stirred for 16 h and allowed to warm to RT. The solvent was evaporated, the solid dissolved in methanol, and 2 mL of concentrated HCl was added and stirred at 60 °C for 15 h. After neutralization and evaporation of the solvent the crude reaction mixture was purified by column chromatography on silica gel with pentane and *tert*-butylmethylether (1:1) as eluent. The yield was 3.2 g, 4.9 mmol, 70% yield:

UV/Vis (ACN): λ_{max}/nm (normalized absorption) = 198 (1), 268 (0.3), 325 (0.1)

HRMS (ESI): m/z = 683.2155 [M+Na] Δmmu =−0.1.

^{1}H-NMR (300 MHz, $CDCl_3$): δ/ppm =7.95 (s, 1H, CarH), 7.28–7.26 (m, CH-CF), 5.07 (s, 2H, Car-CH_2-N), 4.70 (d, 2H, 3J = 7.3 Hz, Car-CH_2-OH), 4.25 (t, 2H, 3J = 6.6 Hz, Car-O-CH_2-R´), 3.99 (s, 3H, O-CH3), 2.62 (q, 2H, 3J = 6.3 Hz, CH_2–en), 1.72 (m, H, CH_2-aliphatic)

^{19}F-NMR (282 MHz, $CDCl_3$): δ/ppm = -162.2.

^{13}C-NMR (75 MHz, $CDCl_3$): δ/ppm = 156.62, 153.57, 148.13, 144.86, 144.26, 138.53, 135.45, 130.75, 129.25, 127.22, 126.77, 113.87, 62.88, 57.02, 44.24, 32.31, 28.60.

References

1. F. Schirrmacher, Das Methusalem-Komplott, *Blessing* **2004**, *1*.
2. World-Health-Organization, Visual impairment and blindness, in: Fact Sheet
3. http://www.dr-gumpert.de/html/grauer_star.html am 23.05.09
4. A. Trinavarat, L.-O. Atchaneeyasakul, S. Udompunturak, *J. Cataract Refrac. Surg.* **2001**, *27*, 775-780.
5. S. P. Pradella, R. Träumer, *Ophthalmologe* **1998**, *95*, 482-485.
6. R. G. Martin, D. R. Sanders, J. Souchek, M. Gold Raanan, *J. Cataract Refrac. Surg.* **1992**, *18*, 333-341.
7. L. Werner, J.-M. Legeais, M.D. Nagel, G. Renard, *J. Biomed. Mat. Res.* **1999**, *46*, 347-354.
8. L. Hesse, L. Freisberg, H. Bienert, H. Richter, C. Kreiner, C. Mittermayer, *Ophthalmologe* **1997**, *94*, 821-825.
9. C. M. Cunanan, N. M. Tarbaux, P. M. Knight, *J. Cataract Refrac. Surg.* **1991**, *17*, 767-773.
10. C. S. Pearlstein, S. S. Lane, R. L. Lindstrom, *J. Cataract Refrac. Surg.* **1988**, *14*, 578-580.
11. C. Heidelberger, N. K. Chaudhuri, P. Dannenberg, D. Mooren, L. Griesbach, R. Duschinsky, R. J. Schnitzer, E. Pleven and J. Scheiner, *Nature* **1957**, *179*, 663-666.
12. S. A. Gandolfi, M. Vecchi, *Ophthalmology* **1997**, *104*, 181-186.
13. M. T. Abdelwahab, M. Kugelberg, U. Kugelberg, C. Zetterström, *J. Cataract Refrac. Surg.* **2006**, *32*, 1955-1960.
14. W. J. Geeraets, E. R. Berry, *Am. J. Ophthalmol.* **1968,** *66*, 15.
15. G. Ciamician, *Science* **1912**, *36*, 385-394.
16. H. D. Roth, *Angew. Chem.* **1989**, *101*, 1220-1234.
17. N. Armaroli, V. Balzani, *Angew. Chem*. **2007**, *119*, 52-67.
18. http://www.uni-leipzig.de/~pwm/web/img/intro_fluorescence_1.png date: 1.7.2012.
19. R. A. Marcus, *Annu. Rev. Phys. Chem.* **1964**, *15*, 155-196.
20. M. Goeppert-Mayer, *Ann. Physik* **1931**, *9*, 273-294.
21. W. Kaiser, C. Garret, *Phys. Rev. Lett.* **1961**, *7*, 229-231.
22. M. Albota, D. Beljonne, J.-L. Bredas, J. E. Ehrlich, J.-Y. Fu, A. A. Heikal, S. E. Hess, T. Kogej, M. D. Levin, S. R. Marder, D. McCord-Maughon, J. W. Perry, H. Roeckel, M. Rumi, G. Subramaniam, W. W. Webb, X.-L. Wu, C. Xu, *Science* **1998**, *281*, 1653-1656.
23. R. B. Woodward, R. Hoffmann, Angew. Chem. **1969**, *81*, 797; *Angew. Chem. Int. Ed.* **1969**, *8*, 781-932.
24. Y. Wen, Y. Song, D. Zhao, K. Ding, J. Bian, X. Zhang, J. Wang, Y. Liu, L. Jiang, D. Zhu, *Chem. Commun.* **2005**, 2732–2734.

25. D. Bryce-Smith, A**.** Gilbert, *Chem. Commun.* **1968**, 1702-1703.
26. H. M. Sheldrake, T. W. Wallace, C. P. Wilson, *Org. Lett.* **2005**, *7*, 4233-4236.
27. D. I. Schuster, G. Lem, N. A. Kaprinidis, *Chem. Rev.* **1993**, *93*, 3-22.
28. P. G. Bauslaugh, *Synthesis* **1970**, 287-300.
29. L. Stella, Z. Janousek, R. Merenyi, H. G. Viehe, *Angew. Chem*. **1978**, *90*, 741-742.
30. H. G. Viehe, Z. Janousek, R. Merényi, L. Stella, *Acc. Chem. Res.* **1985**, *18*, 148–154.
31. G. S. Hammond, N. J. Turro, *Science* **1963**, *142*, 1541-1553.
32. G. Ciamician, P. Silber, *Ber. Dtsch. Chem. Ges.* **1913**, 3077-3084.
33. D. R. Graber, M. W. Grimes, A. Haug, *J. Chem. Phys.* **1969**, *50*, 1623-1626.
34. N. Nizomov, A. U. Kholov, A. A. Ishchenko, V. V. Ishchenko, V. P. Khilya, *J. Appl. Spectrosc.* **2007***, 74,* 626-634.
35. R. S. Becker, S. Chakravorti, C. A. Gartner, M. d. Graca Miguel, *J. Chem. Soc., Faraday Trans.* **1993**, *89*, 1007-1019.
36. B. R. Henry, E. A. Lawler, *J. Mol. Spectrosc.* **1973**, *48*, 117-123.
37. C. H. Krauch, S. Farid, G. O. Schenck, *Chem. Ber.* **1966**, 625-633.
38. D. V. Rao, H. Ulrich, F. A. Stuber**,** A. A. R. Sayigh, *Chem. Ber.* **1973,** *106***,** 388-395.
39. H. Morrison, H. Curtis, T. McDowell, *J. Am. Chem. Soc.* **1966**, *6*, 5414-5419.
40. G. S. Hammond, C. A. Stout, A. A. Lamola, *J. Am. Chem. Soc.* **1964**, *6*, 3103-3106.
41. F. D. Lewis, S. V. Barancyk, *J. Am. Chem. Soc.* **1989**, *111*, 8653-8661.
42. R. Anet, *Can. J. Chem.* **1962**, *40*, 1249-1257.
43. J. W. Hanifin, E. Cohen, *Tetrahedron Lett.* **1966***, 44*, 5421-5426.
44. T. Bach, Synthesis **1998**, *05*, 683-703.
45. J. Svoboda, B. König, *Chem. Rev.* **2006,** *106*, 5413-5430.
46. D. Andrew, D. J. Hastings, A. C. Weedon, *J. Am. Chem. Soc.* **1994**, *116*, 10870-10882.
47. J. L. Broeker, J. E. Eksterowicz, A. J. Belk, K. N. Houk, *J. Am. Chem. Soc.* **1995***, 11*7, 1847-1848.
48. T. Suishu, T. Shimo, K.Somekawa, *Tetrahedron* **1997**, *53*, 3545-3556.
49. E. Lee-Ruff, G. Mladenova, *Chem. Rev.* **2003,** *103,* 1449-1483.
50. T. Bach, H. Bergmann, B. Grosch, K. Harms*, J. Am. Chem. Soc.* **2002**, *124*, 7982-7990.
51. X. Yu, D. Scheller, O. Rademacher, T. Wolff, *J. Org. Chem.* **2003***, 68*, 7386-7399.
52. T. Wolff, H. Görner, *Phys. Chem. Chem. Phys.* **2004***, 6*, 368-376.
53. S. R. Trenor, A. R. Shultz, B. J. Love, T. E. Long, *Chem. Rev.* **2004***, 104*, 3059-3077.
54. F. D. Lewis, D. K. Howard, J. D. Oxman, *J. Am. Chem. Soc* **1983***, 105*, 3344-3345.
55. K. D. Belfield, M. V. Bondar, Y. Liu, O. V. Przhonska, *J. Phys. Org. Chem.* **2003***, 16*, 69-78.
56. J. He, X. Tong, Y. Zhao, *Macromolecules* **2009**, *42*, 4845–4852.
57. J. Motoyanagi, T. Fukushima, N. Ishii, T. Aida, *J. Am. Chem. Soc.* **2006**, *128*, 4220-4221.

58. K. Ohkawa, K. Shoumura, Y. Shirakabe, H. Yamamoto, *J. Mat. Sci.* **2003**, *38*, 3191- 3197.
59. C. Graf, W. Schärtl, *Adv. Mater.* **2000**, *12,* 1353-1356.
60. J. Träger, J. Heinzer, H.-C. Kim, N. Hampp, *Macromol. Biosci*. **2008**, *8*, 177-183.
61. L. Zhao, M. Vaupel, D. A. Loy, K. J. Shea, *Chem. Mater.* **2008,** *20,* 1870-1876.
62. S.-Y. Cho, Y.-K. Song, J.-G. Kim, S.-Y. Oh, C.-M. Chung, *Tetrahedron Lett.* **2009***, 50*, 4769-4772.
63. F. D. Lewis, S. L. Quillen, P. D. Hale, J. D. Oxman, *J. Am. Chem. Soc.* **1988***, 110*, 1261-1267.
64. M. Yoshizawa, Y. Takeyama, T. Okano, M. Fujita, *J. Am. Chem. Soc.* **2003***, 125*, 3243-3247.
65. J. Yang, M. B. Dewal, S. Profeta, M. D. Smith, Y. Li, L. S. Shimizu, *J. Am. Chem. Soc.* **2008***, 130*, 612-621.
66. J. Du, T. P. Yoon, *J. Am. Chem. Soc.* **2009***, 131*, 14604-14605.
67. S. Härtner, H.-C. Kim, N. Hampp, *J. Photochem. Photobiol. A* **2007**, *187*, 242-246.
68. J. Träger, H.-C. Kim, N. Hampp, *Nature Photonics* **2007**, *1*, 509-511.
69. E. J. Corey, J. D. Bass, R. LeMahieu, R. B. Mitra, *J. Am. Chem. Soc.* **1964***, 86,* 5570-5583.
70. R. A. Caldwell, D. Creed, *Acc. Chem. Res.* **1980***, 13*, 45-50.
71. R. Huisgen, *Pure Appl. Chem.* **1980***, 52*, 2283-2302.
72. E. Sato, Y. Ikeda, Y. Kanaoka, *Liebigs Ann. Chem.* **1989**, 781-788.
73. V. Berl, J.-P. Lepoittevin, *Photochem. Photobio.* **1999***, 69*, 653-657.
74. T. Fukuyama, Y. Hino, N. Kamata, I. Ryu, *Chem. Lett.* **2004**, *33,* 1430-1431.
75. J. C. Namyslo, D. E. Kaufmann, *Chem. Rev.* **2003**, *103,* 1485-1537.
76. W. R. Gutekunst, P. S. Baran, *J. Am. Chem. Soc.*, **2011**, *133*, 19076–19079.
77. S. C. Shim, D. Y. Chi, *Chem. Lett.* **1978**, 1229-1230.
78. S. C. Shim, C. S. Ra, K. H. Chea, *Bull. Korean Chem. Soc.* **1980**, *1,* 121-123.
79. J. K. Whitesell, D. E. Allen, *J. Org. Chem.* **1985***, 50*, 3026-3028.
80. H. Suginome, K. Kobayashi, *Bull. Chem. Soc. Jpn.* **1988***, 61*, 3782-3784.
81. N. Yonezawa, M. Hasegawa, *Bull. Chem. Soc. Jpn.* **1983**, *56*, 367-368.
82. N. Yonezawa, M. Kubo, K. Saigo, M. Hasegawa, *Bull. Chem. Soc. Jpn.* **1988**, *61*, 1005-1007.
83. N. Yonezawa, T. Yoshida, M. Hasegawa, *J. Chem. Soc., Perkin Trans. 1* **1983**, 1083-1086.
84. D. Kehrloesser, J. Traeger, H.-C. Kim, N. Hampp, *Langmuir* **2010**, *26*, 3878-3882.
85. R. M. Ortuño, A. G. Moglioni, G. Y. Moltrasio, *Curr. Org. Chem.* **2005**, *9,* 237-259.
86. A. Sergeiko, V. V. Poroikov, L. O. Hanus, V. M. Dembitsky, *Open Med. Chem. J.* **2008**, *2*, 26-37.
87. V. M. Dembitsky, *J. Nat. Med.* **2008,** *62*, 1–33.
88. C. R. Wilke, P. Chang, *A. I. Ch. E. Journal* **1955**, *1*, 264-270.
89. H. Morrison, R. Hoffman, *Chem. Commun.* **1968**, *22*, 1453-1454.
90. R. Hoffman, P. Wells, H. Morrison, *J. Org. Chem.* **1971**, *36*, 102-108.
91. H. Kobashi, R. Kondo, H. Ikawa, T. Morita, *Bull. Chem. Soc. Jpn.* **1984**, *57*, 1197-1201.

92. IUPAC Compendium of Chemical Terminology 2nd Edition (1997) 1996, *68*, 2245.
93. S. Ito, Y. Tanaka, H. Yoshikawa, Y. Ishibashi, H. Miyasaka, H. Masuhara, *J. Am. Chem. Soc.*, **2011**, *133*, 14472-14475.
94. IUPAC Compendium of Chemical Terminology 2nd Edition (**1997**) 1996, *68*, 2231.
95. H. Saito. T. Mori, T. Wada, Y. Inoue, *Org. Lett.* **2006**, *8*, 1909-1912.
96. H. Saito. T. Mori, T. Wada, Y. Inoue, *J. Am. Chem. Soc.* **2004**, *126*, 1900-1906.
97. J. Clark, G. Lanzani, *Nature Photonics* **2010**, *4*, 438-446.
98. K. D. Belfield, M. V. Bondar, Y. Liu, O. V. Przhonska, *J. Phys. Org. Chem.* **2003**, *16*, 69-78.
99. S. R. Trenor. A. R. Shultz, B. J. Love, T. E. Long, *Chem. Rev.* **2004**, *104*, 3059-3077.
100. M. Obi, S. Morino, K. Ichimura, *Macromol. Rapid Commu,* **1998**, *19*, 643-656.
101. J. E. Sturm, *J. Chem. Educ.* **1990**, *67*, 32-33.
102. R. C. Hilborn, *Am J. Phys.* **1982**, *50*, 982-986.
103. B. Trost, J. Stutz, U. Platt, *Atmospheric Environment* **1997**, *31*, 3999-4008.
104. H. E. Zimmerman, *Science* **1956**, *153*, 837-844.
105. J. Yang, M. A. Winnik, *Chem. Phys. Lett.* **1995**, *238*, 25-30.
106. J. S. Seixas de Melo, R. S. Becker, A. L. Macanita, *J. Phys. Chem.* **1994,** *98,* 6054-6058.
107. S. Scypinski, L. C. Love, *Anal. Chem.* **1984**, *56*, 322-327.
108. P. P. Wells, H. Morrison, *J. Am. Chem. Soc.* **1975**, *97*, 154-159.
109. T. Wolff, H. Görner, *J. Photochem. Photobiol. A* **2010***, 209*, 219-224.
110. E. T. Harrigan, A. Chakrabarti, N. Hirota, *J. Am. Chem. Soc.* **1976**, *98,* 3460-3465.
111. D. R. Graber, M. W. Grimes, A. Haug, *J. Chem. Phys.* **1969**, *50*, 1623-1626.
112. D. Seebach, *Angew. Chem*. **1990**, *102*, 1363–1409.
113. C.-M. Chung, Y.-S. Roh, S.-Y. Cho, J.-G. Kim, *Chem. Mater.* **2004,** *16,* 3982-3984.
114. M. Schraub, N. Hampp, *Proc. SPIE* **2011**, 7885, 78851Z/1-78851Z/11.
115. H.-C. Kim, S. Kreiling, A. Greiner, N. Hampp, *Chem. Phys. Lett.* **2003**, *372*, 899-903.
116. D. Kehrlößer, R-P. Baumann, H.-C. Kim, N. Hampp, *Langmuir* **2011**, *27,* 4149-4155.
117. Y. Chen, C. F. Chou, *Polym. Sci., Part A: Polym. Chem.* **1995**, *33*, 2705-2714.
118. Y. Chen, J.-L. Geh, *Polymer* **1996***, 37*, 4481-4486.
119. J. Liese, N. Hampp, *J. Phys. Chem. A* **2011**, *115*, 2927–2932.
120. W. v. E. Doering, W. R. Roth, R. Breuckmann, L. Figge, H.-W. Lennartz , W.-D. Fessner, H. Prinzbach, *Chem. Ber.* **1988**, *121*, 1-9.
121. K. Hesse, S. Hunig, *Liebigs Ann. Chem.* **1985**, 715-739.
122. E. Schaumann, R. Ketcham, *Angew. Chem. Int. Ed.* **1982**, *21*, 225-314.
123. K. Jug, P. L. Müller, *Theoret. Chim. Acta.* **1981**, *59*, 365-372.

124. Z.-w. Qu, H. Zhu, X.-d. Zhang, X.-d. Ai, J.-p. Zhang, X.-k. Zhang, Q.-y. Zhang, *Chem. Phys. Lett.* **2002**, *360*, 283-288.

125. A. Schönberg, A. Mustafa, *Nature* **1944**, *153*, 195.

126. A. Schönberg, N. Latif, *J. Am. Chem. Soc*. **1950**, *72*, 4828-4829.

127. M. T. Silva, R. Braz-Filho, J. C. Netto-Ferrera, *J. Braz. Chem. Soc.* **2000**, *11*, 479-485.

128. U. C. Yoon, Y. C. Kim, J. J. Choi, D. U. Kim, P. S. Mariano, I. S. Cho, Y. T. Jeon, *J. Org. Chem*. **1992**, *57*, 1422-1428.

129. R. S. Givens, P. G. Conrad, A. L. Yousef, J.-I. Lee, *CRC Handbook of Organic Photochemistry and Photobiology, 2nd Edition,* CRC Press LLC, **2004**, 69.

130. M. Goeldner, R. S. Givens, *Studies in Biology,* WILEY-VCH, Weinheim, **2005**, 1-94.

131. V. Hagen, F. Kilic, J. Schaal, B. Dekowski, R. Schmidt, N. Kotzur, *J. Org. Chem.* **2010**, *75*, 2790-2797.

132. M. C. Pirrung, W. H. Pieper, K. P. Kaliappan, M. R. Dhananjeyan, *PNAS* **2003**, *100*, 12548-12553.

133. S. Laimgruber, W. J. Schreier, T. Schrader, F. Koller, W. Zinth, P. Gilch, *Angew. Chem. Int. Ed.* **2005**, *44*, 7901–7904.

134. A. P. Pelliccioli, J. Wirz, *Photochem. Photobiol. Sci.* **2002**, *1*, 441-458.

135. K. Schaper, M. Etinski, T. Fleig, *Photochem. Photobiol.* **2009**, *85*, 1075-1081.

136. T. Schmierer, F. Bley, K. Schaper, P. Gilch, *J. Photochem. Photobio. A* **2011**, *217*, 363-368.

137. G. Wettermark, *Nature* **1962**, *194*, 677.

138. D. Kehrloesser, P. J. Behrendt, N. Hampp, *J. Photochem. Photobio. A* **2012**, *248,* 8-14.

139. E. Reichmanis, R. Gooden, C. W. Wilkins, H. Schonhorn, *J. Polym. Sci. Polym Chem.* **1983**, *21*, 1075-1083.

140. R. K. Russell, J. B. Press, R. A. Rampulla, J. J. McNally, R. Falotico, J. A. Keiser, D. A. Bright, A. Tobia, *J. Med. Chem.* **1988**, *31,* 1786-1793.

141. E. J. Corey, *J. Am. Chem. Soc.* **1972**, *94*, 6190-6191.

142. J. L. Morris, C. L. Becker, F. R. Fronczek, W. H. Daly, M. L. McLaughlin, *J. Org. Chem.* **1994**, 59, 6484-6486.

143. S. S. Agasti, A. Chompoosor, C.-C. You, P. Ghosh, C. K. Kim, V. M. Rotello, *J. Am. Chem. Soc.* **2009**, *131*, 5728-5729.

Supplements

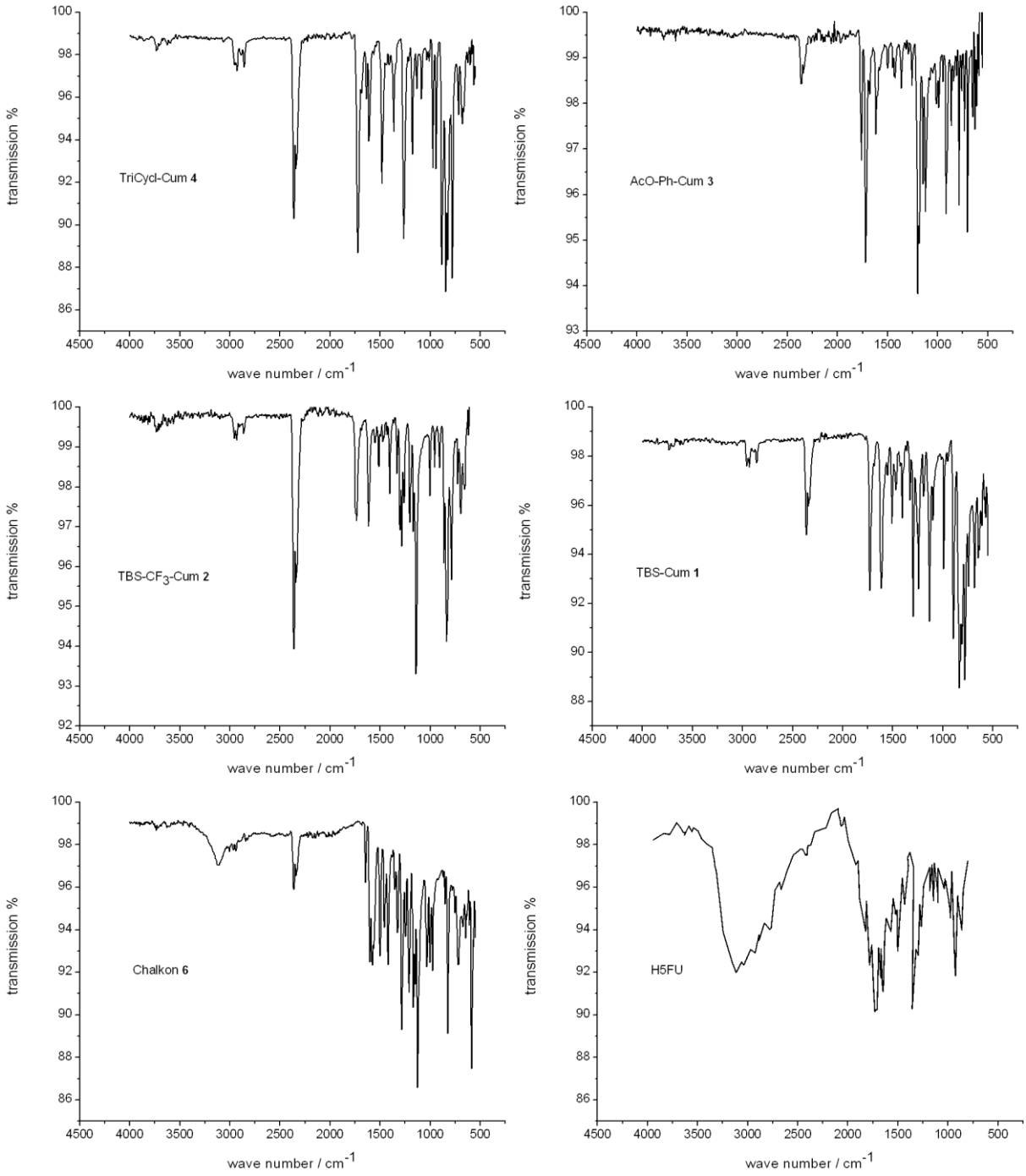

Figure 98: ATIR spectra of kinetic substrates.

Acknowledgment

I would like to thank everybody who has helped and supported me during the time of my degree thesis. In particular I want to thank:

- Prof. Dr. Norbert Hampp for taking me into his work group and allowing me to work on this interesting and intriguing topic. I am grateful for helping me in developing theories, for running with new ideas, as well as for giving me opportunities to meet scientists in foreign countries near and far.

- Prof. Dr. Gerhard Hilt for his expert report.

- The workgroup, with all its members. You supported me and aided me when one person just wasn´t enough. Anne Busch, Philipp Kahler and Pierre Hillebrecht for your invaluable feedback. Hee-Cheol Kim for his continuous help with all things - photochemistry.

- The staff of the University, especially from the machine and the electrical workshop. Often times helping me to construct set ups and experiments, was key to my measurements.

- Jutta Hennen for her assistance with paper work and tutorial registration.

- The students, who contributed to my research by working hard and thinking along the lines of physical chemistry:
  Catarina Nardi-Tironi, Kathrin Wähler, Amanda Beatriz Pineda,
  Stefan Engel x2, Thorben Badur, Maike Noster

- My friends who cheered me on and filled my spare time with joy. You reminded me that there is a life outside of the laboratory and that life is a lot more than molecules and photons.

- Nora for her support and advice.

- My family for always being there for me.

Curriculum vitae

Sept. 2009 - July 2013	Dissertation at the Philipps-University Marburg Physical Chemistry; Workgroup Prof. Dr. N. Hampp “Laser controlled cycloaddition and reversion of crossdimers”
July 2009	Diploma in Chemistry elective subject: Macromolecular Chemistry
Okt. 2008 - July 2009	Diploma thesis in the workgroup of Prof. Dr. N. Hampp “Lasergesteuerte selective, photochemische [2+2]-Cycloaddition von Kreuzdimeren“
Apr. 2004 - June 2008	Study of Chemistry at the Philipps-University Marburg
Aug. 2007 - Apr. 2004	Term abroad at the University of Helsinki, Finland
June 2003	Abitur at the Rottmayr-Gymnasium Laufen